Alma Mater Studiorum – Università di Bologna

DOTTORATO DI RICERCA IN

BIOLOGIA CELLULARE E MOLECOLARE

Ciclo 29

Settore Concorsuale di afferenza: 05/E1

Settore Scientifico disciplinare: BIO10

TARGETING MITOCHONDRIAL RESPIRATORY COMPLEX I: A NOVEL ANTICANCER STRATEGY

Presentata da: ***Renaud Vatrinet***

Coordinatore Dottorato

Prof Giovanni Capranico

Relatore

Prof.ssa Anna Maria Porcelli

Correlatore

Prof. Giuseppe Gasparre

Esame finale anno 2017

TABLE OF CONTENTS

TABLE OF CONTENTS

ABSTRACT

Tumor cells exhibit profound bioenergetic changes with respect to the original non-transformed cell types. One of the main driving mechanism leading to such a metabolic alteration is triggered by hypoxia. Hypoxia is experienced by cancer cells during tumor progression and leads to a significant enhancement of glycolysis in order to sustain tumor growth and survival. The transcription factor hypoxia-inducible factor-1 (HIF1) is the master regulator of cell adaptation to low oxygen condition, and thus of tumor progression. Our group described the lack of HIF1α in low-proliferative oncocytic tumors, which are characterized by the loss of the mitochondrial respiratory Complex I (CI). Hence, we hypothesized that severe CI dysfunctions prevent HIF1α stabilization and impair tumor adaptation to low oxygen levels. Using the zing finger nucleases technology, we generated NDUFS3-deficient cancer cells that display acute CI deficiency. Engineered CI-defective cancer cells showed a lack of HIF1α stabilization in hypoxic condition, likely due to higher intracellular oxygen concentration and increased levels of the metabolite α-ketoglutarate, which both foster HIF1α proteasomal degradation. *In vivo* experiments showed that the lack of CI was associated to an impairment in the growth of the xenografts, together with the lack of HIF1 activation and a significant reduction of the expression of HIF1-responsive genes involved in the glycolytic machinery and tumor vascularization. Further analysis showed that CI-deficient xenografts may have developed a tailored structure to compensate the metabolic restriction caused by the lack of CI and HIF1α. Using a Tet-Off expression system, we thus generated NDUFS3-knock out inducible clones, allowing us to target CI during xenografts growth. Removing NDUFS3 from xenografts have successfully recapitulated key oncocytic features. CI loss induced HIF1α destabilization, the accumulation of defective mitochondria and xenografts growth arrest. Overall, these data showed that cancer cells are unable to sustain proliferation when functional CI is lost during tumor progression.

ABBREVIATIONS

ACO2: aconitase
Ala: Alanine
AMPK: AMP activated kinase
Arg: Arginine
Asn: Asparagine
Asp: Asparate
ATP: adenosine triphosphate
bHLH-PAS: helix–loop–helix - per-arnt-sim
CI: Complex I
CII: Complex II
CIII: Complex III
CIV: Complex IV
CN-PAGE: Clear Native PAGE
CoQ: ubiquinone
CS: citrate synthase
Cys: Cysteine
DAB: diaminobenzidine
DCIP: 2,6-Dichlorophenolindophenol
Dox: doxycycline
DSB: double strand break
EDTA: ethylenediaminetetraacetic acid
ETC: Electron transport chain
F-PCR: Fluorescent PCR
FCCP: carbonyl cyanide-p-trifluoromethoxyphenylhydrazone
FH: fumarate hydratase
FIH-1: factor inhibiting HIF1
FMN: Flavin mononucleotide
GDH: glutamine dehydrogenase
Gln: Glutamine
Glu: Glutamate
GLUT1: glucose transporter 1
Gly: Glycin
H2DCFDA: 2,7-dichlorodihydrofluorescein diacetate
HDR: homology-directed repair
HG: hydroxyglutarate
HIF1: hypoxia inducible factor 1
His: Histidine
HMT: Human Metabolome Technologies
HRE: hypoxic responsive elements
IDH: isocitrate dehydrogenase
Ile: Isoleucine
IMM: Inner mitochondrial membrane
IMS: Inter-membrane mitochondrial space
LDHA: lactate dehydrogenase A
Leu: Leucine
Lys: Lysine
MAS: malate aspartate shuttle
MDH: malate dehydrogenase

Met: Methionine
mtDNA: Mitochondrial DNA
NHEJ: non-homologous end joining
OAA: oxaloacetate
OCR: Oxygen Consumption Rate
OXPHOS: Oxidative phosphorylation
PARP1: poly (ADP ribose) polymerase 1
PCA: perchloric acid
P_D-module: distal half of the P module
PDC: pyruvate dehydrogenase complex
PDK: pyruvate dehydrogenase kinase 1
PHD: prolyl hydroxylases
Phe: Phenylalanine
P_P-module: proximal half of the P module
Pro: Proline
pVHL: Von Hippel Lindau protein
QH_2: ubiquinol
rDNA: recombinant DNA
ROS: Reactive oxygen species
rRna: ribosomal RNA
SA: succinate
SDH: succinate dehydrogenase
Ser: Serine
SIRT: Sirtuin
SRB: Sulforhodamine B
SUCL: succinate Co-A ligase
TALENs: transcription activator-like effector nucleases
TCA: Tricarboxylic acid
Th: Threonine; tRNA: transfer RNA
Trp: Tryptophane
TSG: Tumor suppressor gene
Tyr: Tyrosine
Val: Valine
VEGF: vascular endothelial growth factor
ZFNs: zinc finger nucleases
ZFPs: Zinc finger proteins
WT: wild-type
α-KG: α-ketoglutarate
α-KGDC: α-ketoglutarate dehydrogenase complex

INTRODUCTION

Hallmarks of cancer

Cancer cells are cells gone wrong. They have escaped the yet exceptionally effective genome maintenance systems that prevent pernicious mutations to occur, or else cells to thrive upon serious genetic damage. Thus, malignant cells display genome instability and obtain the capability to sustain chronic proliferation. Homeostasis of cell number is altered, and so are normal tissue architecture and function, ultimately threatening the life of cancer patients.

At first enabled by an alteration in a so-called oncogene or tumor suppressor gene (TSG), the mutations found in the DNA sequence of a cancer cell have further accumulated during the progression of the tumor. As the lump grows, cells divide, a microenvironment settles and evolves, previously gained mutations are inherited and new ones emerge. This succession of genetic alterations in a changing environment implies that tumors are more than insular masses of proliferating cells. Cancer cells found with specific mutant genotypes have not only survived to the particular milieu, but the novel mutations that they harbour might have provided them with selective advantage, hence enabling their outgrowth, or merely their very existence. In this light, one can sense the parallel between Darwinian evolution and the underlying dynamic of cancer. In fact, malignant cells must acquire, through this selection procedure, a set of tailored solutions to sustain their proliferation and progression in the face of all opposition, from cell growth-and-division cycle control, to tumor microenvironment, and to body response.

In 2000, Douglas Hanahan and Robert Weinberg have proposed that six hallmarks govern the transformation of normal cells to malignant cells. These are: sustaining proliferative signalling, evading growth suppressor, resisting to cell death, replicating immortally, acquiring blood supply, and invading and metastasizing (Hanahan and Weinberg, 2000). Because they are specific traits of cancer cells, they are also potential therapeutic targets as documented, for instance, by the broad use of chemo- and radio-therapies that take advantage of cancer cells high proliferation rate. Most recently, in 2011, the same authors have identified four newly emerging hallmarks: cancer cells

display genome instability and chronic inflammation, they evade immune destruction and they reprogram their energy metabolism (Hanahan and Weinberg, 2011) (Figure 1). These research areas are nowadays revealing tremendous promise for cancer treatment.

Figure 1: Hallmarks of cancer (adapted from Hanahan and Weinberg, Cell, 2011)

Mitochondria as the cell powerhouses

Complex life may have arisen from the endosymbiosis between an archaeon and a bacterium, which lately evolved into mitochondria (Lane and Pariseau, 2016). All eukaryotes have or have had mitochondria. Testifying its bacterial heritage, the mitochondrion presents with a circular DNA (mtDNA), a double membrane (Figure 2A), an independent translation machinery and, most importantly, the capacity to produce adenosine triphosphate (ATP), the cell energy currency. Indeed, the complex eukaryotic traits such as the presence of a nucleus, a larger genome, and the ability to form multicellular organisms rely on the fact that these cells possess powerhouses that greatly build on nutrient utilization for ATP production. In the cytosol, glycolysis can quickly and simply degrade a glucose molecule and transfer the energy contained into its chemical bonds into two high energy pyrophosphate bonds, forming two ATP. How mitochondria produce ATP is a far more complex mechanism. These organelles host the electron transport chain (ETC) embedded into their inner mitochondrial membrane (IMM) (Friedman and Nunnari, 2014). The ETC comprises several protein complexes that conduct an electron flow, allowing the latter to pump protons into the intermembrane mitochondrial space (IMS) against their concentration gradient. Protons subsequently move back into the matrix of mitochondria, flowing down through the ATP synthase that ultimately generates ATP. The all apparatus is the oxidative phosphorylation (OXPHOS) system that comprises four enzymatic complexes (CI-IV), two mobile electron carriers and the ATP synthase (Figure 2B). The complete mitochondrial oxidation of a single molecule of glucose provides 36 moles of ATP. To regulate energy transduction efficiency, mitochondria present with IMM invaginations called the “cristae”, whose surface area may be increased or decreased according to cell energetic requirements (Mannella et al., 2013).

Among the 87 polypeptides that constitute the OXPHOS system, only 13 are encoded by the mtDNA (Figure 2C and D), while the remaining part is encoded at the nuclear level and later imported into the mitochondria (Harbauer et al., 2014). The mtDNA, comprised of 16.569 base pair, is double-stranded and is localized in the matrix of mitochondria, where it is present in high copy number,

ranging from tens to thousands copies per cell. The number of mitochondria per mammalian cells vary and may reach more than 2000 in some tissues. Importantly, mtDNA tends to accumulate mutations at a much higher rate than nuclear DNA (Liu and Demple, 2010). Indeed, the mitochondrial genome lacks protective histones, introns and efficient DNA repair system, and it is at the immediate vicinity of the ETC that produces reactive oxygen species (ROS). The phenotypic property and severity induced by a mutation in mtDNA depends on the nature of the mutation and on the proportion of mutant and wild-type mtDNAs present in the cell. When cells contain a mixture of wild-type and mutant mtDNAs, this situation is referred to as heteroplasmy. Instead, when all copies of the mtDNA are identical, this condition is termed homoplasmy.

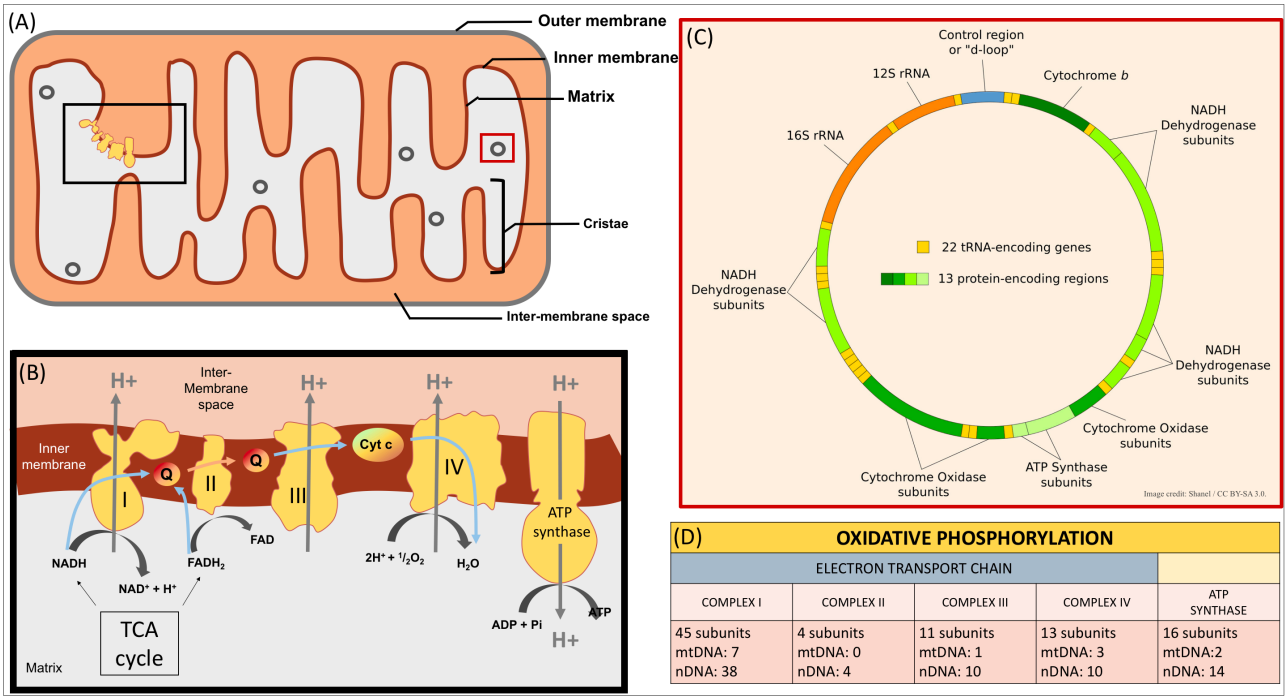

(D) OXIDATIVE PHOSPHORYLATION

ELECTRON TRANSPORT CHAIN				
COMPLEX I	COMPLEX II	COMPLEX III	COMPLEX IV	ATP SYNTHASE
45 subunits mtDNA: 7 nDNA: 38	4 subunits mtDNA: 0 nDNA: 4	11 subunits mtDNA: 1 nDNA: 10	13 subunits mtDNA: 3 nDNA: 10	16 subunits mtDNA:2 nDNA: 14

Figure 2: Mitochondria hosts the respiratory chain and multiple copies of DNA

(A) Overview of the mitochondrial structure with the cristae invaginations into the matrix, which contains multiples copies of mtDNA. The OXPHOS system is embedded into the inner membrane of mitochondria. (B) Representation of the OXPHOS system. The electron transport chain comprises four complexes (CI-IV) that drive an electron flux allowing CI, CIII and CIV to pump protons into the inter-membrane space. The ATP synthase produces ATP when protons move back to the matrix. (C) The mitochondrial DNA is circular and encodes for complexes subunits, transfer RNA (tRNA) and ribosomal RNA (rRNA). (D) Constituents of the OXPHOS system and their origins (nuclear or mitochondrial genome) (Smeitink et al., 2001).

Cancer metabolism

The Warburg hypothesis revisited

Although metabolic reprogramming has been only recently recognized as an emerging hallmark, cancer metabolism is one of the oldest area of research in cancer biology, even predating the discovery of oncogenes and tumor suppressors by some 50 years (Lodish et al., 2000). In the early 20th century, Otto Warburg demonstrated for the first time that cancer and normal cells differ from each other by their metabolic phenotype, the first ones exhibiting an increased glycolytic metabolism regardless the oxygen supply (i.e. aerobic glycolysis). He hypothesized that cancer cells shift their metabolism towards glycolysis because of an accumulation of defective mitochondria, thus preventing the use of OXPHOS as the major contributor for ATP generation (Warburg et al., 1927). Supporting the latter hypothesis, mtDNA mutations have been associated to the upregulation of glycolytic enzymes and to cancer progression (Cuezva et al., 2002; Kirches, 2009; Sánchez-Aragó et al., 2010), and positron emission tomography imaging confirmed the increase in glucose flux in the vast majority of tumors *in vivo* (Zhu et al., 2011). However, while the field of cancer metabolism built on Otto Warburg's work, it also prompted his hypothesis to be revisited. More complex bioenergetic traits have emerged from studies, which clearly demonstrate that increased glycolysis is only rarely the result of mitochondrial dysfunction. Most cancer cells still maintain a significant level of OXPHOS *in vitro* and *in vivo* (Jose et al., 2011; Marin-Valencia et al., 2012; Smolková et al., 2011; Wolf, 2014; Zu and Guppy, 2004). Further, while glycolysis general enhancement may directly quench oxidative metabolism in certain types of cancer (Conley et al., 2001; Crabtree, 1929; Rodríguez-Enríquez et al., 2010), glucose deprivation may instead increase mitochondrial function in cancer cells (Smolková et al., 2010). The latter findings support the fact that OXPHOS may be beneficial to cancer cells, especially in condition of nutritional limitation.

Glycolysis is known to sustain rapid cell division. As a matter of fact, several non-transformed cells display a high glycolytic phenotype during fast proliferation (Lunt and Vander Heiden, 2011). In cancer, enhanced glycolytic machinery has been shown to foster synthesis of nucleotides, fatty acids

and non-essential amino acids for biomass production, to generate energy and reductive equivalents, and to enable metastasis, local invasion and antitumor immunity through lactate production (Chen et al., 2015; Gatenby and Gillies, 2004) (Figure 3). Not surprisingly, numerous studies revealed that oncogenes activation and loss of TSGs directly or indirectly increases glycolysis (Dang, 2012; DeBerardinis et al., 2008; Jones and Thompson, 2009) (Figure 3). Hence, aerobic glycolysis may preferentially be selected by cancer cells as it provides them with substantial growth advantages, making it an attractive target for cancer therapy (Vander Heiden, 2011).

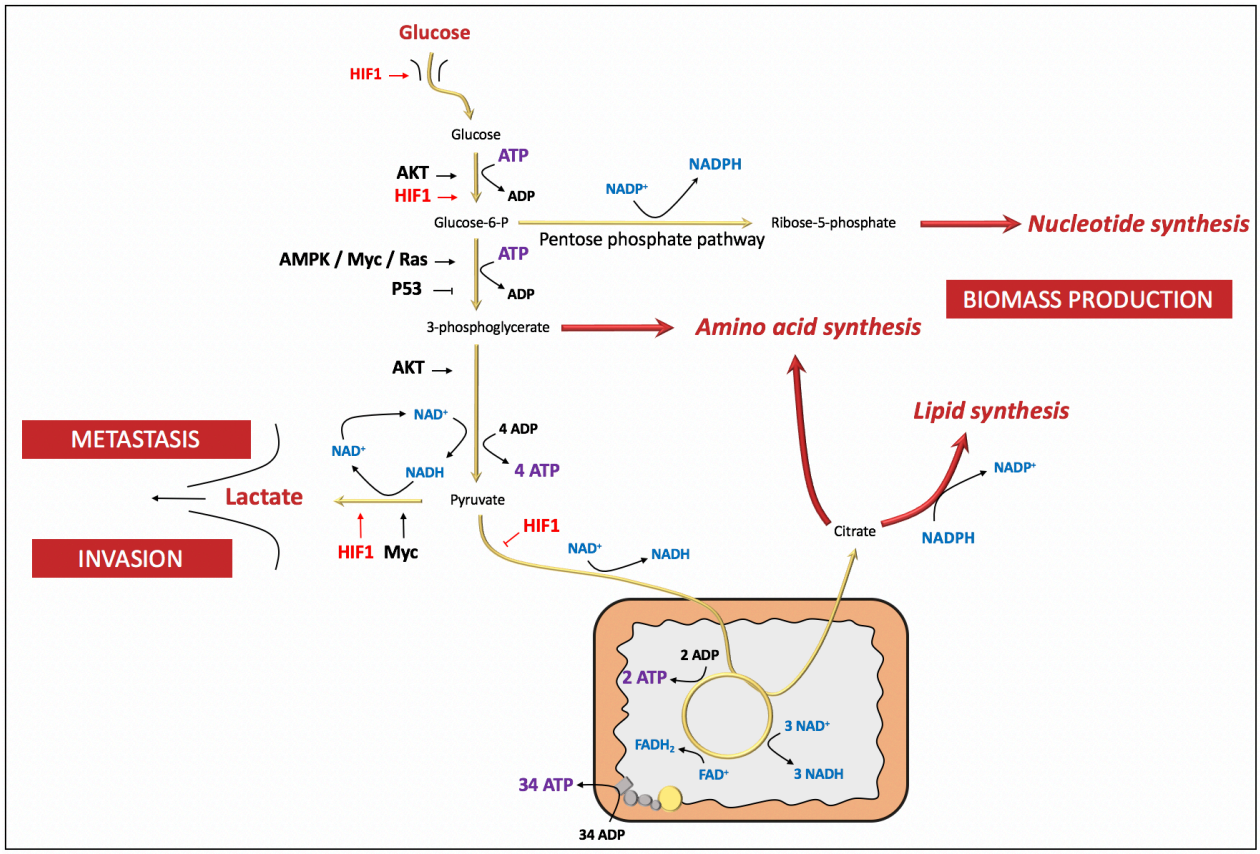

Figure 3: The glycolytic pathway within cell metabolism

Glycolysis is directly controlled by signalling pathways involving known oncogenes and TSGs. This scheme shows how glycolysis, oxidative phosphorylation and biosynthetic pathways are interconnected and regulated. In cancer, the glycolytic pathway is stimulated as it provides new biomass for cell proliferation and lactate for invasion and metastasis. In hypoxia, glycolysis is further stimulated and is disconnected from OXPHOS, pyruvate being mainly redirected toward lactate production. The transcription factor hypoxia inducible factor 1 (HIF1) is the major regulator of glycolytic upregulation in hypoxia and acts at different levels in the glycolytic pathway. Expression of HIF1, AKT, P53, AMPK, Myc and Ras are associated with enhanced glycolysis in cancer.

The environment matters: Hypoxia and the HIF1-signalling

A common feature of solid tumors is that their growth rate often exceeds the speed of new vessels formation and therefore cells rapidly accumulate in poorly vascularized bulks (Jain et al., 2002). Hence, cancer cells cope with fluctuations in oxygen and nutrients levels, which force them to optimize substrate utilization by adjusting metabolic pathways, ultimately allowing them to keep meeting the requirements for malignancy. While nutrient scarcity leads to OXPHOS enhancement and promotes mitochondrial biogenesis (Martin-Montalvo and de Cabo, 2013; Smolková et al., 2011), hypoxia instead induces a typical "Warburg-like" shift from OXPHOS to glycolysis. Hence, an already existing reliance on glycolysis can be further increased when cancer cells face low oxygen tension. The transcription factor hypoxia inducible factor 1 (HIF1) is the master regulator of the hypoxic response and it mediates the complex hypoxic adaptation by modulating the expression of hundreds of genes (Semenza, 2007). HIF1 is composed of an α- and a β-subunit, belonging to the basic helix–loop–helix - per-arnt-sim (bHLH-PAS) protein family, both constitutively produced. In condition of normal oxygen tension (normoxia), HIF1α is hydroxylated on two specific prolyl residues (P402 and P564) in its oxygen-dependent degradation domain by three different prolyl hydroxylases: PHD 1, 2 and 3. This in turn recruits an E3 ubiquitin ligase complex containing the von Hippel Lindau protein (pVHL), resulting in HIF1α ubiquitylation and subsequent degradation by the proteasome (Figure 4). PHDs are Fe(II)/αKG-dependent dioxygenases that use the mitochondrial metabolite α-ketoglutarate (α-KG) and O_2 as co-substrates, and require Fe (II) as a cofactor to produce succinate (SA) and CO_2 (McDonough et al., 2010). Noticeably, even in the absence of oxygen, high levels of α-KG are sufficient to promote the activity of PHDs, making the metabolite an important modulator of the hypoxic response (Tennant et al., 2009). In hypoxia, PHDs low affinity for oxygen does not allow them to hydroxylate HIF1α, which cannot be degraded and becomes stabilized. In this context, HIF1α and HIF1β dimerize to form the transcription factor HIF1 that subsequently translocates into the nucleus (Depping et al., 2008). The modification of genes expression in hypoxia involves the formation of a DNA-binding complex that contain both HIF1 and the pair of transcription

adaptors p300/CBP, which altogether bind DNA at conserved promoter and enhancer-linked HIF1 sites, as hypoxic responsive elements (HRE) (Arany et al., 1996) (Figure 4). Of note, the factor inhibiting HIF1 (FIH-1), another Fe(II)/αKG-dependent dioxygenase, can hydroxylate the asparagine N^{803} of HIF1 and thereby block its interaction with the coactivators p300/CREB or CBP, making it an important modulator of the hypoxic response. The latter includes an attempt to increase vascularization and glycolytic machinery, to get sufficient oxygen levels back and to survive anaerobic conditions, respectively. Hence, genes such as the vascular endothelial growth factor (VEGF), lactate dehydrogenase A (LDHA), pyruvate dehydrogenase kinase 1 (PDK), and glucose transporter 1 (GLUT1), among many other glycolytic enzymes, are upregulated in hypoxia upon HIF1 activation.

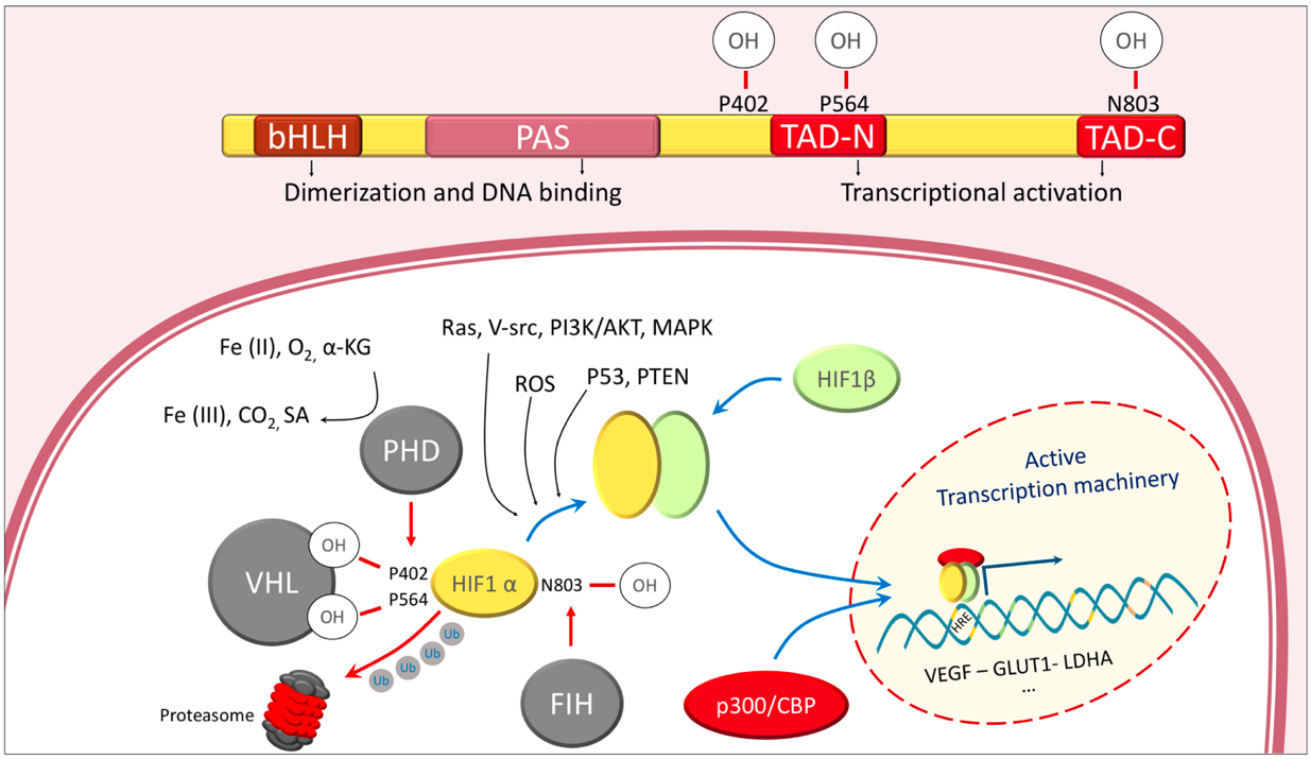

Figure 4: Mechanisms that regulate HIF1 activation (adapted from (Denko, 2008)
HIF1α hydroxylation on P402 and P564 by the prolyl-hydroxylases (PHDs) induces its ubiquitination by the Von-Hippel-Lindau ubiquitin ligase complex (VHL), and its subsequent degradation by the proteasome. The factor inhibiting HIF1 (FIH) may hydroxylate HIF1α on N803, thereby preventing its activation. PHD and FIH are promoted by Fe(II), O_2 and α-KG. When stabilized, HIF1α heterodimerizes with HIF1β and the p300/CBP complex to bind the hypoxia responsive element (HRE) at the promoter of genes, hence fostering their expression.

Besides HIF1α, two other members of the bHLH-PAS superfamily, HIF2α and HIF3α, have also been described. While the role of HIF2α in the hypoxic response has been well established, the mechanisms of action of HIF3α are still poorly understood. HIF1α and HIF2α are closely related and they both activate HRE-dependent gene expression. However, the two transcription factors differ in their transactivation domains and may therefore bind different co-factors and affect the expression of distinct target genes (Loboda et al., 2010). Furthermore, while HIF1α is ubiquitously expressed, HIF2α expression is limited to certain tissues. The latter also presents with different roles in cancer, which may negatively or positively influence tumor progression according to tumor type (Cho and Kaelin, 2016; Favier et al., 2007; Loboda et al., 2010).

Numerous cancer-associated genetic alterations promote HIF1 expression and/or stabilization. Both the overexpression of oncogenes RAS, V-SRC, stimulation of the PI3K/AKT/mTORC1 axis, and loss of the tumor suppressors pVHL, PTEN and p53 have been shown to increase HIF1 levels (Lim et al., 2004; Semenza, 2013) (Figure 4). Similarly, several mitochondrial dysfunctions can further stimulate HIF1 activation. Indeed, ROS were shown to participate to the hypoxia-mediated stabilization of HIF1α (Chandel et al., 2000), suggesting that pathological levels of ROS in cancer may also affect the hypoxic response, independently from O_2 concentration. Accordingly, several mechanisms through which ROS could affect the HIF1-signalling have been proposed, all of which likely to conspire to promote the transcription factor's activity and thereby the tumorigenic potential of cancer cells (Galanis et al., 2008).

Contribution of mitochondrial metabolism to cancer progression

In the canonical view, the tricarboxylic acid (TCA) cycle is a series of chemical reactions that take place in the mitochondrial matrix and drive the oxidation of carbon fuels derived from acetyl-CoA (Ac-CoA), which is mainly provided by glycolysis and fatty acid oxidation. These reactions produce the reducing equivalents NADH and $FADH_2$ that are subsequently utilized by respiratory CI and

respiratory CII, respectively, to generate the mitochondrial membrane potential ($\Delta\psi_m$) required for ATP production (Figure 5).

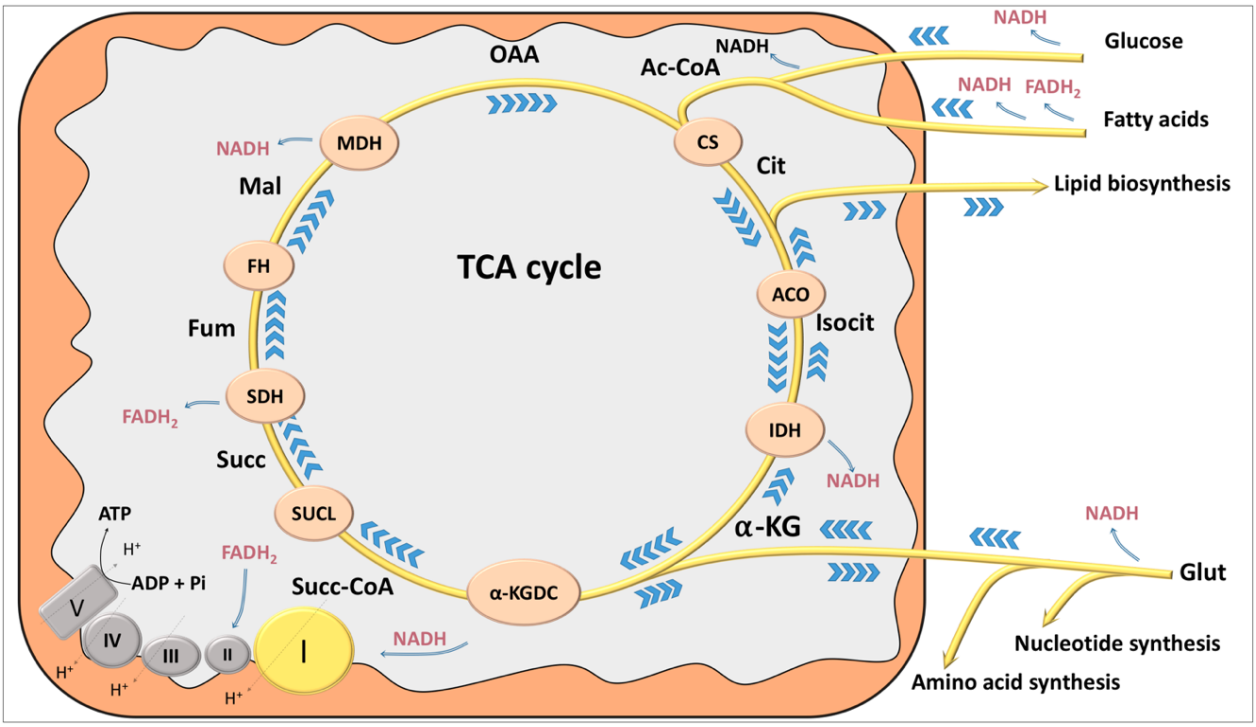

Figure 5: The TCA cycle

The acetyl fraction of Ac-CoA moiety is condensed with oxaloacetate (OAA) by the citrate synthase (CS) to form citrate. The aconitase (ACO) isomerizes citrate into isocitrate, which is then decarboxylated into α-KG by the isocitrate dehydrogenase (IDH) 3. In the second part of the TCA cycle, succinyl Co-A, produced by the second and last decarboxylation reaction, performed by the α-KGDC, is converted back to oxaloacetate through several steps involving production of SA by succinate Co-A ligase (SUCL) and fumarate, malate and finally oxaloacetate by, respectively, succinate dehydrogenase (SDH), fumarate hydratase (FH) and malate dehydrogenase (MDH). Glutamine feeds the TCA cycle at α-KG level. Glucose and fatty acids feed the TCA cycle at Ac-CoA level. The NADH and $FADH_2$ produced by the TCA cycle are utilized by respiratory CI and CII, respectively. TCA metabolic flux is represented by blue arrows (»).

Yet, the TCA cycle exhibits manifold other functions that shape the metabolic profile of cancer cells and influence tumor progression. Glutamine, the most abundant amino acid in plasma, has been widely described as an additional key source of both carbon and nitrogen, especially for rapidly dividing cells (Hosios et al., 2016). Glutamine fuels the TCA cycle at α-KG level, which can enter both energetic and biosynthetic pathways. Indeed, α-KG may either be oxidized by the α-ketoglutarate dehydrogenase complex (α-KGDC) inside mitochondria, or it may be reduced, hence

pushing the TCA cycle towards citrate (DeBerardinis et al., 2007). The latter can be shuttled to the cytosol where it may be converted back into Ac-CoA, which is subsequently used for lipid biosynthesis. This glutamine-dependent biosynthetic pathway is promoted in cancer cells that cope with a low oxygen environment or which exhibit OXPHOS deficiency (DeBerardinis et al., 2007; Fendt et al., 2013; Mullen et al., 2014; Wise et al., 2011). In particular, hypoxia induces a block in glucose and fatty acid oxidation, caused by the inhibition of Ac-CoA entry into the TCA cycle (Huang et al., 2014; Lu et al., 2008). In this context, citrate is generated from glutamine through a TCA cycle running in a reverse manner. Constitutive activation of HIF1 has been shown to promote the rewiring of α-KG fate from oxidative to reductive metabolism in normoxia (Metallo et al., 2011; Wise et al., 2011), highlighting the important role of the transcription factor in modulating TCA metabolites levels (Figure 6). HIF1 reduces the activity of both PDH and α-KGDH, hence likely to contribute to elevating the α-KG/citrate ratio in cells and to promote α-KG reductive carboxylation, by mass action on the TCA cycle flux (Fendt et al., 2013; Sun and Denko, 2014). More recently, HIF1 has also been shown to promote the expression of the glutamine dehydrogenase (GDH), which converts glutamate to α-KG (Jiang et al., 2017). Although Jiang and colleagues demonstrated the importance of the HIF1α-GDH axis for ATP production in hypoxia, its involvement in providing α-KG for reductive carboxylation is however very likely.

Thus, even respiration impairment does not imply a complete shutoff of mitochondrial metabolism. The TCA cycle is fuelled by substrates entering at different gateways and provides the carbon source for both energy production and biosynthesis.

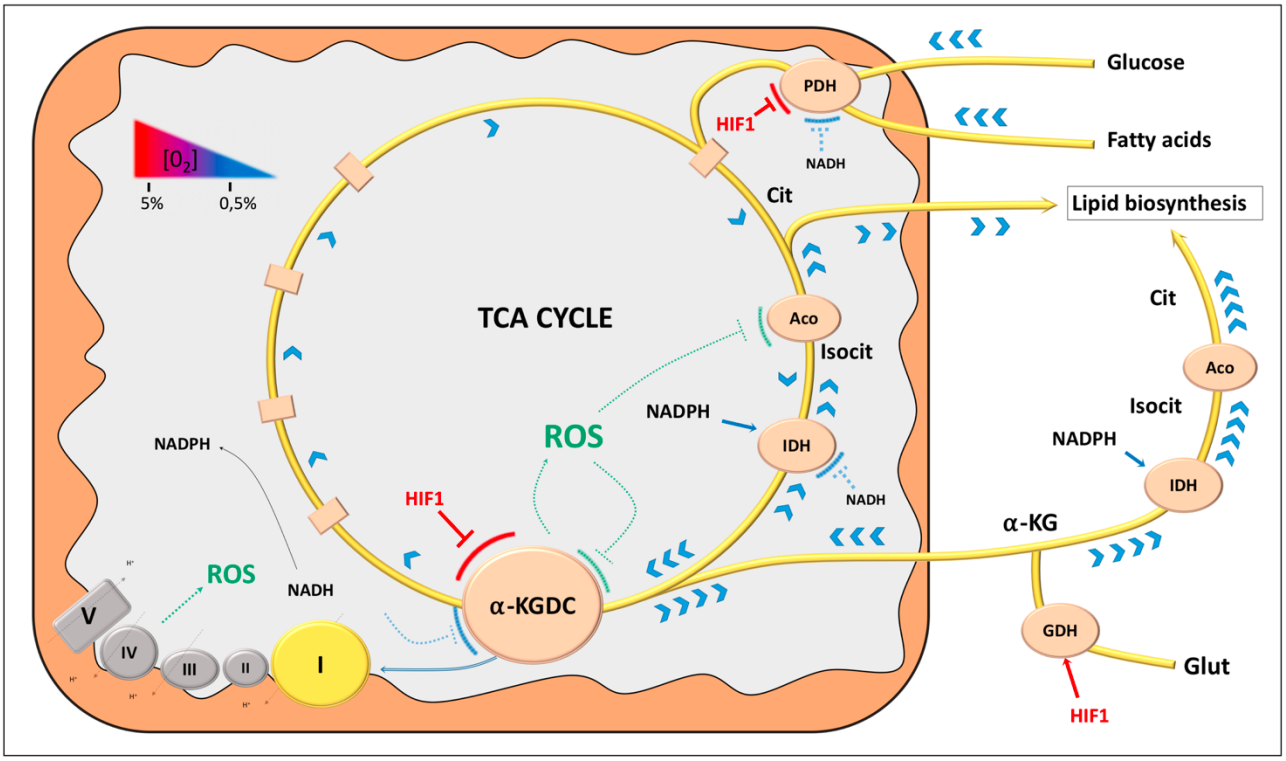

Figure 6: Molecular actors driving α-KG reductive carboxylation in mitochondria upon hypoxia (Adapted from Vatrinet et al., Cancer & Metab, 2017)
Under hypoxia, NADH and HIF1 inhibit the enzymes α-KGDC and PDH, thereby increasing the α-KG/citrate ratio. Besides, ROS production may further participate to the latter by inhibiting the α-KGDC and the aconitase. Anaplerotic source of α-KG may be fostered through the HIF1-mediated increase in GDH activity. TCA metabolic flux is represented by blue arrows (».

Further, mutations in several TCA cycle enzymes, including mutations in fumarate hydratase (FH), succinate dehydrogenases (SDH) and isocitrate dehydrogenase 1 and 2 (IDH1/2) have been reported in multiple types of cancer, which respectively accumulate SA, fumarate, and (*R*)-2-hydroxyglutarate (HG), all conveying broad oncogenic signals. These so called "oncometabolites" share great structural and metabolic similarity to α-KG, retaining therefore the capacity to regulate Fe(II)/αKG-dependent dioxygenases (Morin et al., 2014), likely to influence on HIF1-signalling through the modulation of PHDs and FIH activity. Accordingly, PHDs are allosterically inhibited by SA and fumarate (Selak et al., 2005), while (R)-2-HG occupies α-KG's binding site and acts as a competitive inhibitor (Xu et al., 2011). Furthermore, chronic inhibition of PHDs in both SDH-deficient and FH-deficient tumors is associated with the stabilization of HIF1α and activation of downstream hypoxic pathways, even in normoxia (i.e. pseudohypoxia) (Pollard et al., 2005). Contrariwise, α-KG is

sufficient to oppose SA, fumarate, and hypoxia-mediated activation of HIF1α, resulting in the reversal of enhanced glycolysis and cell death (MacKenzie et al., 2007; Tennant et al., 2009). The Fe(II)/αKG-dependent dioxygenases are a family of more than 60 enzymes involved in nutrient sensing, oxygen sensing, and epigenome editing (Loenarz and Schofield, 2008; Rose et al., 2011). The K_M of Fe(II)/αKG-dependent dioxygenases for α-KG is close to its physiological concentration. Therefore, even a modest variation in the α-KG levels may profoundly modify dioxygenases-mediated signals. In this light, and building on ours and others precedent studies, our group has recently hypothesised an essential role for the α-KG signal in continuously restructuring the metabolic and epigenetic landscape of cancer cells to survive internal and environmental pressures (Vatrinet et al., 2017).

Hence, mitochondria are not bystanders in the process of carcinogenesis and tumor progression. Far from being only the powerhouses of cells, these organelles are the hub of multiple metabolic pathways and the source of signalling metabolites whose levels can significantly impact on cancer cells fate within tumors.

What did we learn from oncocytomas?

Oncocytomas are low proliferative tumors named after their characteristic of bearing oncocytes' mitochondria, which display aberrant cristae and show low electron density on micrographs, thus being most likely non-functional. Accordingly, oncocytic tumors share the common but rare feature that they harbour high burden of disruptive mutations in mitochondrial genes encoding for OXPHOS complexes subunits (Gasparre et al., 2011a). Instead, such severe mtDNA mutations have been shown to be purified in aggressive cancer, where they are often found at low heteroplasmy levels (Iommarini et al., 2013; Ju et al., 2014; Kurelac et al., 2015; Pereira et al., 2012).

In a recent review published by our group, De Luise et al. identified three factors that must be reached in order to achieve the oncocytic phenotype (De Luise et al., 2017)., namely: i) a lesion hitting the mitochondrial energy production capacity, which triggers a bioenergetics crisis; ii) an imbalance

between mitochondrial biogenesis and autophagy/ mitophagy, which may predispose to the accumulation of damaged organelles; iii) the contribution of oncogenes/TSGs/modifier genes to the onset of the previous two conditions. Strikingly, mutations were often found in genes encoding CI subunits. In most cases, they were stop codon or frameshift mutations, known to disrupt the assembly of the multisubunit complex whose activity was found substantially reduced (Mayr et al., 2008; Simonnet et al., 2003; Zimmermann et al., 2011). For instance, while low heteroplasmy levels of a MT-ND5 mutation were observed in several cancer types (Brandon et al., 2006; Larman et al., 2012; Pereira et al., 2012), the homoplasmic variant was only found in oncocytic tumors (Gasparre et al., 2009). In this light, and given the low aggressiveness of oncocytic tumors, the potential anti-tumorigenic effect of CI loss ought to be further investigated.

The mitochondrial respiratory Complex I

The complex I within the respiratory chain

The mammalian CI (NADH:ubiquinone oxidoreductase) is the first and largest complex of the respiratory chain and is comprised of 45 subunits that are encoded by both nuclear and mitochondrial DNA (Hirst, 2013). Seven subunits are encoded by the mitochondrial genome and synthesized on mitochondrial ribosomes. The 38 remaining subunits are encoded by the nuclear genome and synthesized on cytoplasmic ribosomes (Koopman et al., 2009). CI has a L-shaped structure with one hydrophobic arm embedded into the inner membrane and one hydrophilic arm pointing into the matrix (Zhu et al., 2016) (Figure 7). The multi-subunit complex can be subdivided into three structurally and functionally defined modules: the N-module (NADH binding and oxidation), the Q-module (transfer of electrons to ubiquinone), and the P-module (proton pumping). The role of CI is to oxidize the NADH produced by mitochondrial dehydrogenases and malate aspartate shuttle (MAS), both dependent on TCA cycle and glycolytic flux rates. Flavin mononucleotides (FMN) mediate the electron transfer along a chain of FeS clusters to the terminal cluster and to ubiquinone (CoQ) that is consequently reduced to ubiquinol (QH_2). This process allows 4 protons to be pumped

from the mitochondrial matrix into the intermembrane space (IMS). QH_2 is subsequently oxidized in CoQ by complex III to reduce cytochrome c, concomitantly with the release of 4 additional protons into the IMS. Finally, complex IV uses cytochrome c to reduce molecular oxygen, the final electron acceptor, releasing 2 protons into the IMS (Figure 2B). The electrochemical proton gradient provided ultimately allows ATP production as the protons accumulated in the IMS flow back through the ATP synthase into the matrix of mitochondria (Nelson and Cox, 2017).

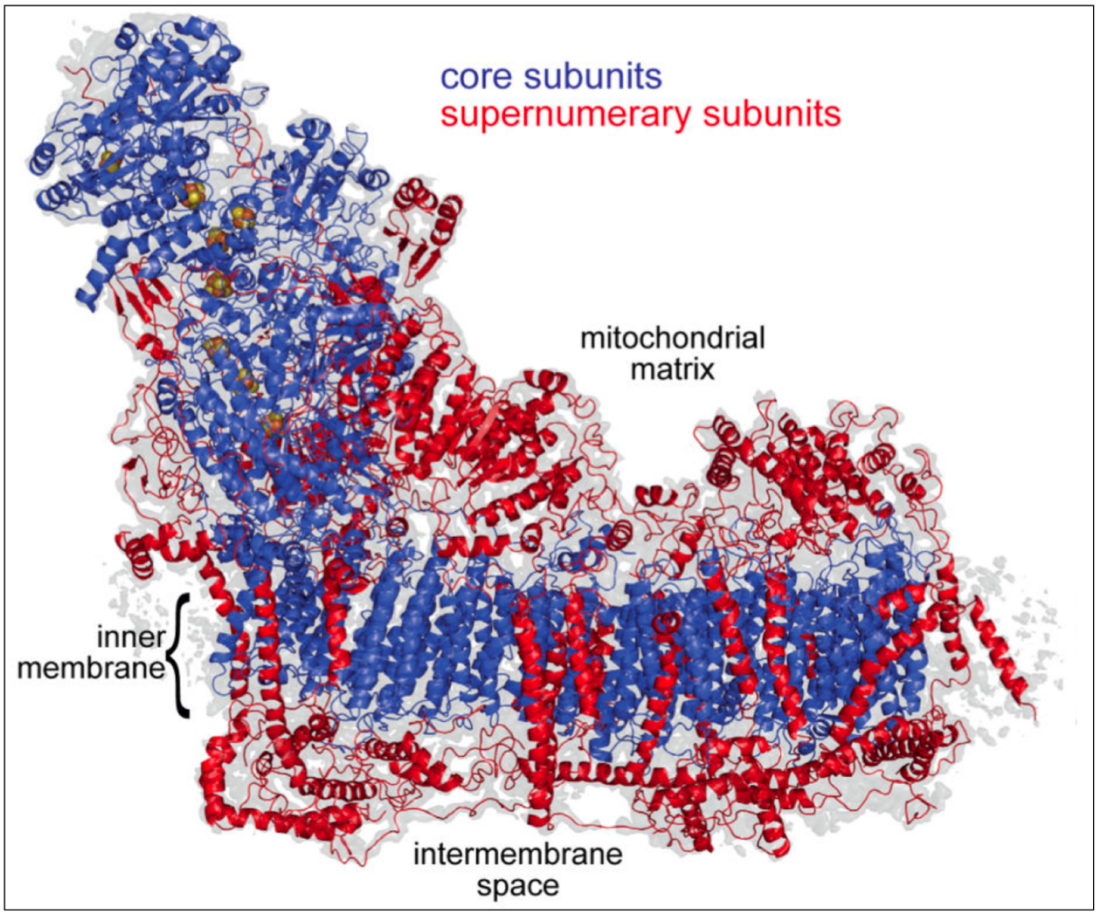

Figure 7: Structure of the mammalian respiratory complex I (Zhu et al., Nature, 2016)
Overview of the complex with 31 supernumerary subunits (in red) that are wrapped around a core of 14 subunits (in blue). FeS clusters are found in the hydrophilic arm (in yellow/orange).

Complex I assembly

Functional CI requires a multifaceted and coordinated process of assembly (Guerrero-Castillo et al., 2017) (Figure 8). Briefly, the assembly of the different modules are initiated separately. An 89 kDa complex containing the subunits NDUFS2 and NDUFS3, and the accessory subunit NDUFA5, is formed as a preliminary Q module, around which converge the remaining subunits of the Q module together with additional subunits of the proximal half of the P module (PP-module), to form a larger complex with predicted mass of 283 kDa.

The PP-module consists initially of 3 core subunits that bind 4 assembly factors, which subsequently accumulate 3 additional subunits and assembly factors. This 386 kDa complex subsequently bind a part of the distal half of the P module (PD-module), and then the entire Q module associated to the remaining subunits of the PP-module.

The PD-module arises from the assembly of two separate subcomplexes with predicted mass of 230 kDa and 154 kDa, with the first one originating from the accumulation of further subunits around a smaller complex of 53 kDa. The two blocks bind each other only after the 230 kDa subcomplex has combined with the large complex introduced above, containing both the PP and Q modules.

The N module is the last constituent of CI. It comprises 8 subunits, which arise from the initial convergence of two subcomplexes of two subunits, which subsequently bind a larger complex that comprises 4 subunits, together with the rest of the respiratory CI.

Studying CI assembly and its regulation is challenging, but it provides essential knowledge to understand genotype to phenotype correlation in disease, to provide diagnosis and to elaborate therapeutic strategy. On the other hand, studies point to the crucial role of specific subunits for CI architecture and function. Noticeably, NDUFS3 is of great interest. Not only this subunit is involved in the very early phases of CI assembly, but it is a core constituent of the Q module, at the interface between the P and N modules, and thereby between the hydrophilic and hydrophobic arms. In this light, the removal of NDUFS3 would most likely induce CI disassembly.

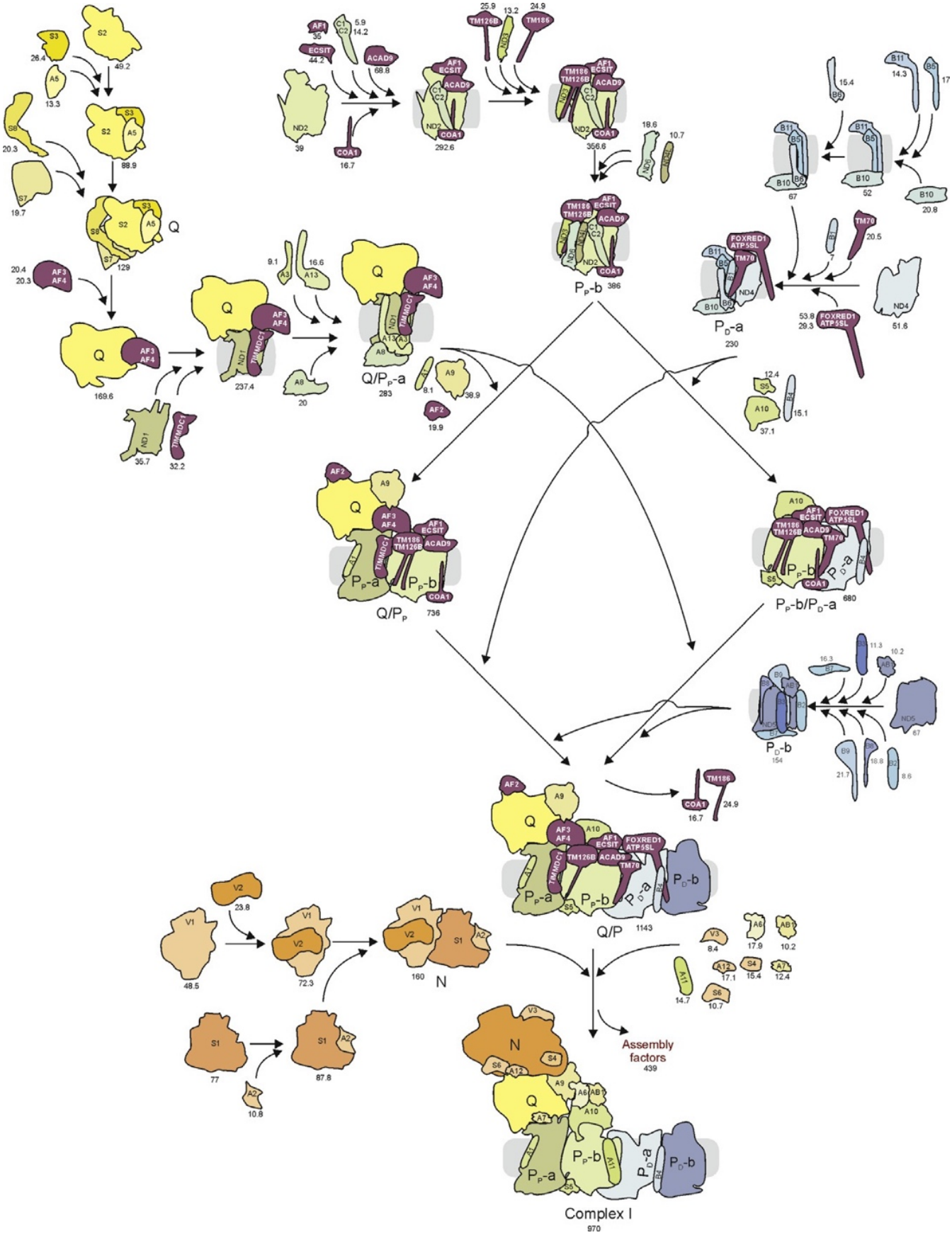

Figure 8: Comprehensive model of CI assembly (Guerrero-Castillo et al., 2017)

Complex I: a modulator of tumor progression

CI activity and dysfunctions are reflected on the cellular redox state, energetic status and intracellular oxygen levels, all impacting on tumor progression (Figure 9) (Vatrinet et al., 2015).

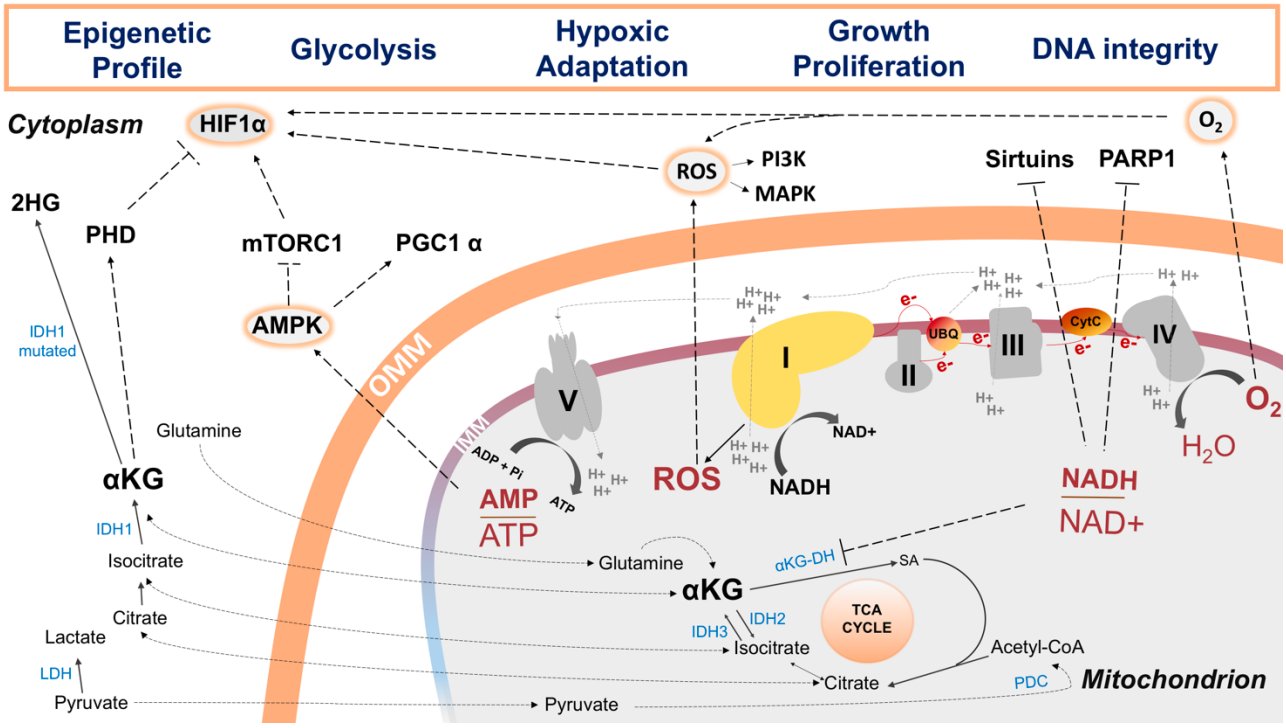

Figure 9: The mechanisms by which CI modulate tumor progression (adapted from Vatrinet et al., The IJBCB, 2015)

CI activity influences ROS levels, NADH/NAD$^+$ and AMP/ATP ratios, and oxygen and TCA metabolites levels. This scheme illustrates the crucial position of HIF1α, whose stabilization may be regulated by all the actors cited above. Besides, signalling pathways such as AMPK, PI3K, MAPK, Sirtuins and PARP1 may indirectly be regulated by CI function, thereby impacting on key mechanisms that drive cancer progression.

Complex I, ROS production and oxygen consumption

ROS are by-products of mitochondrial oxidative metabolism and, at physiological concentration, they are crucial for cell survival (Murphy, 2009). They include the superoxide anion ($O^{\cdot}{}_2^-$), hydrogen peroxide (H_2O_2), and the hydroxyl radical ($OH^{\cdot}$). The O_2 consumed (0.1- 0.5%) by mitochondria is converted into $O^{\cdot}{}_2^-$ (Giorgio et al., 2007), which is rapidly and spontaneously converted into H_2O_2 (Wang et al., 2008). In turn, ROS regulate several mechanisms essential for normal cell function such

as protein turnover, posttranscriptional modification of proteins, transcriptional regulation, and modifying redox-sensitive enzymes activity and protein interactions (Trachootham et al., 2008). In contrast, when a situation of oxidative stress is reached, H_2O_2 and $O^{\cdot}{}_2^-$ give rise to $OH^{\cdot}$, in presence of reduced transition metal (Murphy, 2009).

ROS levels are a reliable indicator of ETC damage and their overproduction may participate to cancer progression by inducing genomic instability, modifying gene expression and acting as regulatory molecules (Ray et al., 2012; Szatrowski and Nathan, 1991), or they may induce cell death when chronically oversupplied (Shen and Liu, 2006). The two main producers of $O^{\cdot}$ in mitochondria are the CI and the α-KGDC, which are also targets of ROS that inhibit both enzymes in a reversible manner. Importantly, CI and α-KGDC activity and ROS generation depend on the mitochondrial NAD^+/NADH ratio (Adam-Vizi and Chinopoulos, 2006), indicating a functional link between the two-enzymatic complex.

Importantly, hypoxia induces mitochondrial ROS production, which have been shown to participate to cell metabolic adaptation by promoting the HIF1 signalling pathway (Chandel et al., 1998). Although contradicting with the dependence of mitochondrial $O^{\cdot}{}_2^-$ production to oxygen concentration, it has been proposed that upon hypoxia, changes in $[NO^{\cdot}]$ may change the redox state of the cytochrome oxidase and therefore CIII response to low oxygen levels, thereby increasing H_2O_2 production. In fact, loss of cytochrome c or Rieske FeS center of CIII eliminates ROS generation (Guzy et al., 2005). Other mechanisms through which hypoxia increases H_2O_2 production have been proposed, such as through cell signalling pathway, but further investigation are needed to clarify the phenomenon (Murphy, 2009). In turn, several processes through which ROS mediate HIF1 activation have been described. On the one hand, H_2O_2 may induce the conversion of Fe^{2+}, substrate of the PHDs, into Fe^{3+}, thereby inactivating the dioxygenases and resulting in HIF1α stabilization (Pouysségur and Mechta-Grigoriou, 2006). On the other hand, ROS may promote several signalling pathways, such as PI3K/Akt and p38 MAPK, which all may inactivate PHDs (Emerling et al., 2005; Mottet et al., 2003).

Recent studies suggest that the role of CI in the interplay between ROS and HIF1 is essential for the hypoxic response. While CI may promote ETC activity and thereby ROS promotion under hypoxia, HIF1 has instead been shown to promote the expression of NDUFA4L2, subunit of the CI, thus reducing the activity of the enzymatic complex and thereby lowering ROS production in hepatocellular carcinoma cell lines. Contrariwise, inactivation of the HIF1/NDUFA4L2 axis resulted in ROS accumulation and apoptosis (Lai et al., 2016). The importance of this CI subunit in coordinating the hypoxic response has been discovered only very recently (Tello et al., 2011). In 2016, four separate studies have identified NDUFA4L2 as a marker of poor prognosis in cancer patients (Lai et al., 2016; Liu et al., 2016; Lv et al., 2016; Minton et al., 2016).

Hence, CI plays a pro-active role in the multiple ROS-mediated mechanisms of cancer cells. Importantly, while mild CI dysfunction may induce a severe oxidative stress and contribute to tumor progression and metastasis (Ishikawa et al., 2008; Sharma et al., 2011), strong CI impairment may instead not be associated to a significant increase in ROS production, due to the lack of the FMN sites where ROS are generated (Gasparre et al., 2011b; Iommarini et al., 2014).

Additionally, increased evidences point to mitochondrial oxygen consumption as an additional potent modulator of tumor progression. Indeed, the concentration of oxygen in cells does not only depend on its delivery, and therefore on extracellular oxygen levels, but it is also defined by the rate of its conversion into H_2O by CIII, and therefore by ETC activity. Oxygen is a signalling molecule, as it influences the activity of several oxygenases, including the Fe(II)/αKG-dependent dioxygenases (Loenarz and Schofield, 2008). Inhibiting CI may reduce HIF1α stabilization in hypoxia by increasing oxygen tension and promoting PHDs activity (Bastian et al., 2017). Further, several studies have shown that decreased oxygen consumption impairs the hypoxia-mediated resistance to radiotherapy of cancer cells (Gallez et al., 2017). In line with this, inhibiting CI has been shown to improve the oxygenations of tumors and therefore their radiosensitivity (Zannella et al., 2013).

Complex I and the cellular energetic status

Increasing evidence shows that cellular energetic crisis may impact on cancer progression. Given the pivotal role of CI in ETC function, defects in the enzyme activity are likely to affect cancer cells energetic status and metabolism, narrowing the possibilities of nutrient utilization for ATP production. As a matter of fact, cells with mitochondrial dysfunction are more sensitive to low glucose conditions and calorie restriction, and combination of complex I inhibition and glucose deprivation might be selectively lethal for cancer cells (Agarwal et al., 2016; Bikas et al., 2015; Birsoy et al., 2014; Guo et al., 2011; Morscher et al., 2015). Energetic crisis is translated to cells through the energy sensor AMP activated kinase (AMPK), which inhibits biosynthetic pathways and supports catabolic events in order to restore intracellular energetic balance (Hardie et al., 2012). We recently showed that CI-defective cancer cells displayed a clear-cut increase in AMP/ATP ratio and AMPK activation under metabolic stress conditions (Iommarini et al., 2014). It has been shown that AMPK activation represses mTORC1 signalling, thereby preventing cell growth and proliferation, and suppressing HIF1α translation (Faubert et al., 2013). Consistent with this, lack of AMPK enhanced glycolysis in a HIF1-dependent mechanism, suggesting that AMPK acts as a tumor suppressor by repressing HIF1-signalling (Faubert et al., 2013).

Complex I and the NAD^+/NADH ratio

The NAD^+/NADH ratio regulates several metabolic routes and signalling pathways that greatly impact on cancer progression. Importantly, cancer cells may exhibit a dependency on metabolic pathways regulated by NAD^+ (Gui et al., 2016; van Horssen et al., 2013). Recently, studies have demonstrated that an essential role of the respiratory chain is indeed to transfer electrons from NADH to oxygen, thereby maintaining an adequate redox state that allows aspartate synthesis and therefore cancer proliferation (Birsoy et al., 2015; Sullivan et al., 2015). In line with this, the NADH/NAD^+ ratio would correlate with tumor growth *in vivo* (Gui et al., 2016). In this light, lower CI-mediated NADH oxidation may negatively affect cancer cell proliferation. Accordingly, Vander Heiden's

group showed that the effects of CI inhibition on the tumorigenic potential of various cancer cells may depend on their reliance on NAD+ synthesis and aspartate production. These metabolic exigencies may vary broadly with environment changes, which would therefore determine cancer cells sensitivity to CI inhibition (Gui et al., 2016).

Conversely, it has been shown that maintaining a minimal concentration of NADH is essential for reductive carboxylation to operate. This is explained by the requirement of cancer cells with respiratory defects to transfer reducing equivalent from NADH to NADPH, a reducing agent that subsequently drive citrate production from α-KG, thereby maintaining cell proliferation (Mullen et al., 2014).

Further, an unbalanced NADH/NAD^+ ratio may also affect Sirtuins (SIRTs)-dependent signalling pathway and the poly (ADP ribose) polymerase 1 (PARP1) control of DNA integrity and cell proliferation (Chiarugi et al., 2012). The role of PARP in promoting tumor progression is well known, as it sustains aberrant DNA repair mechanism (Davar et al., 2012), and five PARP inhibitors are now in late-stage development in clinical trials (Dulaney et al., 2017). In contrast, although all the seven Sirtuins (SIRT1-7) have been shown to be involved in cancer, their precise roles and influences on tumor progression ought to be clarified (George and Ahmad, 2016). While SIRT1 overexpression reduces the formation of carcinomas and sarcomas (Herranz and Serrano, 2010), it has also been found highly expressed in other cancers (Yuan et al., 2013a), where it would promote carcinogenesis and resistance to chemotherapy (Herranz and Serrano, 2010; Liang et al., 2008). Mitochondrial SIRT3 and SIRT5 have also been found overexpressed in different cancer types (Alhazzazi et al., 2011a, 2011b; Lu et al., 2014). Nevertheless, the latter were also shown to be down-regulated in other tumors (Lai et al., 2013; Yang et al., 2014), where they might act as tumor suppressors by regulating ROS production and hypoxic response (Finley et al., 2011). SIRT4 would instead act exclusively as a tumor suppressor by restricting glutamine utilization and repressing Myc-induced B cells lymphomagenesis (Jeong et al., 2016).

Lastly, variations of the NADH/NAD^+ ratio directly influence TCA fluxes and metabolites levels.

NADH allosterically regulates the activity of the TCA cycle checkpoints pyruvate dehydrogenase complex (PDC), IDH 3, and α-KGDC. In respiration-defective cancer cells, the accumulation of NADH may inhibit these enzymes while promoting the activity of the NADPH-dependant IDH1/2, consequently fostering the reductive carboxylation of α-KG. Increase in cellular NADH levels may also promote the activity of the MDH 1 and 2, the phosphoglycerate dehydrogenase and LDHA. In this context, the latter enzymes may consume rather than produce NADH, together with converting the accumulating α-KG into L-2HG, hence re-equilibrating cellular redox state and shaping signalling pathways to adapt both cell metabolic and epigenetic landscape (Vatrinet et al., 2017). Accordingly, NADH accumulation may lead to an increase in cytosolic α-KG levels through α-KGDC inhibition. In this frame, our group has shown that CI-defective cancer cells displayed an unbalanced NAD^+/NADH ratio together with an accumulation of α-KG, associated to a constitutive destabilization of HIF1α (Calabrese et al., 2013; Gasparre et al., 2011b; Iommarini et al., 2014) (Figure 10). These cells were unable to enhance the glycolytic machinery during hypoxia and displayed a lower tumorigenic potential *in vitro* and *in vivo* compared to CI competent cancer cells (Calabrese et al., 2013).

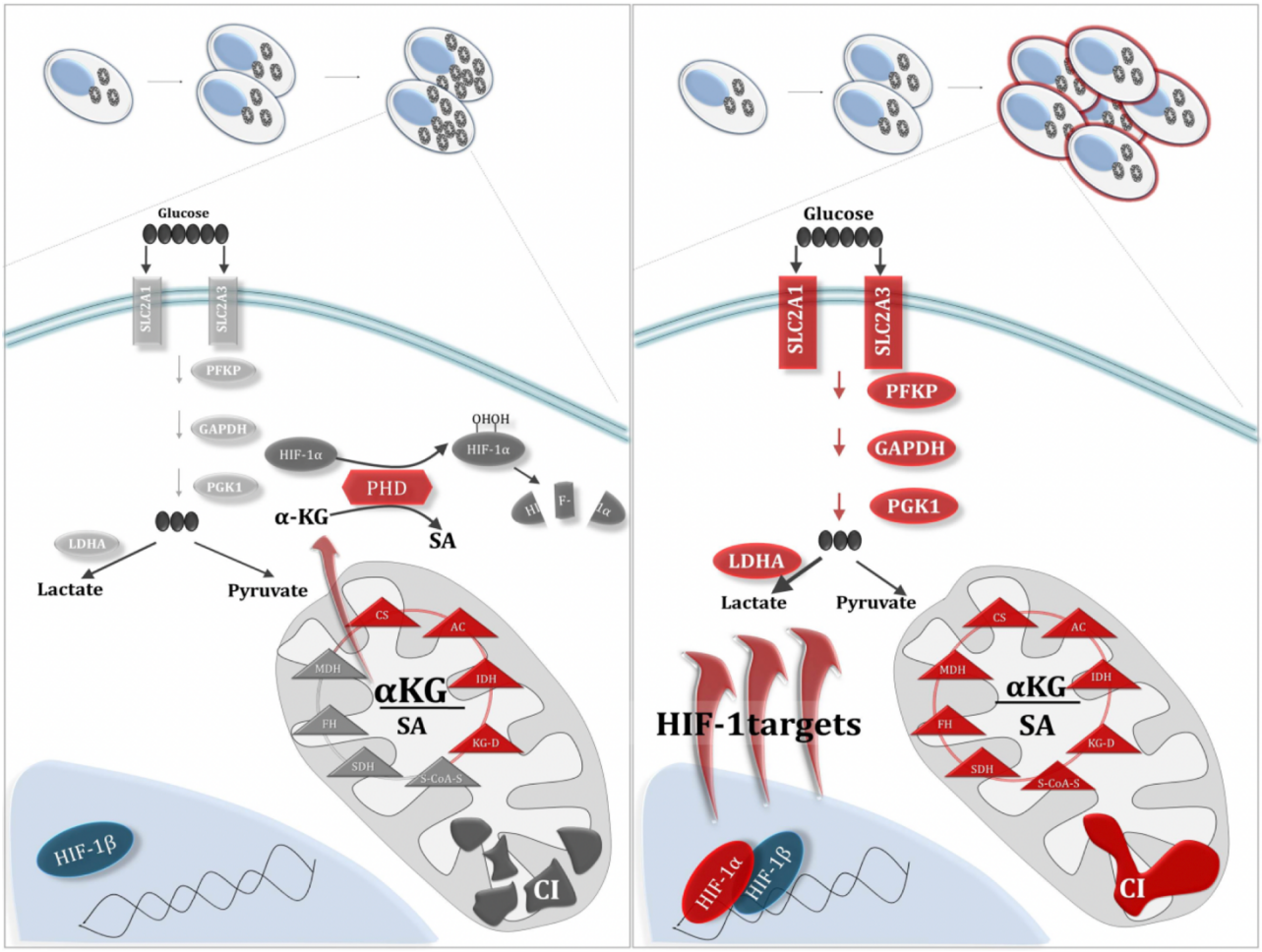

Figure 10: Metabolic changes in the absence/recovery of functional CI in cancer cells (Calabrese et al., 2013)

The increase in the α-KG/SA ratio that is associated to the lack of CI may foster the activity of the PHD, hence destabilizing HIF1α (left panel). Inactivation of HIF1α prevents the upregulation of the glycolytic machinery normally requested to compensate for the defective mitochondrial respiration. This scenario may not allow the metabolic adaptation of tumor cells, possibly inducing a short-circuited mitochondrial compensatory proliferation. CI rescue recovers NADH consumption and therefore the α-KG/SA balance (right panel). In this scenario, HIF1α remains stabilized and may therefore translocate into the nucleus where it dimerizes with HIF-1β and activate transcription of target genes (red ovals and rectangles), among which those contributing to increase the glycolytic flux. Red elements indicate activation or overexpression.

Hence, CI might affect tumorigenesis and cancer progression through different mechanisms. Modulating CI activity influences ROS production, oxygen consumption rate, NADH levels and usage, ATP generation, metabolic pathways utilization, and the amount of signalling metabolites. Various degrees of CI dysfunctions have been shown to differently affect tumor progression (Iommarini et al., 2014; Park et al., 2009). Accordingly, not all nDNA-encoded CI core subunits

defects have equal prognostic significance and may instead have opposite effects (Ellinger et al., 2016; Su et al., 2016). Furthermore, beside the severity of CI impairment, the effect may also be context dependant. In fact, although loss of CI is associated to low-tumorigenic potential (Calabrese et al., 2013), it might help SDH-mutant tumors to survive by promoting glutamine metabolism (Lorendeau et al., 2016). This recent study further accentuates the oncojanus role of CI as previously defined by our group (Gasparre et al., 2011b). Overall, considering the essential role of CI in controlling metabolism, hypoxic adaptation and cell proliferation, this enzyme may be envisioned as a target for the development of new adjuvant anticancer therapies.

Targeting Complex I

Pharmacological compound

Several compounds affecting CI have been studied as anticancer drugs (Table 1). The plant alkaloid rotenone, piericidin A and capsaicin are specific inhibitors of CI and have been shown to be selectively cytotoxic for cancer cells (Palorini et al., 2013). More recently, biguanides have been recognized as a new class of CI inhibitors. These antihyperglycemic agents prevent ubiquinone reduction in a non-competitive manner, thereby stimulating ROS production (Bridges et al., 2014). Metformin is the most-known biguanide as it is the first line medication for the treatment of diabetes mellitus. Interestingly, clinical studies revealed a potential anti-neoplastic effect of the drug, the therapies being associated with lower risk for patient to develop cancer (Becker et al., 2014; Evans et al., 2005). However, these effects are still debated and warrant more investigation (Farmer et al., 2016). Notwithstanding this, following the great surge of interest in biguanides, several *in vitro* and *in vivo* studies have been conducted and have provided a body of evidence for metformin-mediated anti-neoplastic effects (Andrzejewski et al., 2014; Wheaton et al., 2014). Upon glucose starvation, cancer cells were found to be more sensitive to biguanides-mediated inhibition of CI (Birsoy et al., 2014). Accordingly, metformin, in combination with the glycolysis inhibitor 2-deoxyglucose, has been shown to induce cell death *in vitro*, AMPK activation, and it decreased the growth of several

xenografts models (Cheong et al., 2011). Metformin has also been shown to inhibit mitochondrial-dependent biosynthetic processes in cancer cells (Griss et al., 2015).

Inhibitor	Family	Mechanisms of action	References
Rotenone (II/B)	Rotenoids	- Induces cell death in association with glucose starvation - Synergistic effect with Forskolin	Palorini et al., 2013; Wheaton et al., 2014
Piericin A (I/A)	Piericidins	- Induces cell death in association with glucose starvation - Synergistic effect with Forskolin	Hwang et al., 2008; Palorini et al., 2013
Capsaicin (C)	Vanilloids	- Induces cell death in association with glucose starvation - Synergistic effect with Forskolin - Stimulates ROS production and promotes apoptosis	Pramanik et al., 2011; Palorini et al., 2013
Rolliniastatin-1 (I/A)	Annonaceus acetogenins	- Induces the mitochondrial apoptotic pathway	de Pedro et al., 2013
Metformin	Biguanides	- Reduces HIF1α stabilization under hypoxia - Activates AMPK pathway - Modulates IGF pathway	Wheaton et al., 2014; Andrzejewski et al., 2014; Birsoy et al., 2014
Phenformin	Biguanides	- Reduces HIF1α stabilization under hypoxia - Activates AMPK pathway - Modulates IGF pathway	Wheaton et al., 2014; Birsoy et al., 2014
Canagliflozin	Gliflozin	- Reduces ATP production - Activates AMPK pathway - Reduces cell proliferation and clonogenicity	Villani et al., 2016
BAY 87-2243	Aminoalkyl pyrimidine	- Inhibits oxygen consumption - Decreases HIF1 activation - Increases ROS generation - Reduces ATP production - Activates AMPK pathway	Ellinghaus et al., 2013; Helbig et al., 2014; Schokel et al., 2015
AG311	Pyrimidoindoles	- Inhibits oxygen consumption - Decreases HIF1 activation - Decreases metastatic potential	Bastian et al., 2016
ME-344	Isoflavonoids	- Induces cell death and inhibits tumor proliferation and metastasis	Lim et al., 2015
JCI-20679	Annonaceus acetogenins	- Inhibits cancer cell proliferation	Akatsuka et al., 2016

Table 1: Respiratory complex I inhibitors used as anticancer molecules.

Furthermore, both metformin and phenformin may synergize BRAF inhibitors to most effectively decrease the proliferation of BRAF-mutated melanoma cell lines (Niehr et al., 2011; Yuan et al., 2013b). Similarly, combination of metformin and the chemotherapeutic agent doxorubicin induce cancer cell death more efficiently than either drug alone and prevent tumor relapse *in vivo* (Hirsch et al., 2009).

Therefore, metformin, in combination with anti-proliferative or anti-glycolytic drugs, may be an effective adjuvant anti-cancer therapeutic. Nevertheless, it is important to note that beside CI inhibition, several other signalling pathways may be responsible for the anti-tumorigenic effects induced by metformin, which displays only very low specificity for the respiratory complex (Bridges et al., 2014; Lei et al., 2017).

Many other pharmacological compounds have been recently developed (Table 1). Another anti-diabetic drug, Canagliflozin, has also been studied as anticancer agent. Canagliflozin has been shown to inhibit complex I, to decrease glucose uptake and ATP production, and to activate AMPK in prostate and lung cancer cells. Treatment with this drug decreased cells proliferation and clonogenicity *in vitro* (Villani et al., 2016). On another hand, BAY-87-2243 has been shown to decrease mitochondrial oxygen consumption, to increase ROS generation, to reduce ATP production and to activate AMPK, and this was associated to a reduction of cancer cell survival *in vitro*. Furthermore, the molecule decreased hypoxia and HIF1 activation in melanoma mouse xenografts and sensitized them to radiation therapy (Helbig et al., 2014; Schöckel et al., 2015). Similarly, AG311, a compound that has been shown to exert anticancer and anti-metastatic activity, inhibits complex I and thereby oxygen consumption and HIF1 activation (Bastian et al., 2017). Isoflavonoids are instead mild CI and CIII inhibitors but induce the destabilization of the OXPHOS complexes upon long term treatment. In particular, the synthetic isoflavan analogue ME-344 induce cell death and inhibit tumor proliferation and metastasis (Lim et al., 2015). Finally, JCI-20679 is an additional CI inhibitor that has been shown to inhibit cancer cell growth (Akatsuka et al., 2016).

Development of CI inhibitors is thus in full swing in cancer research. Nonetheless, given the adverse

effects and the wide-spread response of the compounds, the mechanisms underlying the anti-tumorigenic effects observed upon suppression of CI activity are still poorly understood and ought to be further dissected. For that purpose, an accurate and specific targeting of the multisubunit complex in cancer cells is required.

Zinc finger nucleases technology as a useful tool for CI activity suppression

Gene inactivation is a powerful way to provide conclusive information on its function. This approach is referred to as reverse genetics and can be summarize as a "from gene to phenotype" approach, in contrast with "forward genetic", which aims at identifying the genetic cause of a specific phenotype. For instance, the latter approach has demonstrated that the oncocytic phenotype may likely arise from severe CI mutations. Knocking out CI in cancer cells would instead provide important insights on the role of this enzymatic complex in cancer progression, *via* phenotypic analysis. The reverse genetics strategy has first been possible with the emergence of recombinant DNA (rDNA) technology in the 70's, and has enabled remarkable advances in biological and medical sciences (Capecchi, 2005). Yet, this technique was far from being affordable for any research laboratories. rDNA technology showed low efficiency and required the development of time-consuming selection/screening strategies. Moreover, the occurrence of adverse mutagenic effects was common (Gaj et al., 2013).

In the past 15 years, the emergence of the zinc finger nucleases (ZFNs), transcription activator-like effector nucleases (TALENs) and CRISPR/Cas technologies has sparked a second revolution that has further extended the frontiers of biological research. They all consist in non-specific engineered nucleases that are fused to investigator-designed DNA binding domains that can virtually recognize any sequence in any genome. These new genome-editing tools were rapidly assimilated and utilized by the whole research community, by means of their ever-higher simplicity and efficiency in inducing site-directed mutagenesis.

The ZFNs were the first engineered molecular scissors that hit the scene (Figure 11). Zinc finger proteins (ZFPs) are the most common DNA binding domains found in eukaryotes, being involved in

many functions such as transcription processes. One zinc finger domain can recognize three DNA base pairs (bps) *via* an α-helix (Figure 11).

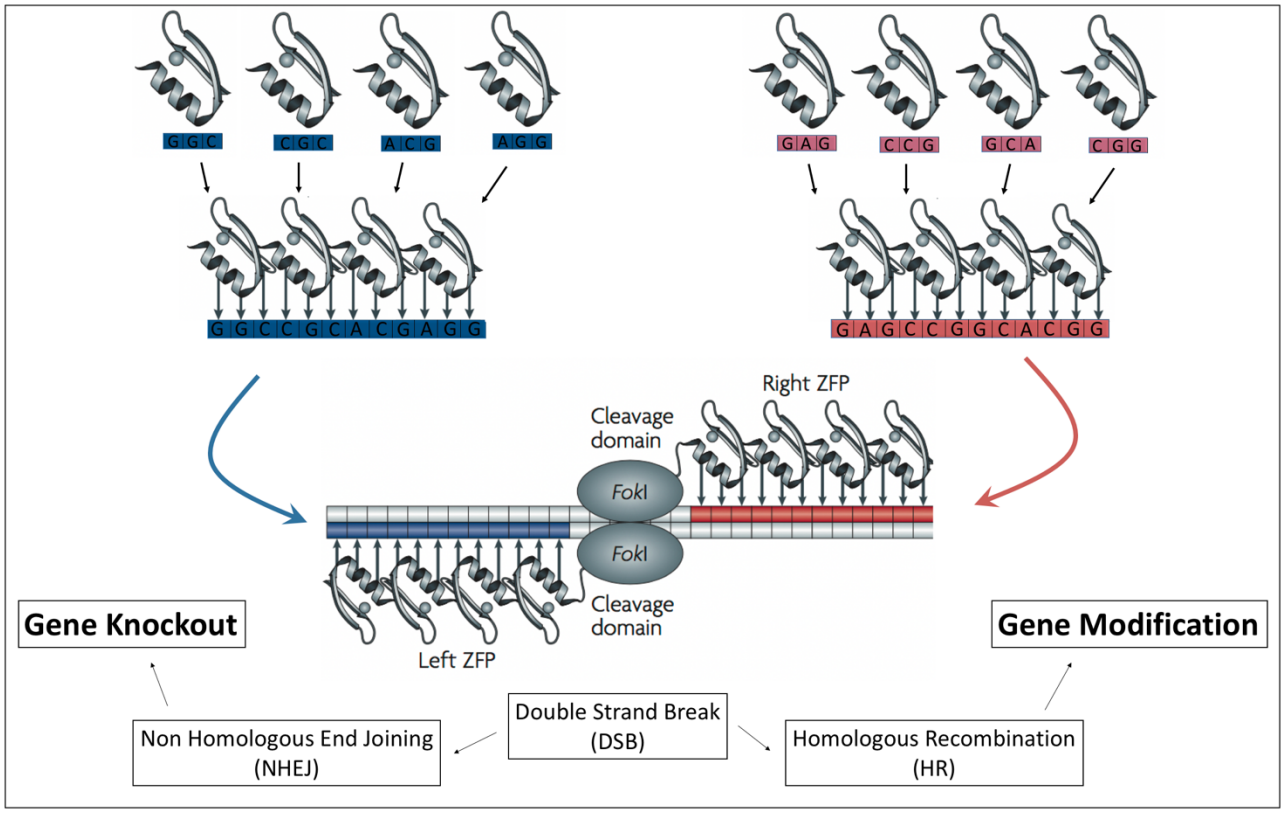

Figure 11: Structure and design of zinc finger nucleases
One zinc finger protein (ZFP) can recognize 3 DNA base pairs and several ZFPs are used to specifically recognize a DNA sequence in the genome. ZFPs are fused to FokI restriction enzymes. The latter can catalyse a DNA double strand break (DSB) only when they dimerize. DSBs can be repaired by Non-Homologous End Joining (NHEJ) or Homologous Recombination (HR). NHEJ is utilized to insert mutations that may prevent the production of the functional protein. HR is utilized when a specific sequence should be inserted.

Three clustered domains are frequently found associated and enable the zinc finger proteins to recognize a set of 9 bps, with different levels of selectivity. Conversely, engineered ZFPs have been designed to bind up to 18 bps of a DNA sequence, by means of 6 zinc finger domains, thereby conferring a specificity within 68 billion bps of DNA (Gaj et al., 2013). ZFPs are fused with the nuclease domain of the Fok1 restriction enzyme. The latter was of great interest since it must dimerize to cleave DNA. Hence a double strand break (DSB) can be induced only upon two adjacent and independent binding events, with correct orientation and appropriate spicing to allow the formation

of the dimer (Urnov et al., 2010). These conditions greatly favour ZFNs site-specificity together with reducing off-target effects.

Once a DSB has been introduced at the locus of interest, cells can repair it via homology-directed repair (HDR) or non-homologous end joining (NHEJ) pathway. HDR canonically utilizes the homologous sequence of a paired chromosome as a template to correctly repair the harmful break. Taking advantage of this, the DNA repair processes may therefore be driven by the addition of a user-specified donor DNA, which is usually aimed at correcting a mutation or inserting a new gene. Conversely, the NHEJ pathway rapidly ligates the two broken ends, a process which occasionally introduces small insertions/deletions. The latter is therefore exploited as a strategy towards gene disruption, as the mutations may introduce a frameshift that prevents the production of the protein.

Nowadays, ZFN technology has been largely replaced by the CRIPR/cas system, far more attractive for its specificity, cost and ease of use.

AIMS

Prior to the present work, ours and other groups have shown that severe CI dysfunctions can be disadvantageous to tumor growth by negatively impacting on tumors metabolic adaptation to hypoxia, therefore disclosing this enzyme as a potential target for cancer therapy. These studies were performed on oncocytomas samples harbouring CI-disruptive mtDNA mutations, and on cancer cybrid models, where the load of the latter mutations could be monitored. The pseudonormoxic feature of CI-deficient cancer cells evidenced a two-way relationship between mitochondria and the transcription factor HIF1α, whose stabilization requires CI activity. However, the mechanism underlying HIF1α destabilization in CI-deficient cancer cells remained to be demonstrated. Further, whether the latter was the primary cause of the low tumorigenic profile observed was still unclear.

This study aims at mimicking the effects of severe CI-disruptive mtDNA mutations in cancer cells. For this purpose, the ZFN technology is utilized to create stable cancer cell models lacking CI. The former approach will permit to dissect the biochemical and metabolic profiles of CI-deficient cancer cells, together with identifying the molecular actors that drive HIF1α destabilization. Moreover, the genetic stability provided by such a tool prevents any genetic drift otherwise triggered when studying mtDNA mutations. In this light, *in vivo* studies will provide important insights on the effect of CI irreversible loss on tumor growth and progression. A proof of concept study will further confirm the results obtained by re-inserting NDUFS3 in CI-deficient cancer cells. Conversely, the effect of CI loss during tumor progression will be investigated by suppressing NDUFS3 expression while CI-competent xenografts have already reached advanced development stage.

Lastly, this work is expected to establish the backbone of a more complex investigation that will help to further confirm the pivotal role of HIF1α loss in preventing tumor growth, while discriminating the relative significance of CI disruption in carcinogenesis and cancer progression.

EXPERIMENTAL PROCEDURES

Genome editing

Plasmids containing cDNA of *NDUFS3*-targeted zinc finger endonucleases were purchased from Sigma-Aldrich and used following the manufacturer's instructions. The plasmids were purified and transcribed in vitro using MessageMax caping kit (Cell Script), Poly adenylation kit (Epicentre) and purified using MegaClear kit (Life Technologies). The pool of zinc finger endonucleases mRNAs (2.5ug each) was transfected using Transit-mRNA transfection kit (Mirus) into 70% confluent cells. Cells were split 48 hours after transfection and DNA was extracted using Mammalian Genomic DNA Miniprep Kit (Sigma-Aldrich). Non-homologous repair efficiency was evaluated by Fluorescent PCR using KAPA2G taq polymerase (Kapa Biosystems) with 58°C annealing and primers forward CTGCCACAAGGAGCTAGGAC and reverse GCACAGGGAGATAAAAGGCA. Clonal selection was performed in order to identify the cells with frameshift *NDFUS3* mutations (Figure 12). Selection media used for the growth in 96-well plates was composed of DMEM High glucose supplemented as described below with subsequent modifications: 20% FBS, L-Tryptophan (32mg/l, Sigma-Aldrich) and Nicotinamide (8mg/l, Sigma-Aldrich). Genotyping was performed after DNA extraction from 96-well plates using 8µl of Lysis Solution (Sigma-Aldrich) and 80µl of Neutralization Buffer (Sigma-Aldrich) per sample. Heterozygous clones were first expanded and a subsequent second transfection with NDUFS3 zinc finger pool was performed as described above. This step led to the selection of homozygous frameshift *NDUFS3* mutants and homozygous wild-type (WT) revertants. The latter were used as controls in all experiments described here. Three clones per genotype were obtained for 143B and two for HCT116 cells. *NDUFS3* genotype was confirmed by Sanger sequencing using KAPA2G taq polymerase (Kapa Biosystems) and Big Dye protocol (Life Technologies).

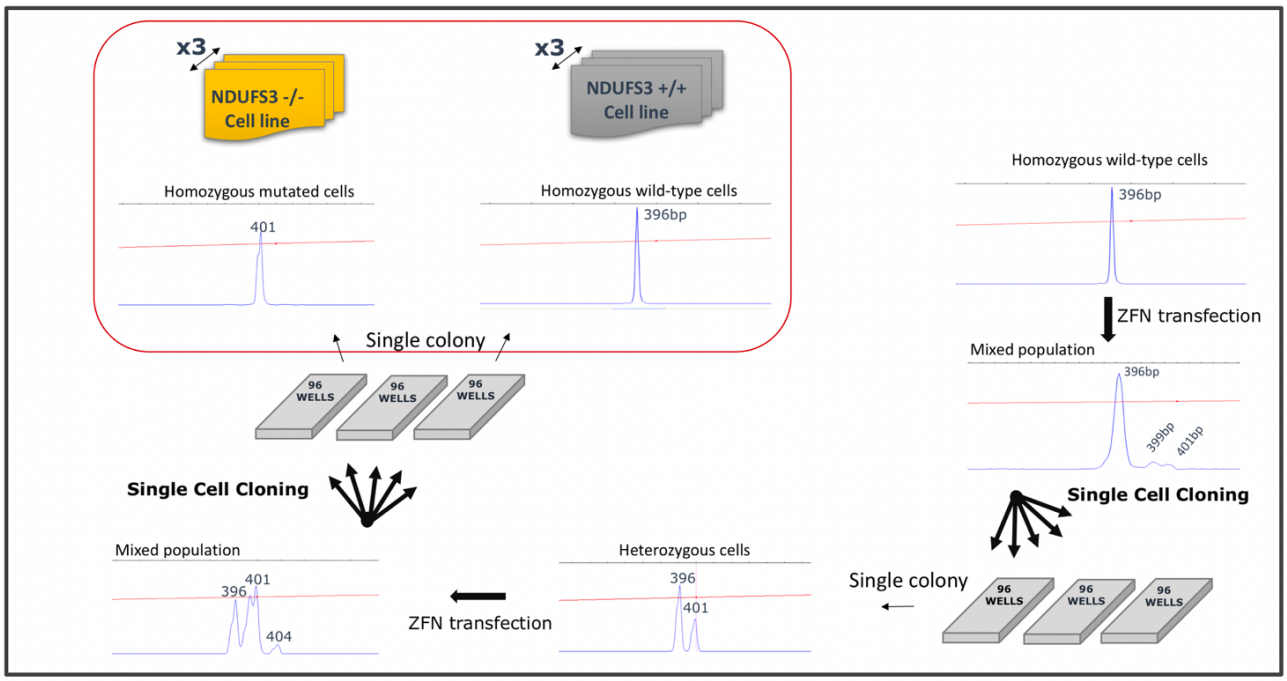

Figure 12: Illustration of the cell selection procedure

Blue pics are F-PCR results for a selected population of cells. The horizontal position of the pic is defined by the length of the PCR-amplicon while its height is proportional to the number of amplicons at this specific length, hence representative of the number of alleles bearing one, two or no mutation in the given population of cells analysed. Briefly, after a first transcription with the ZFNs, a population of cells bearing potential interesting mutations is obtained (i.e. 5 insertions). Single cells are distributed in each well of three 96 well plates. F-PCR on the colonies obtained allowed to isolate a population of cancer cells whose one NDUFS3 allele presented with 5 insertions. These cells were transfected again with the ZFNs. A second screening has led to the isolation of cells with two alleles with frameshift mutations and cells that have reverted the mutations and are therefore NDUFS3 wild type.

Cell culture

Osteosarcoma 143B Tk$^-$ cells and colorectal cancer HCT116 cells were cultivated in Dulbecco's modified Eagle medium (DMEM) High Glucose (Euroclone), supplemented with 10% fetal bovine serum (Euroclone), L-glutamine (2mM, Euroclone), penicillin/streptomycin (Euroclone) and uridine (50µg/ml, Sigma-Aldrich), in an incubator with a humidified atmosphere at 5% CO_2 and 37°C. Cells were replaced by a fresh batch upon 15 passages and mycoplasma testing was performed before disposal and after each thawing (approximately every two months). Experiments in hypoxia were performed inside the Invivo2 300 (Baker Ruskinn) chamber, set up at 5%CO_2, 37°C and 1% O_2. Where indicated, cells were incubated for 5 hours with dimethyloxalylglycine [DMOG (1mM),

Sigma-Aldrich] or MG132 (10μM, Sigma-Aldrich) and 1 hour with pimonidazole (100μM, Hypoxiprobe) at indicated concentrations. Cell origin was authenticated using AMPFISTRIdentifiler kit (Applied Biosystems).

SDS-PAGE and Western blot analysis

Whole lysates of cultured cells and freshly snap frozen xenograft samples were prepared in RIPA buffer [TrisHCl pH7.4 (50mM), NaCl (150mM), SDS (1%), Triton (1%), EDTA pH7.6 (1mM)] supplemented with protease inhibitors (Roche) and quantified by Lowry protein assay (Biorad). Samples were separated by SDS-PAGE and transferred to the nitrocellulose membrane using Turbo-pack system (Biorad). The membranes were blocked 30 minutes at 37°C and incubated with primary antibodies using following dilutions/conditions: anti-NDUFS3 (Abcam) 1:1000/1 hour at room temperature (RT); anti-HIF1a (GeneTex) 1:2000/1 hour at RT; anti-Vinculin (Sigma-Aldrich) 1:10000/1-hour at RT; anti-pimonidazole (Hydroxyprobe) 1:3000/2 hours at 37°C; anti-HIF2a (Novus Biologicals) 1:1000/1 hour at RT, anti-HIF1a-OH (Cell Signalling) 1:500/O/N at 4°C. Washes were performed 4 x 5 minutes using TBS-Tween [0.1% Tween 20 (Sigma-Aldrich) in Tris Buffered Saline] and incubation with secondary antibodies (Jackson ImmunoResearch Laboratories), diluted 1:20000 in TBS-Tween, was performed for 30 minutes at RT. Developing was performed by using Clarity Western ECL Substrate (Biorad) and exposing with ChemiDoc XRS+ (Biorad). For anti-HIF1α-OH, anti-phospho-AKT and anti-phospho-ERK antibodies Western Breeze system (Life Technologies) was used in terms of secondary antibody and developing solutions, following the manufacturer's instructions.

Mitochondrial isolation

Crude mitochondria were obtained by $15x10^6$ cells. Cells were suspended in cold isolation buffer containing 200 mM D-Mannitol, 70 mM Sucrose, 1 mM EGTA, 10 mM HEPES, pH 7.6, with protease inhibitor cocktail (Roche) and mechanically homogenized with 50 strokes using a glass-teflon potter in melting ice. Unbroken cells and nuclei were centrifuged at 3000 rpm for 10 minutes at 4°C, and the supernatant, containing mitochondria, was centrifuged at 13000 rpm for 20 minutes at 4°C. The mitochondrial pellet was suspended with cold isolation buffer and stored at -80°C. Protein content was quantified according to Bradford's protocol (Bradford, 1976).

Membrane fractions enriched of mitochondrial proteins (mitoplasts) were isolated from cell pellets ($10x10^6$ cells) using digitonin (final concentration 50 µg/mL). Digitonin binds to membrane cholesterol, destabilizing and solubilizing the cellular membranes. The inner membrane, unlike the outer membrane, is almost devoid of cholesterol, therefore digitonin solubilizes cellular membranes, except the inner membrane, which remaining intact can be isolated. Briefly, cells were centrifuged and pellet suspended at a concentration of $10x10^6$ cells/mL with cold PBS (154 mM NaCl, 1 mM KH_2PO_4, 3 mM Na_2HPO_4), and after addition of digitonin, incubated on ice for 1 minute. Cold PBS was then added to 2.5- fold dilute the suspension volume, thus interrupting cell permeabilization. The digitonin treatment was repeated until at least 90% of the cells were permeabilized, as detected at the microscope by Trypan blue cell permeabilization. Cells were then centrifuged at 13000 rpm for 15 minutes at 4°C and the pellet was stored at -80°C. Protein content was quantified according to Bradford (Bradford, 1976).

CN-PAGE

Complex I was separated through Clear Native PAGE (CN-PAGE) (Wittig et al., 2006). Cells were resuspended at 10^7 cells/ml in PBS, permeabilized with 50 µg/ml digitonin, centrifuged at 13000 rpm for 10 minutes and the mitochondrial pellet was stored at -80°C. The day after it was resuspended in mitochondrial buffer (750 mM 6-aminocaproic acid, ACA; 50 mM BisTris, pH 7.0), the proteins

quantified and DDM (n-Dodecyl β-D-maltoside) added at 2,5-fold the protein quantity. Afterwards samples were incubated in ice for 10 minutes and then centrifuged at 13000 rpm for 15 minutes at 4°C. The supernatant containing the mitochondrial proteins was then recovered and proteins quantified. The supernatant collected was diluted in CN-Sample Buffer (0.1% Red Ponceaux and 50% Glycerol). 50 μg of mitochondrial protein samples were loaded onto a native gel constituted by a gradient of polyacrylamide from 4% to 12%, made with a gradient building machinery and a peristaltic pump (Delta-Pump). Running gels were prepared adding to established acrylamide concentrations 25 mM Imidazole, 0.5 M ACA, pH 7, 0.02% APS and 0.02% TEMED; 10% glycerol was added to the gradient with higher concentrations. Stacking gel contained 4% acrylamide. Anode buffer and Cathode buffer were used for CN-PAGE (50 mM Tricine, 7.5 mM Imidazole, 0.02% DDM, 0.05% NaDOC pH 7). The electrophoresis was carried at 80V. After electrophoresis, gels were submerged for 15 minutes at room temperature, in the dark, in a solution containing 2 mM Tris-HCl, 0.5% 3-(4,5-dimethylthiazol-2-yl)-2,5-diphenyltetrazolium bromide (MTT) and 0.02% NADH. The CI appeared as a black band due to the reduction of MTT to tetrazolium salts by NADH oxidation through CI.

Measurement of complex-specific ATP synthesis

The rate of mitochondrial ATP synthesis driven by CI, CII and CIII was measured in digitonin-permeabilized cells as previously described (Ghelli et al., 2013). Briefly, after trypsinization, cells (10×10^6/ml) were suspended in a buffer containing 150mM KCl, 25mM Tris–HCl, 2mM EDTA (ethylenediaminetetraacetic acid), 0.1% bovine serum albumin, 10mM potassium phosphate, 0.1mM $MgCl_2$, pH 7.4, kept at room temperature for 15 minutes, then incubated with 50μg/ml digitonin until 90-95% of cells were positive to Trypan Blue staining. Aliquots of 3×10^5 permeabilized cells were incubated in the same buffer in the presence of the adenylate kinase inhibitor P^1,P^5-di(adenosine-5′) pentaphosphate (0.1mM) and OXPHOS complexes substrates. Chemiluminescence was determined as a function of time with Sirius L Tube luminometer (Titertek-Berthold, Pforzheim, Germany). The

chemiluminescence signal was calibrated with an internal ATP standard after the addition of 10μM oligomycin. The rates of the ATP synthesis were normalized to protein content and citrate synthase (CS) activity (Trounce et al., 1996).

Measurement of complexes activity

Crude mitochondria were used to measure redox activities with a UV-Vis spectrophotometer (V550 Jasco). For CI and CII activity, spectrophotometric assay was performed at 600nm wavelength, at 37°C and under continuous stirring, by following the 2,6-Dichlorophenolindophenol (DCIP) reduction. Kinetic was calculated using the DCIP molar extinction coefficient (19.1 $mM^{-1}cm^{-1}$). The CIII and CIV activities were analyzed with a dual-wavelength spectrophotometer (540 nm-550 nm) at 37 °C and under stirring, following the reduction or oxidation of cytochrome *c* (molar extinction coefficient 19.1 $mM^{-1}cm^{-1}$).

25 μg of crude mitochondria were used in each assay. The specific activity was measured after subtraction of non-specific activity conducted in a separate assay, adding the specific complex inhibitors at the beginning of the reaction (CI: 1 μM Rotenone; CII: 5 mM Malonate; CIII: 1 μM Antimycin A; CIV: 300 μM KCN) (Carossa et al., 2014; Ghelli et al., 2013). For details about reaction components see Table M1.

The activity of CS was evaluated in mitochondria suspended in a buffer containing 125 mM Tris-HCl, 0.1% Triton X-100, 100 μM DTNB (ε= 13.6 mM^{-1}), 300 μM Acetyl-CoA, pH 8. The reaction was started by addition of 500 μM Oxaloacetate (Trounce et al., 1996) and measured at 412 nm at 30°C with UV-Vis spectrophotometer (V550 Jasco).

Reaction component for OXPHOS Complexes Activity measurements	
COMPLEX I	**COMPLEX II**
50mM KP_i pH 7,8 3,5mg.mL^{-1} BSA 25µg crude mitochondria 70µM DUB 60µM DCIP (in 5mM KP_i pH 7,8) 1 µM Antimycin A **Starter:** 70µM NADH	100mM KP_i pH 7,8 1mg.mL^{-1} BSA 2mM EDTA 25µg crude mitochondria 200 Mm ATP 50µM DUB 80µM DCIP 1µM Antimycin A 1µM Rotenone 1µM KCN **Starter**: 10mM Succinate
COMPLEX III	**COMPLEX IV**
50mM KP_i pH 7,8 3,5mg.mL^{-1} BSA 300µM KCN 20µM Cytochrome c Oxidized 25µg crude mitochondria 1µM Rotenone 5mM Malonate **Starter:** 50µL DBH_2	50mM KP_i pH 7,8 3,5mg.mL^{-1} BSA 1mM EDTA 20µM Cytochrome c Reduced 1µM Antimycin A **Starter**: 25µg crude mitochondria

Table M1: Reaction component for OXPHOS complexes activity measurements

Oxygen consumption rate

Oxygen Consumption Rate (OCR) was measured using the Seahorse XFe24 Extracellular Flux Analyzer (Seahorse Bioscience) as previously described (Iommarini et al., 2013). Cells were seeded ($3x10^4$ cells/well) into XFe24 cell culture plate and allowed to attach for 24 hours. Cell culture media was replaced with XF media (Seahorse Bioscience). OCR was measured over a 3 minutes period, followed by 3 minutes mixing and re-oxygenation of the media. For Mito Stress Test, complete growth medium was replaced with 670µl of unbuffered XF media supplemented with 10mM glucose pH 7.4 pre-warmed at 37°C. Cells were incubated at 37°C for 30 minutes to allow temperature and pH equilibration. After an OCR baseline measurement, 70µl of oligomycin, carbonyl cyanide-p-trifluoromethoxyphenylhydrazone (FCCP), and rotenone plus antimycin A were sequentially added

to each well to reach final concentrations of 1µM oligomycin, 0.25µM FCCP, and 1µM rotenone and antimycin A. Three measurements of OCR were obtained following injection of each drug and drug concentrations optimized on cell lines prior to experiments. At the end of each experiment, the medium was removed and SRB assay was performed to determine the amount of total cell proteins as described above. OCR was normalized to total protein levels (SRB protein assay, see below) in each well. Each cell line was represented in 5 wells per experiment (n = 3 replicate experiments). Data are expressed as pmoles of O_2 per minute (OCR) normalized on SRB absorbance.

Cell viability

Cell viability was measured by the Sulforhodamine B (SRB) assay (Sigma-Aldrich) and by cell counting after Trypan Blue (Sigma-Aldrich) staining. Cells were seeded in 24-well plates ($7.5x10^3$ cells/well for 143B and $10x10^3$ cells/well for HCT116) in complete medium. For additional conditions, 24 hours post-seeding cells were washed twice in PBS and incubated in indicated media. Evaluation of growth in galactose condition was performed as described in (Ghelli et al., 2003). Briefly, at the end of incubation time, cells were fixed with 50% trichloroacetic acid for 1 hour at 4°C, washed 5 times with H_2O and finally dried for 1 hour at room temperature. Cells were then stained with SRB 0.4% diluted in 1% acetic acid for 1 hour at room temperature, washed 4 times with 1% acetic acid, and disrupted with 10 mM Tris-HCl pH 9.8. The absorbance of SRB was detected with Victor3 plate reader (Perkin Elmer) at the wavelength of 560 nm.

Metabolomics

Metabolite concentrations were measured with Carcinoscope analysis [Human Metabolome Technologies (HMT)] which uses capillary electrophoresis coupled to time of flight/triple quadrupole mass spectrometry and provides absolute quantification of 116 targeted metabolites. Metabolites were extracted using 100% methanol supplemented with 550µl of Internal Standard Solution provided by HMT from 2-5 million cells seeded on 90mm plate. The metabolite concentrations were

normalized to the number of viable cells. For mass isotopomer analysis, cells were incubated for 3 hours either with DMEM High glucose (Euroclone) supplemented with [^{13}U] labelled glutamine (2mM) or with DMEM (Life Technologies) supplemented with [^{13}C] labelled glucose (25mM) and sodium pyruvate (110mg/l, Sigma-Aldrich). Nutrients labelled with ^{13}C were purchased from Cambridge Isotope Laboratories. Metabolite extraction was performed as described above and the isotopomer distribution was evaluated with F-Scope analysis (HMT) that enables determination of metabolic flux by measuring absolute concentrations and tracer-labelled fractions of 54 targeted metabolites.

ATP measurements

Aliquots of 1.5×10^6 cells were washed, resuspended in 1 ml of ice-cold PBS and extracted for ATP determination. Briefly, cell suspension was treated with 1M perchloric acid (PCA), immediately cooled on ice and centrifuged at 48°C to remove insoluble material. PCA was neutralized with potassium hydroxide and samples were centrifuged immediately before injection. The supernatant (100 ml) was injected on C18 column. ATP was extracted and detected as described by Jones (Jones, 1981) on a Kinetex reversed phase C18 column (250 × 4.6 mM, 5mm; Phenomenex, CA, USA), with a two pump Waters 510 system equipped with a variable volume injector. Absorbance at 260 nm was monitored by a photodiode array detector (Waters 996). ATP peak was identified by comparison of its retention time with those of standards and confirmed by co-elution with standards. The quantification was obtained by peak area measurement compared with standard curves and data were normalized for protein content, determined by Bradford assay (Bradford, 1976).

Glucose uptake

Glucose consumption was determined by using the Glucose (GO) Assay Kit (Sigma-Aldrich) scaling down the manufacturer protocol to a final volume of 1 ml. Briefly, cells were seeded in 6-well plates (1×10^5 cells/well) in high glucose medium. After 48 hours, cells were washed in PBS and incubated with DMEM-high glucose without phenol red. Aliquots of 100 ml of medium were taken at time 0 and after 24 hours of incubation and 3 ml of samples were used to determine the glucose concentration, by the enzymatic reaction of glucose oxidase coupled to peroxidase-mediated oxidation of reduced o-Dianisidine (l l⁄4 540 nm, 30 min, 378C). The data obtained were normalized on cell number.

Lactate production

Cells were seeded in 6-well plates ($3x10^5$ cells/well) in 2ml of high-glucose medium. After 24 hours and 48 hours aliquots of medium were collected and deproteinated with 6% PCA, vortexed and incubated in ice for 1 minute. Samples were centrifuged at 13000rpm at 4°C for 2 minutes and the lactate concentration in supernatants was determined by measuring NADH (λ=340nm; ε=6.22mM^{-1} cm^{-1}) production in a buffer containing 320mM glycine, 320mM hydrazine, 2.4mM NAD^+ and 2U/mL L-lactic dehydrogenase (Sigma-Aldrich) after 30 minutes of reaction at 37°C. Data were expressed as pmoles of lactate produced by 1000 cells.

Clonogenic assay

The ability of cells to maintain survival and mitotic ability was determined by seeding cell suspensions (500 cells per 32-mm dish) in growth medium and incubated at 37°C in a humidified 5% CO_2 atmosphere. Colonies were fixed after 10 and 14 days, for 143B and HCT116, respectively, using 50% Trichloracetic acid (Sigma-Aldrich), colored with SRB (Sigma-Aldrich) and destained with 1% acetic acid (Sigma-Aldrich). Images were acquired using ChemiDoc XRS+ (Biorad) and counted using ImageJ (Collins, 2007).

Anchorage-independent growth assay

Anchorage-independent cell growth was determined in 0.33% agarose with a 0.5% agarose underlay. Cell suspensions ($1x10^4$ cells per 32-mm dish) were plated in semisolid medium (growth medium plus agar 0.33%) and incubated at 37°C in a humidified 5% CO2 atmosphere (Iommarini et al., 2013). Colonies were counted after 10 days at a magnification of 10× with an inverted microscope (Nikon Diaphot, Nikon Instruments). Images were acquired with Gel Logic 1500 molecular imaging apparatus (Kodak).

2D-migration assay

Cells were cultured to confluence in 6-well plates. Under aseptical conditions a thin wound was induced by scratching with a 200µl pipette tip and detached cells were rinsed with PBS. Using a phase contrast set up and a 10× magnification wound healing was monitored to identify invading cells at different time points. For quantitative evaluation, images of 20 sequential open wound areas were acquired using digital photo camera mounted on the microscope and analyzed with T-scratch software (CSElab). The capacity to invade was expressed as the percentage of open wound area.

***In vivo* studies**

For in vivo studies, nu/nu mice (CD-1® Nude Mouse Crl:CD1-Foxn1n) were used, purchased from Charles River Laboratories. The animals were treated according to institutional guidelines and regulations and experiments were performed following the protocol approved by the SALK ethical committee. Five to six weeks old female mice were subcutaneously inoculated with a 200µl suspension of $15x10^6$ cells in serum free medium and matrigel (BD Bioscience, Franklin Lakes, NJ, USA) in the right flank of the animal. Xenograft size was measured with a sliding caliper twice a week, according to the formula (width x height x length/2). Mice were sacrificed either simultaneously, when the first xenograft reached $3cm^3$, or consecutively, when each animal reached

xenograft volume of $3cm^3$ (or met the termination criteria). For the experiments with doxycycline (Dox), A total of 3% sucrose with or without $1mg.ml^{-1}$ Dox was added into the drinking water of mice once each tumor with the inducible lentiviral system has exceeded $450mm^3$, and the water was changed twice a week. Prior to the sacrifice (3 hours before) all animals were injected intraperitoneally with pimonidazole (60 mg/kg, (Hypoxyprobe) diluted in saline solution. The xenografts were snap frozen for protein, DNA and RNA extraction and formalin fixed for IHC analysis.

Measurement of H_2O_2 production

Production of H_2O_2 was measured in cells grown in complete high glucose medium. 100,000 cells were treated with 2,7-dichlorodihydrofluorescein diacetate (H2DCFDA) (Life Technologies) to a final concentration of 100 mM, and incubated at 37°C for 30 minutes. The cells were then collected and the reaction was stopped by placing them in an ice bath for 5 minutes. The cells were disrupted by treatment with Triton X-100 (2%) and centrifuged at 2,500g for 20 minutes at 4°C. The supernatant was used to measure fluorescence emission (excitation, 485 nm; emission, 535 nm) in a multilabel counter Victor3 (Perkin Elmer). The amount of H_2O_2 produced was calculated by using a standard curve of 2,7-$DCFH_2$ in which 1 mM of 2,7-$DCFH_2$ represented 1 mM of H_2O_2.

Immunohistochemical staining

For immunohistochemical staining, the following antibodies were used: rabbit monoclonal anti-complex I subunit NDUFS3 (1:200; Abcam), rabbit polyclonal anti- HIF1a (1:350; Sigma-Aldrich), mouse monoclonal anti- pimonidazole (1:400; Hypoxyprobe), rabbit monoclonal anti-CD-31 (1:50; Abcam), mouse monoclonal anti-human ki67 (1/100Dako). All antibodies were diluted in Dako antibody diluent with background reducing components (Dako).

Tissue sections (4mm) were deparaffinised by three changes of xylene, rehydrated in three changes of absolute 2-propanol followed by heat-induced epitope retrieval in TE-T buffer (10 mM Tris pH

9.0, 1 mM EDTA, 0.05% Tween 20) for 40 minutes at 95°C and 20 min at room temperature. Sections were equilibrated with phosphate-buffered saline containing 0.5% Tween 20 (PBS-T pH 7.4). Staining was carried out using the Envision Detection System (Dako) according to the manufacturer's instructions followed by visualisation with diaminobenzidine (DAB) for 10 minutes. Slides were counterstained with haematoxylin.

Masson's Trichrome

Tissue sections (4mm) were deparaffinised by two changes of xylene and then dehydrated by two changes of industrial methylated spirit and subsequently washed in tap water. Nuclei were stained in Weigert's Iron Haematoxylin in 15minutes. Cytoplasms were stainined in red using Ponceau 2R-/acid Fuchsin Solution for 4 minutes. Collagen fibres are stained in Aniline Blue in 1% Acetic Acid for 5 minutes, after being decolourised by 1% Aqueous Phosphomolybdic Acid. For details about the solutions utilized see Table M2.

Weigert's Iron Haematoxylin Solution (Mix of A and B at equal part)	2 R-/acid Fuchsin Solution	1% Aqueous Phosphomolybdic Acid Solution	0.5% Aniline Blue in 1% Acetic Acid Solution
Stock Solution A: Haematoxylin: 1 g 95% Alcohol:100 ml	1% Ponceau 2R (Ponceau De-Xylidine) in 1% Acetic Acid : 2 parts	Phosphomolybdic Acid: 1g Distilled Water: 100ml	1% Acetic Acid Solution Acetic Acid, Glacial: 1ml Distilled Water: 99ml
Stock Solution B: 29% Ferric Chloride in water: 4ml Distilled water:95ml Hydrochloric acid concentrated: 1ml	1% Acid Fuchsin in 1% Acetic Acid: 1 part		0.5% Aniline Blue in 1% Acetic Acid Working Solution Aniline Blue: 0,5g 1% Acetic Acid: 100ml

Table M2: Preparation of solutions for Masson's Trichrome staining

Electron microscopy

Directly after xenograft removals, small sections ($\leq 5mm^3$) were immersed in cacodylate buffer 0,1M with 2.5% glutaraldehyde and 4% paraformaldehyde and stored during 24 hours at 4°C. After 24 hours, this fixation solution is replaced by a solution of cacodylate buffer 0,1M without glutaraldehyde and paraformaldehyde. Within 3 weeks after samples collection, sections (1 µm) were

stained with 1% toluidine blue for morphology control and electron microscopy area selection. Thin sections were observed with JEM-1011 Transmission Electron Microscope (JEOL Ltd).

Generation of NDUFS3 inducible knock-out cells

To create a stable inducible transgenic cell line re-expressing NDUFS3, the Retro-X Tet-Off Advanced Inducible Expression Systems (Clonetech) was utilized following the manufacturer's instructions. Two separate infections were performed with the following vectors: pRetro-X Tet-Off Advanced, which constitutively expresses the transactivator tTA-Advanced, controlled by the tetracycline analogous Dox, and the pRetroX-Tight-Pur in which wild-type NDUFS3 cDNA sequence was cloned, therefore called pRetroX-Tight-Pur-NDUFS3, which expresses NDUFS3 under the control of an inducible promoter recognized by tTA-Advanced. NDUFS3 cDNA has been obtained through a retrotranscription reaction after that RNA was extracted from human blood using the high capacity cDNA retrotranscription kit (Life Technologies) and primers containing the restrictions sites NotI and EcoRI.

First, the gene has been inserted in the pGEM®-T Easy Vector (Promega), which was utilized to transform *E. cloni* 10G Chemically Competent DUOs cells (Lucigen). Colonies have then been selected through a white/blue screening. After DNA extraction from a positive clone, the integrity of the NDUFS3 gene and the presence of the regulatory element requested for its expression were confirmed by Sanger sequencing using KAPA2G taq polymerase (Kapa Biosystems) and Big Dye protocol (Life Technologies).

Secondly, the plasmid pGEM®-T/NDUFS3 has been digested with the *Not*I and *Eco*RI digestion enzymes and the cDNA was cloned inside the pRetroX-Tight-Pur. This vector has been used to transform the *E.coli* 10G Chemically Competent DUOs cells. Colonies were selected with ampicillin and the screening has been performed

The pRetroX-Tet-Off Advanced vector was transduced in 143B NDUFS3$^{-/-}$ cells. The selection of cells that have integrated the plasmid was performed using G418 (400µg/ml, Sigma). Cells were then maintained in a medium containing G418 (100µg/ml). Single cell cloning of selected cells was then

performed. Cells with optimal tTA-Advanced activity were identified by measuring luciferase activity as it follows. The pRetroX-Tight-Pur-LucControl Vector was transiently transfected using X-treme GENE HP DNA Transfection Reagent (Roche) into cells (8.10^4) seeded in 6-well plates incubated with a medium containing Clonetech tetracycline-free FBS (Clonetech). Each clone was then treated with or without Dox (concentration 100ng/ml, Geneticin, Life technologies). After 48 hours, cells were harvested and processed with the Luciferase assay kit (Dual-Luciferase(R) Reporter Assay System, Promega) protocol. The luciferase activity was analyzed by Luminometer (Titertek-Berthold). As expected, the intensity was high in absence of Dox (cDox) and low in cells cultivated with 100ng/ml of Dox (+Dox) in the medium. Two clones with the lowest + Dox luciferase activity were pooled together and the second viral transduction was performed as described above, using the pRetroX-Tight-Pur-NDUFS3 Vector. The selection of cells that have incorporated the plasmid was performed using 0.5µg/ml of puromycin (Gibco). Cells were then cultured in a medium containing puromycin 0.25 µg/ml. Single cell cloning of selected cells was performed to select clones without NDUFS3 in a +Dox medium, while able to express NDUFS3 in a –Dox medium. Four of the selected clones were pooled to obtain 143B NDUFS3$^{-/-\ ind}$.

RESULTS

Generation and biochemical characterization of NDUFS3$^{-/-}$ cancer cells.

With the aim of generating CI-deficient cell models, the knock-out of *NDUFS3* (NDUFS3$^{-/-}$) was induced in the osteosarcoma cell line 143B and the intestinal carcinoma cell line HCT116 by using the ZFN technology. After cells transfection with the ZFNs, single cell cloning has allowed the isolation of individual cells with potential genotypes of interest. Fluorescent PCR (F-PCR) and Sanger sequencing performed on the population of cells obtained have permitted to identify and to select the clones containing frameshift mutations at the 5' end of one or the two alleles of the NDUFS3 gene (NDUFS3$^{-/-}$), which are likely to prevent the proper translation of the mRNA (Figure 12). Western Blot analysis on three selected cell lines confirmed the absence of the protein in NDUFS3$^{-/-}$ clones (Figure 13 upper panel). Importantly, three NDUFS3$^{+/+}$ cells are clones having reversed the mutations induced and therefore they express NDUFS3 (Figure 13 upper panel). Given the fact that the latter have followed the same selection processes than NDUFS3$^{-/-}$ cells, they represented appropriate control for all the further analysis, and they were used as such.

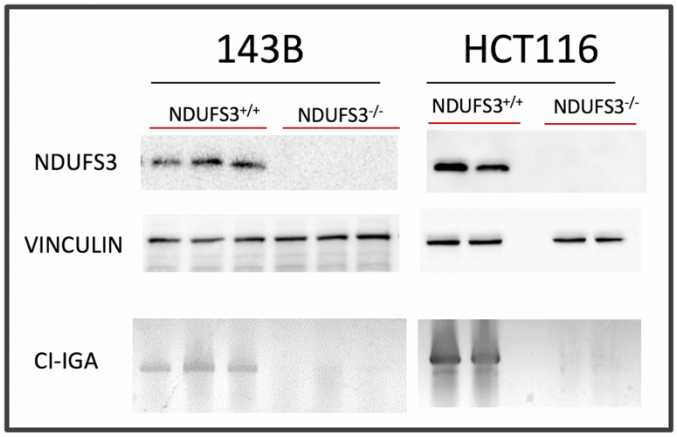

Figure 13: NDUFS3$^{-/-}$ clones lack NDUFS3 and display a significant reduction of CI activity
SDS page followed by western blot analysis on three 143B clones and two HCTT116 clones for each genotype (upper panel). Clear-Native PAGE followed by CI-in gel activity on the same clones. Black bands appear only upon NADH oxidation by CI (lower panel).

The assembly and the activity of the CI were then investigated in the different models obtained. As initially hypothesised, and confirming the crucial role of NDUFS3 for CI assembly, in-gel activity analysis showed a significant reduction of CI activity in NDUFS3$^{-/-}$ clones compared to their WT counterparts (Figure 13 lower panel). This finding was further confirmed by the measurement of ATP

synthesis mediated by the CI, whose values were found drastically decreased in CI-deficient clones, while CII and CIII showed no altered capacity to participate to ATP production (Figure 14). In line with the above, among all the complexes of the respiratory chain and citrate synthase, only complex I showed a decrease in its activity in 143B NDUFS3$^{-/-}$ clones (Figure 15).

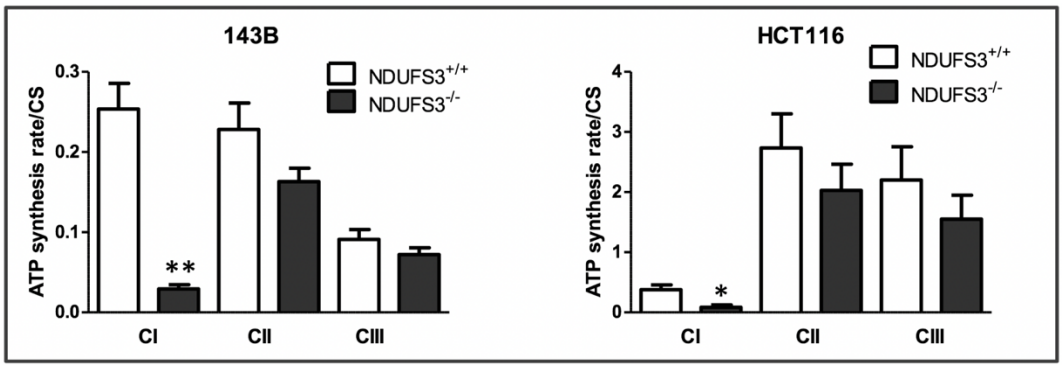

Figure 14: CI-mediated ATP synthesis is significantly reduced in 143B cells and HCT116 cells
*The ATP synthesis rate driven by complex I (pyruvate and malate) or complex II (succinate plus rotenone) or complex III (DBH_2) was determined in isolated mitochondria by the luciferase assay using a luminometer. The values (nmol/min*mg protein) were normalized for CS activity. Data are means ± SEM of three experiments. * P<0.05; ** P<0.01*

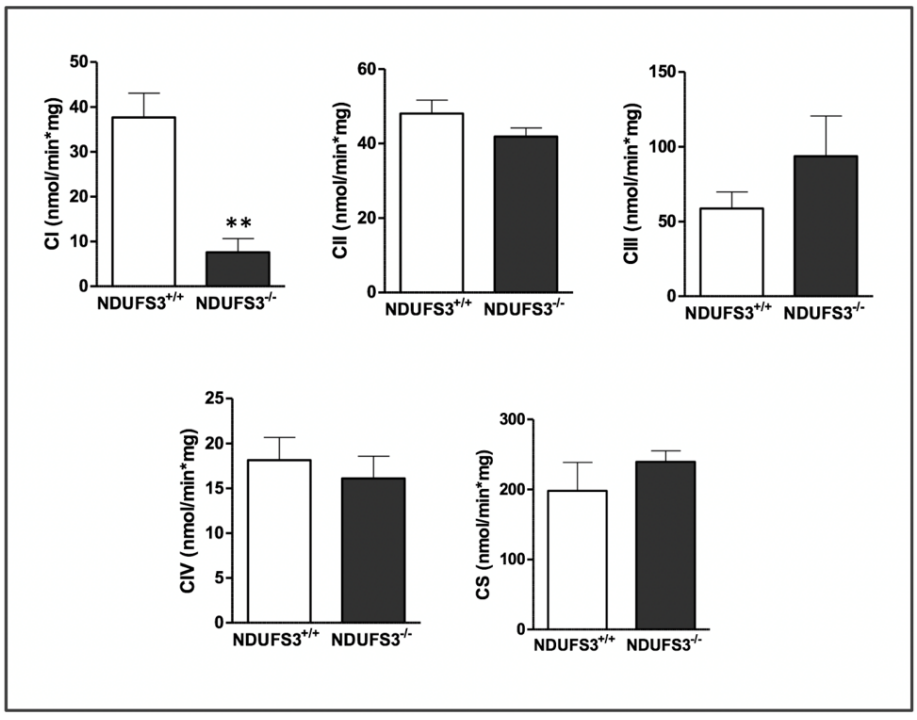

Figure 15: Only the activity of the CI is significantly reduced in NDUFS3$^{-/-}$ 143B clones
*Analysis of the respiratory complexes redox activity. Measurement of CI, CII, CIII and CIV redox activity and CS synthase activity in crude mitochondria extracted from 143B clones. Data are means ± SEM of three experiments. ** P<0.01.*

Notwithstanding the fact that the rest of the respiratory chain remained unaltered, oxygen consumption rate measurement revealed that disruption of CI in NDUFS3$^{-/-}$ cell lines was sufficient to abrogate mitochondrial respiration, while, contrariwise, NDUFS3$^{+/+}$ cells significantly utilized the respiration chain (Figure 16).

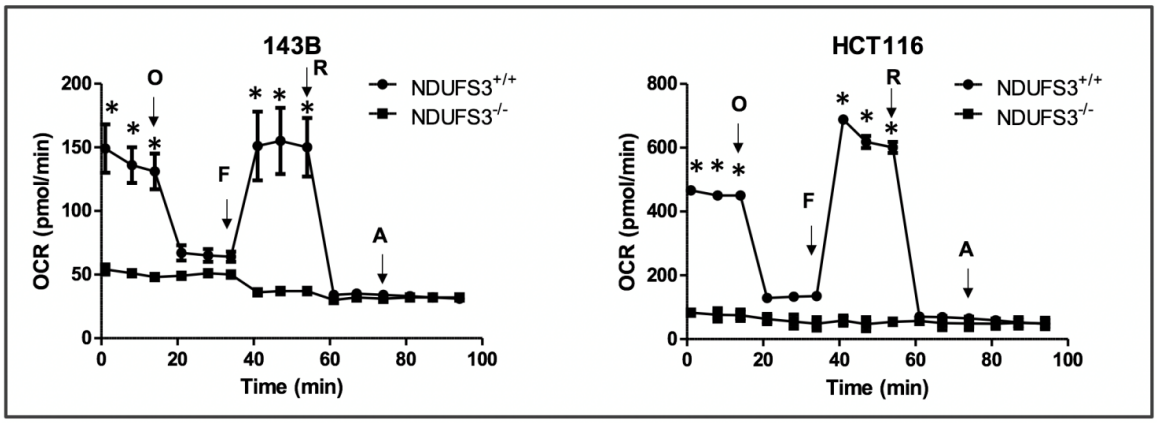

Figure 16: Loss of CI abrogates mitochondrial respiration in 143B and HCT116 clones
*Oxygen consumption rate measurement by Seahorse assay. After addition of oligomycin (O), the subsequent decrease of the OCR represents the respiration that served for ATP production. The slopes induced upon addition of FCCP (F) and then rotenone (R) and antimycin (A) permits to calculate the maximal capacity of cells to respire. Data are means ± SEM of three experiments. * P<0.05.*

Accordingly, only NDUFS3$^{+/+}$ clones could grow in a glucose-free, galactose medium, which forces cells to rely on respiration to proliferate (Figure 17A). Quantifying ATP levels in the latter condition confirmed that NDUFS3$^{-/-}$ clones were no longer able to produce ATP though OXPHOS (Figure 17B).

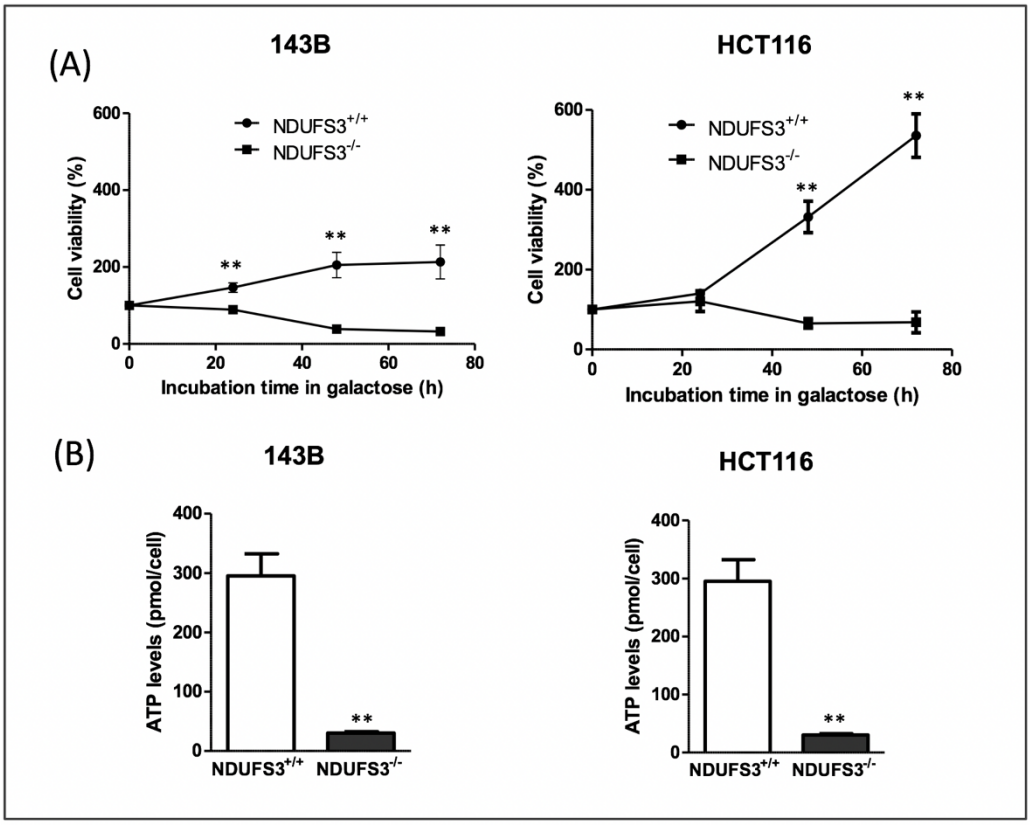

Figure 17: NDUFS3$^{-/-}$ clones do not sustain proliferation nor they maintain ATP levels when forced to rely on mitochondrial respiration

*(**A**) Time course of 143B and HCT116 clones' viability in DMEM-galactose The SRB absorbance value at time zero corresponds to 100% viable cells. (**B**) ATP is detected by HPLC and absorbance is measured at 260nM. Values are normalized for cell number. Data are means ± SEM of three experiments. * P<0.05; ** P<0.01.*

In line with previous studies, HMT metabolomics revealed that the strong OXPHOS defects induced in 143B clones is associated with a significant reduction of aspartate levels, while the amount of the other amino acids remained unchanged, thus not impacting on total amino acids quantity (Figure 18). Nevertheless, when cultured in similar, high glucose conditions, no significant difference was found regarding ATP production (Figure 19A) and only CI-deficient HCT116 cells, and not 143B, displayed a slight reduction of viability (Figure 19B). Altogether, these data indicate that CI-deficient cells may use alternative metabolic routes to sustain ATP synthesis and proliferation, and that decreased aspartate levels is most likely not a limiting factor for the proliferation of NDUFS3$^{-/-}$ clones.

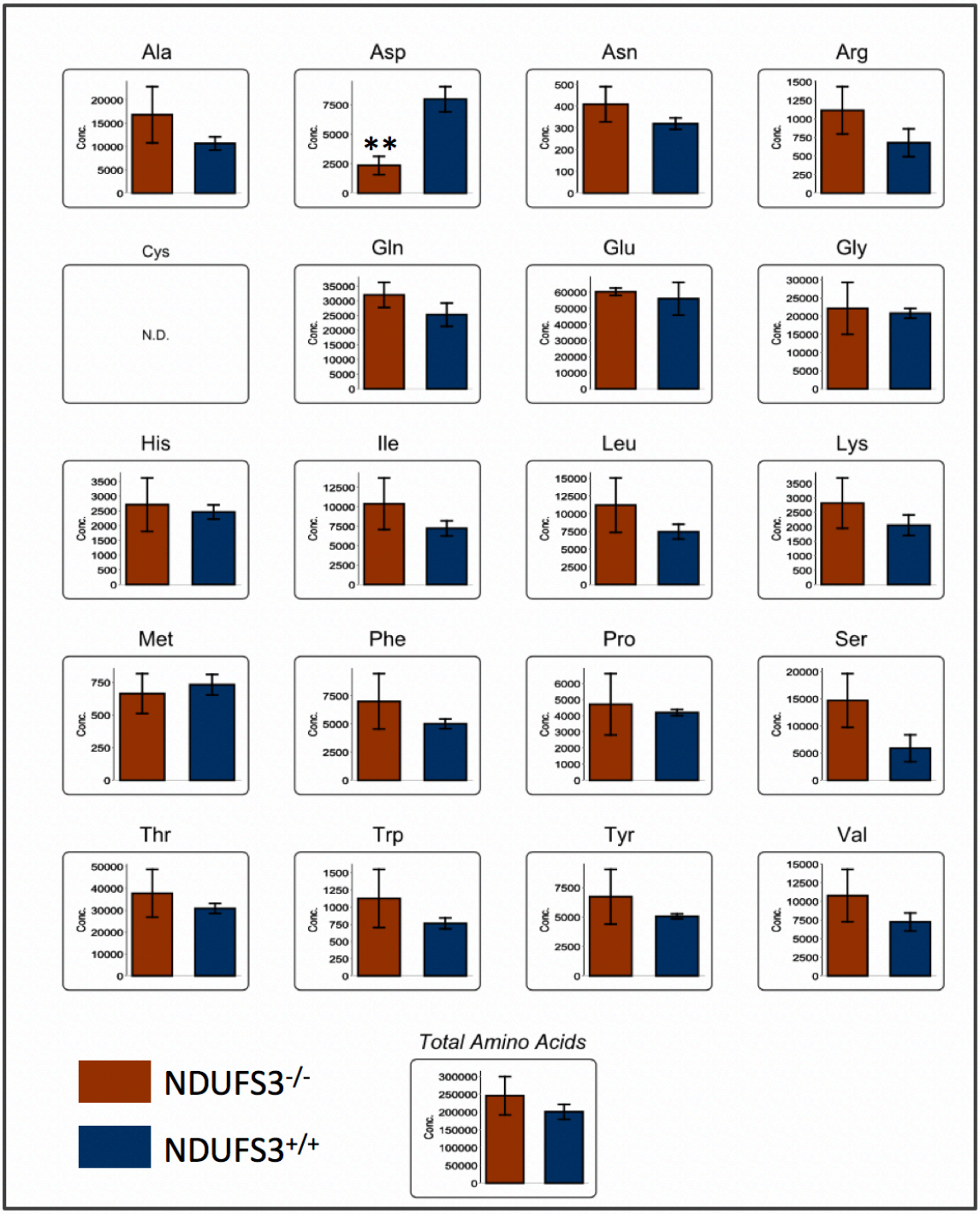

Figure 18: Aspartate levels are significantly reduced in NDUFS3$^{-/-}$ 143B clones

*Clones were cultured in high glucose medium and all the 20 proteinogenic amino acids, but cysteine (cys), could be quantified by carcinoscope analysis. Total amino acids are the summation of all the 20 proteinogenic amino acids. Alanine (Ala); Arginine (Arg); Asparagine (Asn); Asparate (Asp); Glutamine (Gln), Glutamate (Glu), Glycine (Gly); Histidine (His); Isoleucine (Ile); Leucine (Leu); Lysine (Lys); Methionine (Met); Phenylalanine (Phe); Proline (Pro); Serine (Ser); Threonine (Th); Tryptophane (Trp); Tyrosine (Tyr); Valine (Val). Data are means ± SEM of three experiments. * P<0.05; ** P<0.01.*

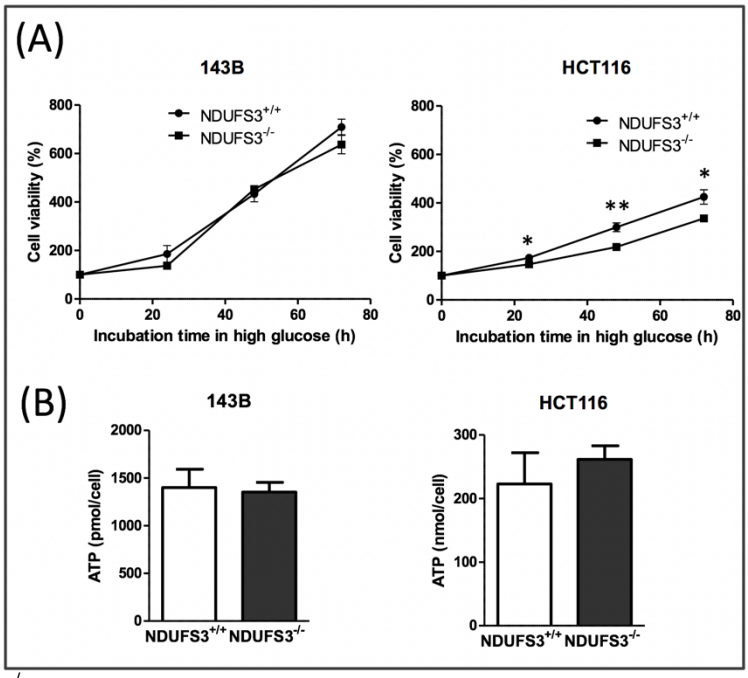

Figure 19: NDUFS3$^{-/-}$ 143B and HCT116 clones sustain ATP production and cell proliferation in high glucose condition

*(**A**) Time course of 143B and HCT116 clones' viability in DMEM-high glucose. The SRB absorbance value at time zero corresponds to 100% viable cells. (**B**) ATP is detected by HPLC and absorbance is measured at 260nM. Values are normalized on cell number. Data are means ± SEM of three experiments. * P<0.05; ** P<0.01.*

Interestingly, the measurement of HCT116 cells viability in galactose and glucose medium may indicate their higher dependence on mitochondrial respiration for proliferation than 143B cells, which divide much faster in high glucose condition than in galactose medium (Figures 17A and 19A).

Upon ETC impairment, increased glycolytic machinery and reductive carboxylation of α-KG are two well characterized escape routes that allow cancer cells to keep meeting the metabolic requirements for proliferation. In line with this, a higher uptake of glucose was observed in both 143B and HCT116 NDUFS3$^{-/-}$ cell lines compared to the WT (Figure 20A), together with an increase in the production of lactate (Figure 20B).

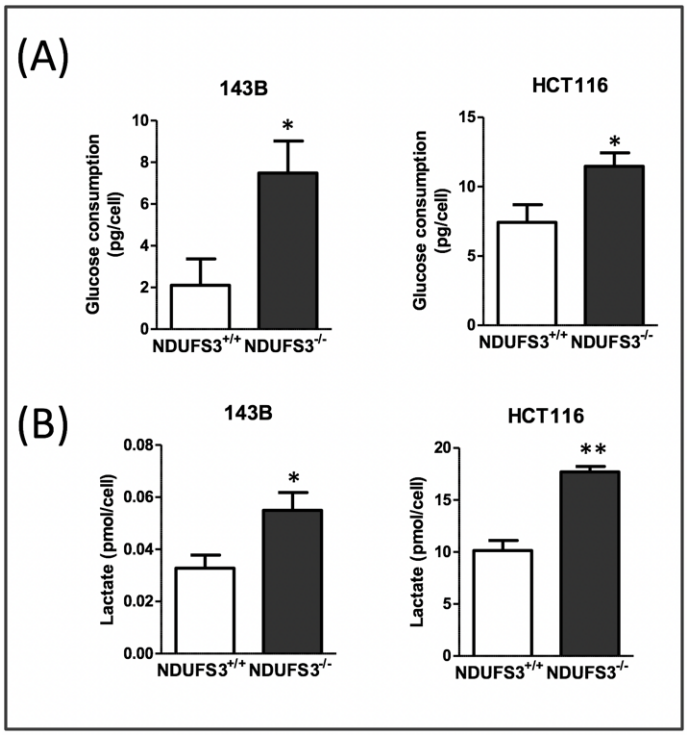

Figure 20: CI-deficient 143B and HCT116 clones consume more glucose and produce more lactate than CI-competent cells.

*(**A**) Glucose uptake and (**B**) Lactate production are measured by spectrophotometric assay. Data are means ± SEM of three experiments. * P<0.05; ** P<0.01.*

Furthermore, HMT analysis has revealed a higher α-KG/Citrate ratio in CI-deficient cells (Figure 21A), which is a "trademark" of reductive carboxylation (Fendt et al., 2013). This last finding is further corroborated by mass isotopomer analysis that allows the tracking of glucose and glutamine carbons distribution into metabolic pathways. In NDUFS3$^{-/-}$ 143B cell lines, glucose contribution to citrate (m+5) is lower than in NDUFS3$^{+/+}$ cells (Figure 21B), while glutamine contribution to citrate generation is greater in CI-deficient cell lines (Figure 21C).

Altogether, these data demonstrate that CI loss abolishes mitochondrial respiration in 143B and HCT116 cells but does not induce any energetic crisis nor severe proliferation impairment. The latter phenomenon may be due to CI-deficient cells ability to increase glycolysis and to trigger glutamine-dependent reductive carboxylation, when adequately supplied in nutrients.

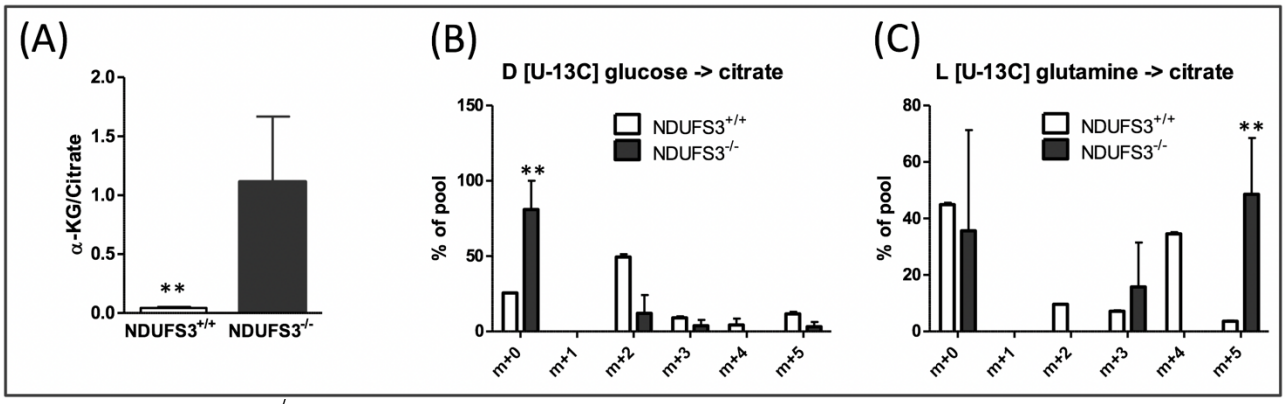

Figure 21: NDUFS3$^{-/-}$ 143B cells trigger glutamine reductive carboxylation
*(**A**) Determination of the α-KG/citrate ratio following carcinoscope analysis of metabolite levels in 143B cells cultured in high glucose condition. (**B**) Mass isotopomer analysis of D [U-13C] glucose and (**C**) L [U-13C] glutamine distribution. Data are means ± SEM of three experiments. ** P<0.01.*

CI-deficient cancer cells display decreased tumorigenic potential

The metabolic prerequisites for malignancy are complex and ought to be clearly understood. While the lack of CI does not affect proliferation *in vitro*, it can nevertheless be expected that the alteration would negatively affects the intricate machinery that drive cancer formation and progression. Several methods have been developed to evaluate the tumorigenic potential of cancer cells *in vitro*, being valuable informative primary steps from which further *in vivo* experiment can be performed. All analysis confirmed the hypothesis stated above. The *in vitro* anchorage independent growth assay in soft agar has evidenced the lower ability of CI-deficient clones to grow in an anchorage independent atmosphere, compared to CI-competent cells (Figure 22A). The clonogenic assay has showed their reduced capacity to survive and to maintain mitotic activity (Figure 22B) and, lastly, the wound healing assay showed the lower capability of NDUFS3$^{-/-}$ cells to repopulate the scratched area, illustrating their weakened migration ability (Figure 22C). Interestingly, this set of experiments suggested that CI loss may have affected more the tumorigenic potential of HCT116 than 143B cells, since the difference in all measurements between the two genotypes is higher in the model of epithelial origin. Overall, these data demonstrate that CI loss reduces the tumorigenic potential of osteosarcoma and intestinal cancer cells *in vitro*.

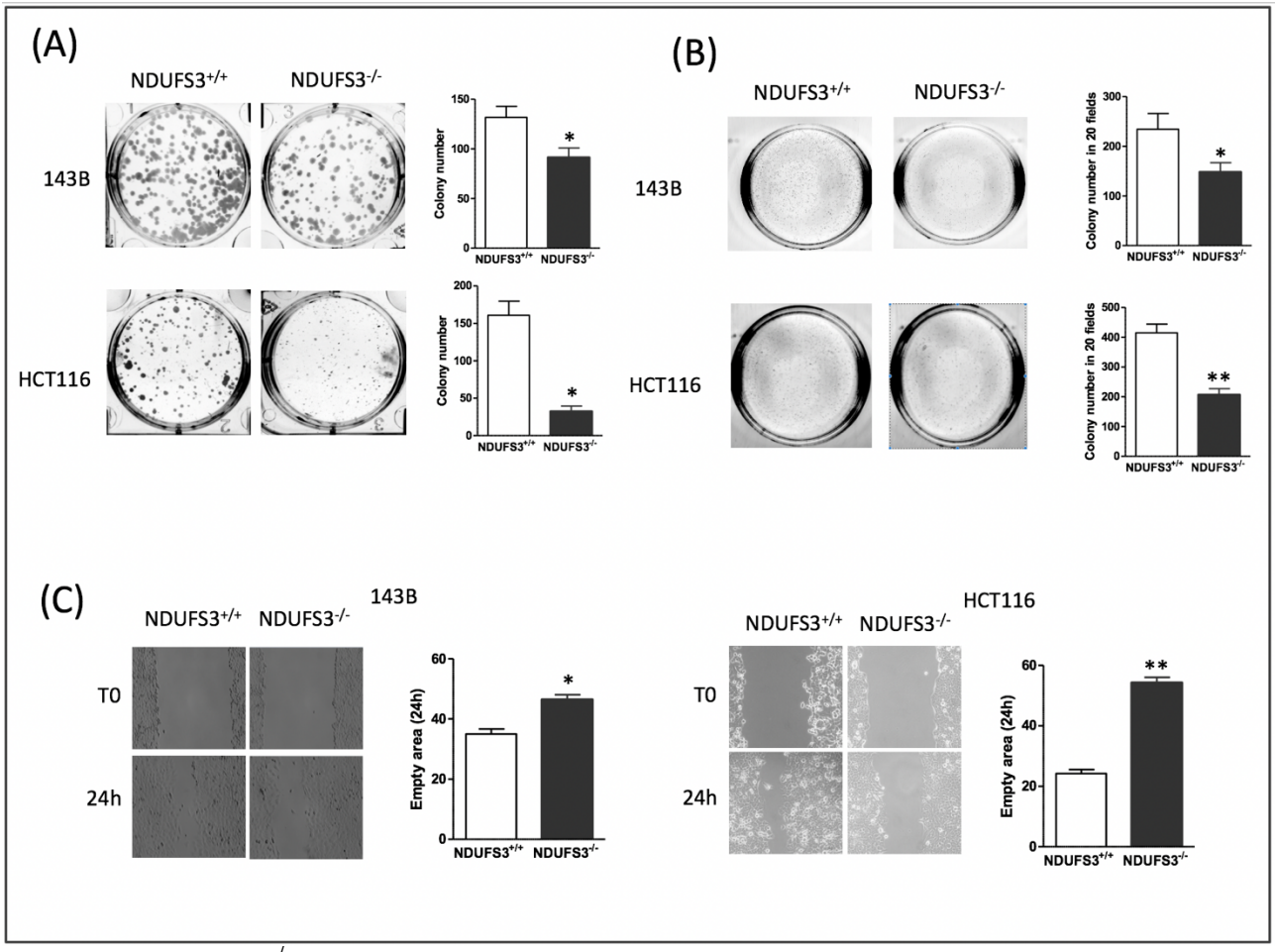

Figure 22: NDUFS3$^{-/-}$ cancer cells showed reduced tumorigenic potential in vitro
*(**A**) Representative images of anchorage independent growth in soft agar of HCT 116 and 143B cells clones (**left**), and colony count after 10 days (**right**). (**B**) Representative images of clonogenic assay results (**left**) and count of HCT 116 and 143B colonies on soft agar plate after 14 and 10 days, respectively (**right**). (**C**) Representative images of wound healing assay results (**left**) and percentage of open wound areas after 24 hours for HCT 116 and 143B clones (**right**). Data are means ± SEM ≥ 3 experiments * P<0.05; ** P<0.01*

Contrariwise to *in vitro* studies, *in vivo* experiments allow the microenvironmental influence on tumor progression to be considered. Indeed, vascularization density, oxygen and nutrient availability, surrounding cells, molecules and extracellular matrix are inherent to tumor biology. The latter characteristics, together with the unstable and always evolving genetics of cancer cells, considerably participate to intra-tumoral heterogeneity and render difficult the prediction of tumor evolution. This taken into consideration, different strategies have been employed to assess the effects of CI loss on tumorigenesis and cancer progression. Both 143B and HCT116 CI-deficient and CI-competent cells have been inoculated in nude mice. However, HCT116 NDUFS3$^{-/-}$ failed to engraft (Figure 23),

confirming the higher sensibility of the intestinal cancer cells to the suppression of CI activity, as evidenced by the previous *in vitro* experiments (Figure 19A and 20), and restricting *in vivo* studies to the 143B model.

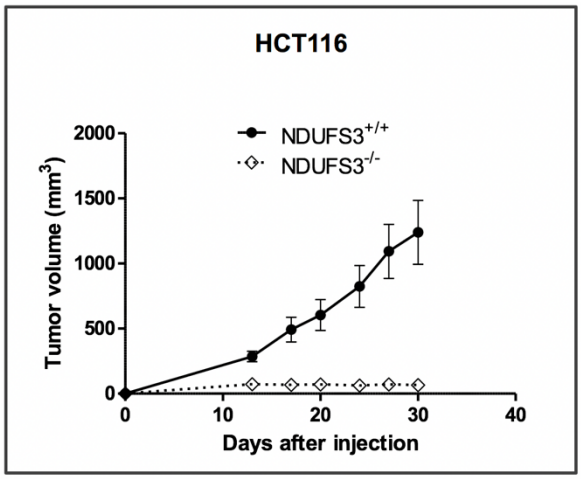

Figure 23: HCT116 NDUFS3$^{-/-}$ failed to engraft *in vivo*
Xenograft growth after subcutaneous injection of HCT 116 clones in nude mice. NDUFS3$^{-/-}$ cells did not grow. Data are means ± SEM = 8 experiments

In a first experiment, mice were sacrificed when each one of them met the termination criteria, so that a proper evaluation of each xenograft growth over time could be performed. Instead, the second experiment stopped when the first xenograft reached the maximal volume, hence limiting any time-related bias for the proper biochemical and molecular characterization of the masses. In both experiments, the lack of NDUFS3, confirmed by IHC (Figure 24B), is associated to a significant reduction of xenograft growth rate (Figure 24A and 25A) and mice survival (Figure 25B). In line with this, less NDUFS3$^{-/-}$ cells presented with positive Ki67 staining, marker of proliferation, compared to the WT (Figure 24C).

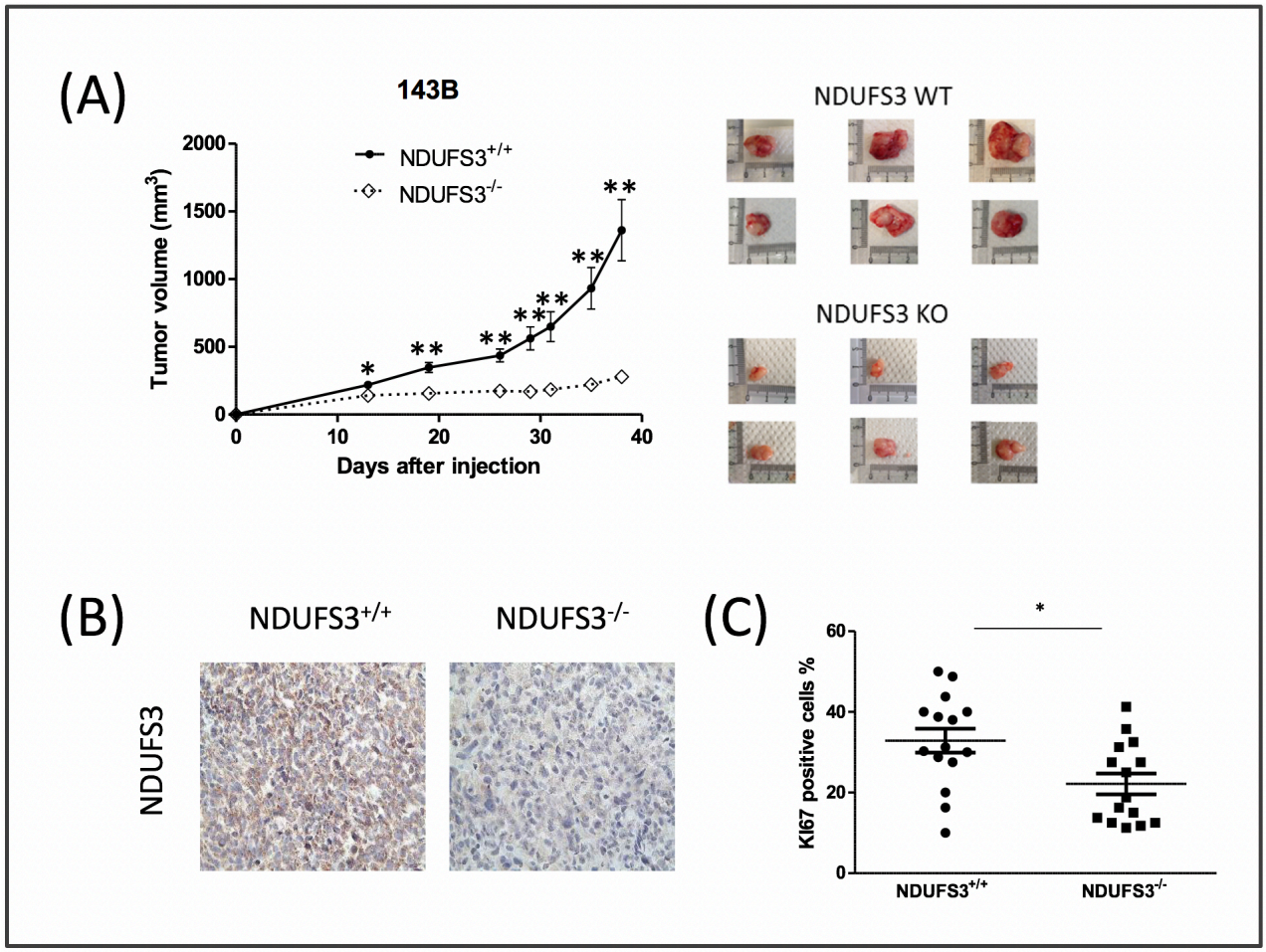

Figure 24: NDUFS3$^{-/-}$ 143B xenografts displayed reduced tumorigenic potential *in vivo*

*(**A**) Xenografts growth after subcutaneous injection of 143B clones in nude mice (**left**), representative pictures of the masses after 38 days (**right**). Data are means ± SEM = 15 animals (**B**) Representative IHC staining of NDUFS3 at 40X magnification. (**C**) Percentage of KI67 positive cells on tumor slices after IHC staining. Data are means ± SEM = 15 samples.*

** P<0.05; ** P<0.01*

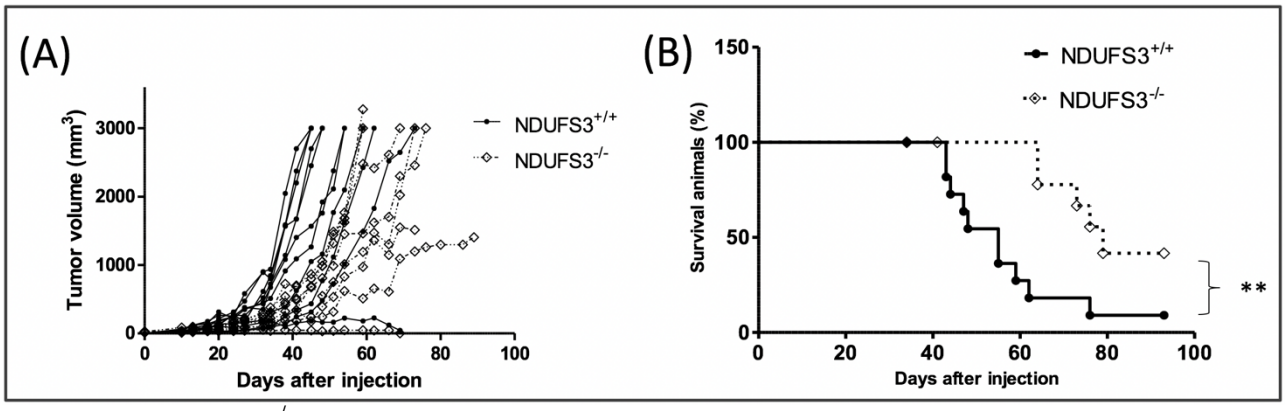

Figure 25: NDUFS3$^{-/-}$ 143B xenografts do not recover tumorigenic potential over time

*(**A**) Xenografts growth after subcutaneous injection of 143B clones in nude mice (**B**) Proportion of animals that reached the termination criteria over time. Data are means ± SEM ≥ 8 animals; ** P<0.01*

Finally, first in a preliminary experiment (Figure 26 upper panel), and then confirmed by a full experiment (Figure 26 lower panel), after that both 143B NDUFS3$^{-/-}$ and NDUFS3$^{+/+}$ cells were inoculated together in mice, xenografts growths correlated with the abundance of NDUFS3$^{+/+}$ cells. In fact, when more NDUFS3-positive cells were present in the masses (Figure 26B and D), higher were the xenograft growth rates (Figure 26A and C). This last data confirmed the tumor advantage of having functional CI for growth and progression.

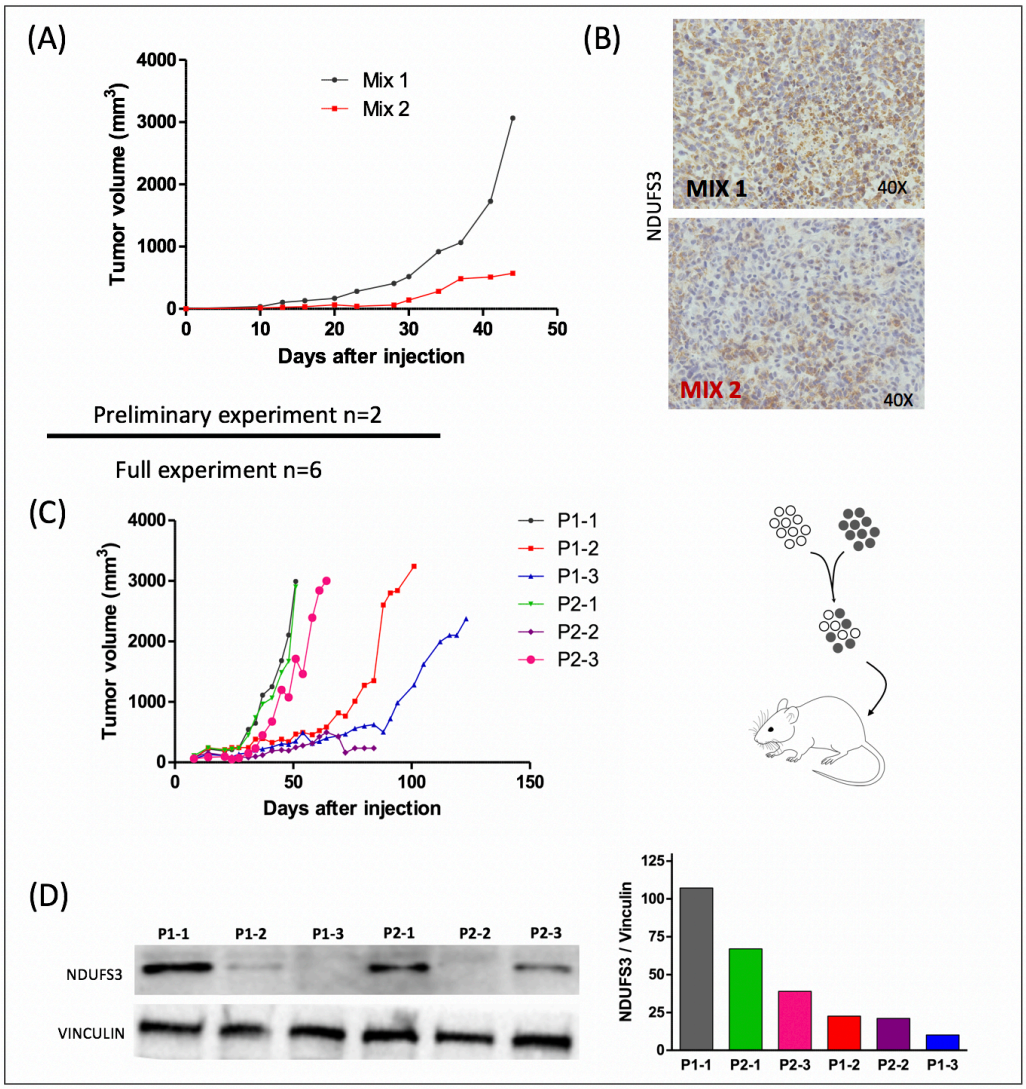

Figure 26: Xenograft growth rates correlate with the presence of NDUFS3$^{+/+}$ cancer cells
*(**A**) Xenografts growth after subcutaneous injection of a same mix of both 143B CI-deficient and CI-competent clones at equal proportion in two nude mice (**B**) IHC staining against NDUFS3 for each resulting xenograft, at 40X magnification. (**C**) Xenografts growth after subcutaneous injection of two different cell pools containing both 143B CI-deficient and CI-competent clones at equal proportion (P1 and P2), in 3 nude mice for each pool. (**D**) SDS page followed by western blot analysis on each tumor samples (left) and quantification of bands intensity (right). The antibody specifically recognizes human NDUFS3.*

CI-deficient cancer cells are unable to trigger the HIF1- mediated response to hypoxia.

Our group has previously shown the correlation between the absence of CI and the lack of stabilized HIF1α. In line with this, western blot analysis indicated that all NDUFS3$^{-/-}$ xenografts lacked HIF1α whereas all NDUFS3$^{+/+}$ xenografts stabilized the transcription factor (Figure 27A), suggesting that NDUFS3$^{-/-}$ did not activate any hypoxic response. Accordingly, real-time PCR on the same samples showed that the expression of the HIF1 responsive genes VEGF, GLUT1 and LDHA, is significantly lower in NDUFS3$^{-/-}$ than in NDUFS3$^{+/+}$ xenografts (Figure 27B).

HIF1 gene expression is not altered in NDUFS3$^{-/-}$ xenograft, demonstrating that the mechanisms responsible for the absence of HIF1α in these masses occur at least at the post transcriptional level (Figure 27B).

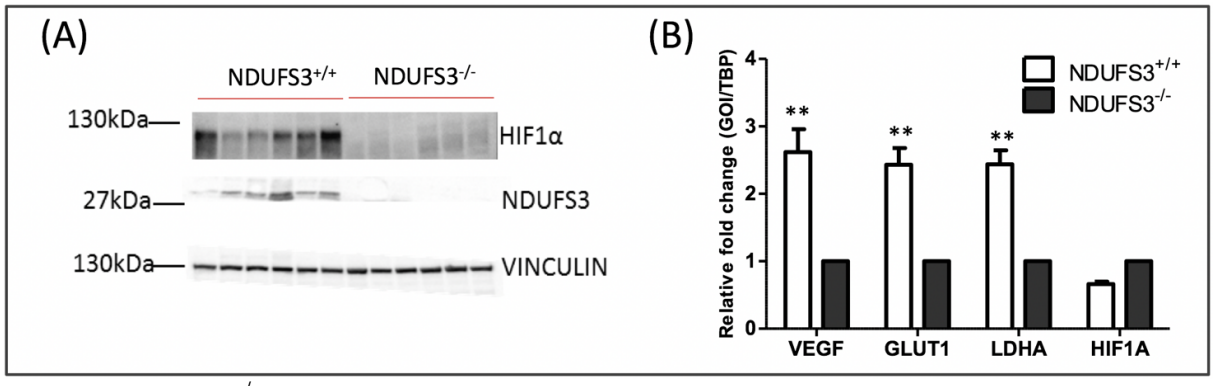

Figure 27: NDUFS3$^{-/-}$ xenografts do no activate the HIF1 pathway
*(**A**) SDS page followed by western blot analysis on 6 representative tumor samples removed 38 days after cell injection, for each genotype. (**B**)Real-Time PCR after total RNA extraction from xenografts tissues. Data are means ± SEM = 3 samples. ** P<0.01; VEGF: vascular endothelial growth factor; GLUT1: Glucose transporter 1; LDHA: lactate dehydrogenase.*

HIF1α stabilization is regulated by both oxygen, α-KG levels and reactive oxygen species (ROS).

In order to investigate the role of oxygen content, mice were injected subcutaneously with a solution of pimonidazole that forms adducts in hypoxia, recognizable by an antibody (Figure 28A). Strikingly, no hypoxic adduct was detectable by immunohistochemistry in the NDUFS3$^{-/-}$ xenografts removed 38 days after mice inoculation, indicating that contrariwise to NDUFS3$^{+/+}$ masses, they did not face hypoxia (Figure 28A). Further, HIF1α staining on the same paraffin sections revealed that CI-

competent tumors stabilized the transcription factor, with a clear nuclear staining, whereas all CI-deficient ones did not (Figure 28A).

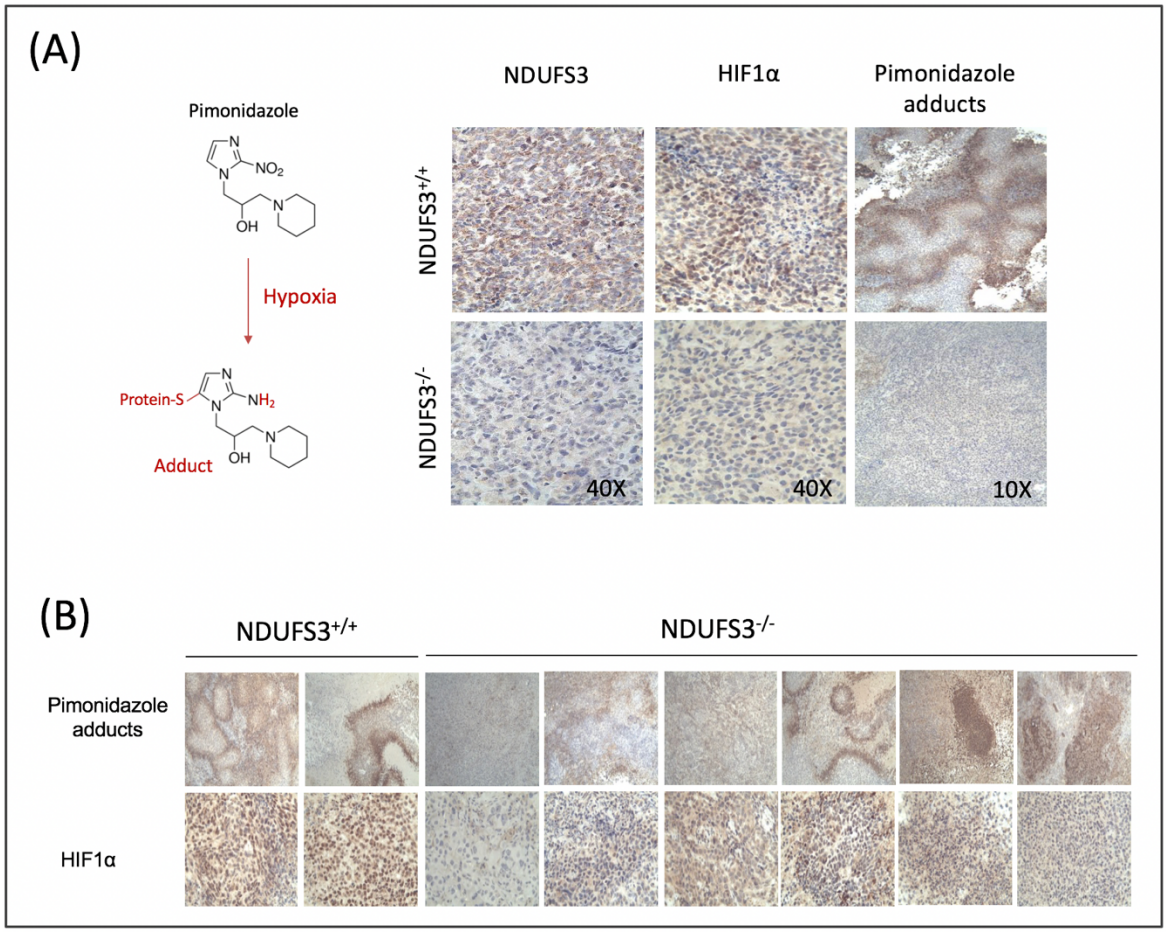

Figure 28: NDUFS3$^{-/-}$ xenografts do not stabilize HIF1α.
*(**A**) Illustration of pimonidazole adduct formation in hypoxia (left) and representative IHC staining on xenograft samples removed 38 days after cell injection, at 40X magnification (NDUFS3 and HIF1α) and at 10X magnification (pimonidazole adducts) (right). NDUFS3$^{-/-}$ xenografts do not show any positive staining for each targeted protein. (**B**) Representative IHC staining for HIF1α (40X) and pimonidazole adducts (10X) on xenograft samples removed at maximal volume. The last three NDUFS3$^{-/-}$ samples on the right show the absence of HIF1α staining despite the presence of pimonidazole adducts.*

Remarkably, however, when masses were removed at maximum volume, few NDUFS3$^{-/-}$ xenografts presented with small hypoxic areas but no stabilization of HIF1α (Figure 28B), suggesting their inability to trigger a proper response to hypoxia. Confirming the latter hypothesis, western blot analysis showed that both 143B and HCT116 NDUFS3$^{-/-}$ clones delayed HIF1 stabilization when cultured *in vitro* in hypoxia, and ultimately failed to reach the same levels than NDUFS3$^{+/+}$ with time (Figure 29A). Furthermore, upon 24 hours in hypoxia, CI-deficient cell models displayed a

significantly lower expression of HIF1-responsive genes compared to CI-competent cells (Figure 29B).

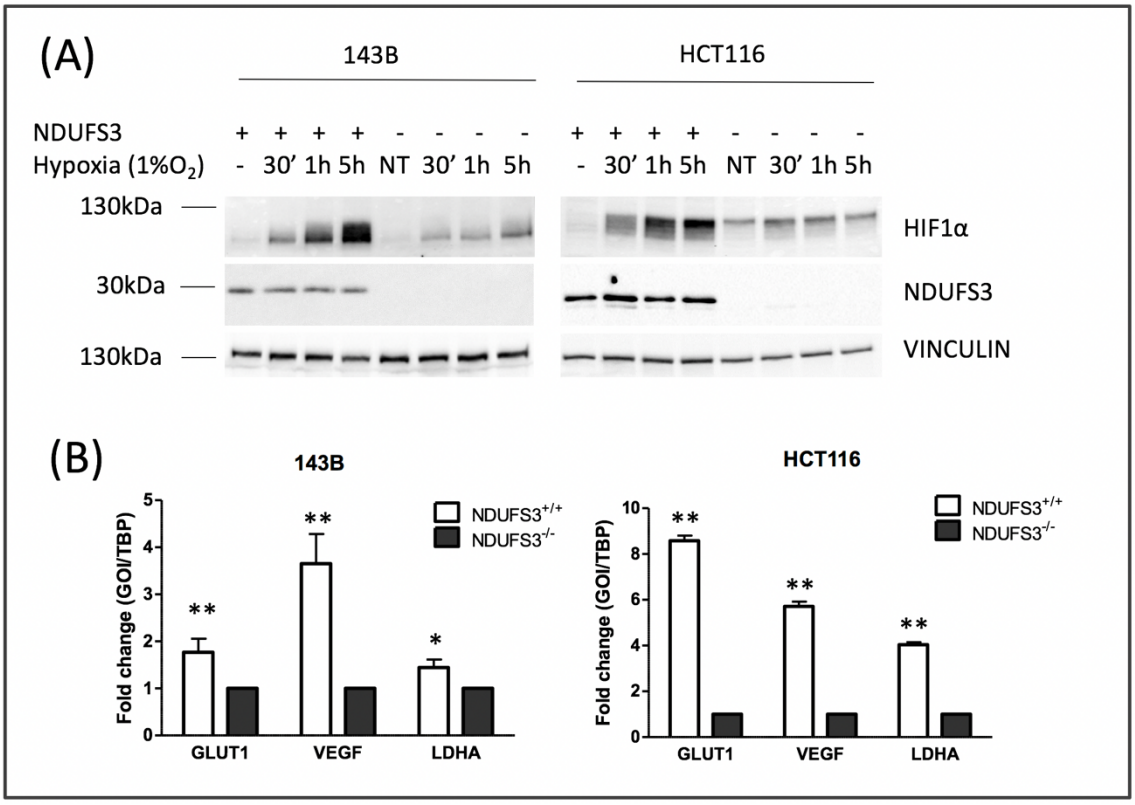

Figure 29: CI-deficient cancer cells display reduced HIF1 activation *in vitro* in hypoxia
*(**A**) SDS page followed by western blot analysis on 143B and HCT116 clones cultured in normoxia or incubated 30', 1h or 5h in hypoxia. (**B**) Real-Time PCR after total RNA extraction from cells incubated 24h in hypoxia. Data are means ± SEM = 3 samples; * P<0.05; ** P<0.01*

Overall, these data are in line with the previous studies conducted by our group that showed the pseudonormoxic feature of CI-deficient tumors, arising from their inability to stabilize HIF1α even in hypoxic condition, due to NADH accumulation and subsequent rise of α-KG levels that promote its proteasomal degradation. In line with this, carcinoscope analysis evidenced a higher $NADH/NAD^+$ ratio and increased α-KG levels in 143B $NDUFS3^{-/-}$ clones (Figure 30A and B). Moreover, after cell treatment with pimonidazole in hypoxia, western blot analysis indicated that intracellular oxygen content of $NDUFS3^{-/-}$ clones was higher than their WT counterparts, as evidenced by the weaker bands corresponding to the hypoxic adducts, despite the same extracellular level of oxygen (Figure

30C). This is in line with previous studies showing that upon ETC impairment the resulting decrease in mitochondrial oxygen consumption participate to raising its cytosolic concentration.

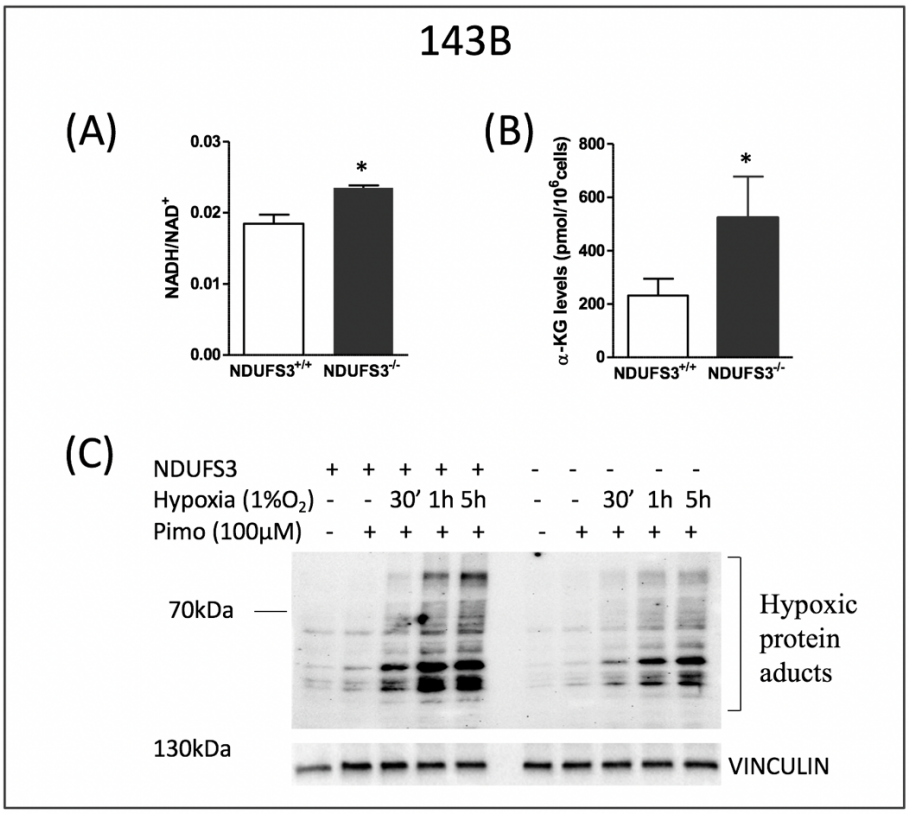

Figure 30: NDUFS3$^{-/-}$ 143B clones display a higher NADH/NAD^{+} ratio and increased intracellular levels of α-KG and oxygen

*(**A**) Determination of the NADH/NAD+ ratio and (**B**) α-KG by carcinoscope analysis in 143B clones cultured in high glucose condition. Data are means ± SEM = 3 samples; * P<0.05. (**C**) SDS page followed by western blot analysis on 143B clones cultured in normoxia or incubated 30', 1h or 5h in hypoxia, in presence or absence of pimonidazole (100µM).*

Finally, the *in vitro* measurement of H_2O_2 production in both 143B and HCT116 clones revealed that NDUFS3$^{-/-}$ cells had no increase in oxidative stress compared to the NDUFS3$^{+/+}$ clones (Figure 31). In this light, and given the inability of NDUFS3$^{-/-}$ to use the respiratory chain, it is unlikely that ROS levels may further increase upon any environmental factors *in vivo*.

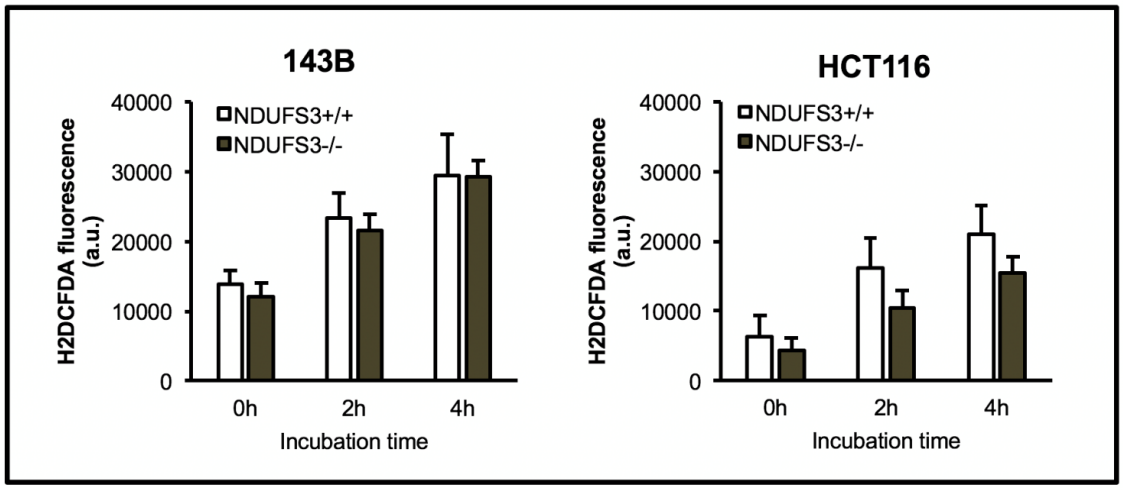

Figure 31: NDUFS3$^{-/-}$ clones do not display increased H_2O_2 production
Measurements of H_2O_2 production after cell incubation in a complete high glucose medium containing 2,7-dichlorodihydrofluorescein diacetate (H2DCFDA).

Hence, no increase in ROS production and high levels of α-KG and intracellular oxygen may, altogether, participate to activate PHDs in CI-deficient cells and xenografts, even in hypoxia (i.e. low extracellular oxygen levels). Supporting the latter hypothesis, inhibiting PHDs with DMOG in NDUFS3$^{-/-}$ clones restored HIF1α stabilization, and the inhibition of the proteasome by MG132 induced the accumulation of the hydroxylated form of HIF1α, as observed by western blot analysis (Figure 32). Altogether these data suggest that the absence of HIF1α in NDUFS3$^{-/-}$ xenografts may originate from intracellular normoxic condition and perturbation of TCA metabolite levels.

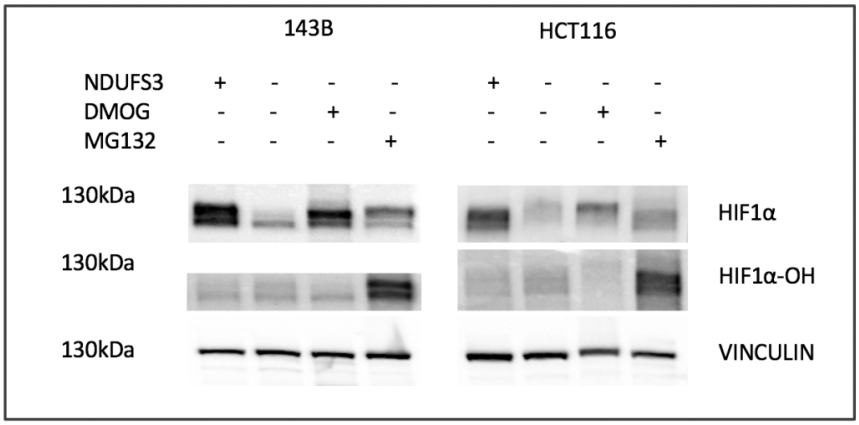

Figure 32: Destabilization of HIF1α in NDUFS3$^{-/-}$ clones is cause by its hydroxylation and subsequent proteasomal degradation.
SDS page followed by western blot analysis on 143B and HCT116 clones cultured in hypoxia and incubated with DMOG (1mM) or MG132 (10μM) for 5 hours.

CI-deficient xenografts display a tailored structure that may sustain nutrient supply.

Notwithstanding HIF1α destabilization and severe respiration impairment, NDUFS3$^{-/-}$ xenografts could sustain a low but constant proliferation rate (Figure 25A), underlying a minimal adaptation to meet the growth requirements. Additionally, as mentioned above, CI-deficient cells could sustain proliferation only when adequately supplied in nutrients that feed alternative metabolic pathways (Figure 17 and 19). In this light, the typical feature of solid tumors that is low vascularization, leading to oxygen and nutrient shortage, is expected to be highly deleterious for NDUFS3$^{-/-}$ xenografts growth and progression. Surprisingly, immunohistochemical staining directed against CD31, marker of endothelial cells, revealed that 143B NDUFS3$^{-/-}$ xenografts may be more vascularized than NDUFS3$^{+/+}$ masses (Figure 33A). Nevertheless, it is important to note that the difficulty to discriminate between mature and immature vessels may lower the relevance of this data. Pattern of vascularization were nevertheless clearly different between the two genotypes. NDUFS3$^{-/-}$ masses presented with clustered vessels that formed extended "highway" septa, while the rest of the tumor showed very little and potentially immature vessels (Figure 33B). Contrariwise, NDUFS3$^{+/+}$ xenografts showed rare, scattered but likely mature vessels that were surrounded by cancer cells that agglomerated in bulks, delimited by a hypoxic area that separated viable cells from a necrotic area (Figure 33C). Further, immunohistochemical analysis of collagen fibres by Masson's trichrome staining, revealed that 143B CI-deficient masses, and not CI-competent ones, displayed stromal invasion containing host vessels (Figure 33B and 34). Altogether, these data indicate that CI-deficient may have developed a tailored architecture to better respond to the metabolic needs that were required for their growth.

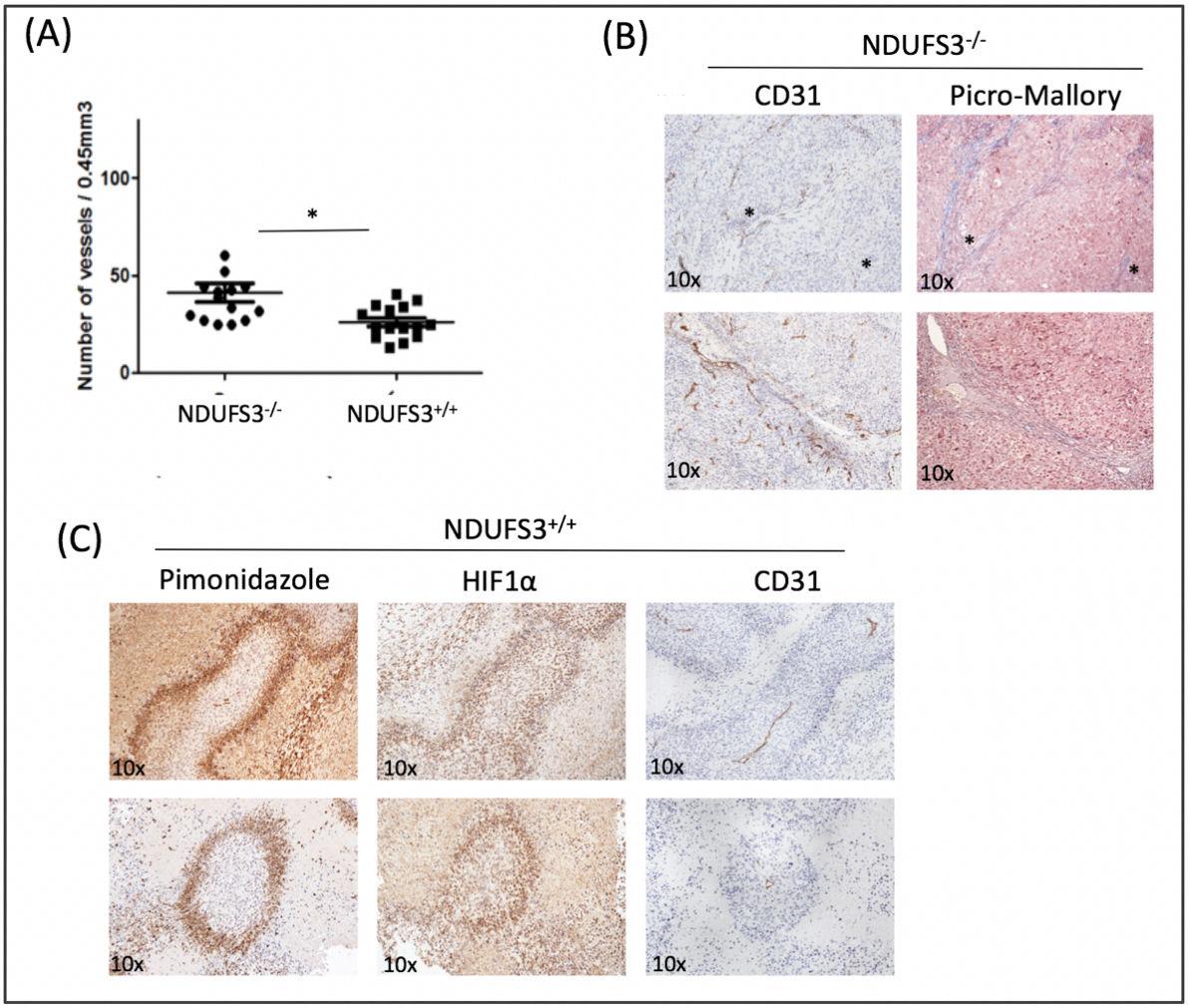

Figure 33: NDUFS3$^{+/+}$ and NDUFS3$^{-/-}$ masses display a different pattern of vascularization. *(**A**) Quantification of vessels following CD31 staining of all NDUFS3$^{+/+}$ and NDUFS3$^{-/-}$ xenografts removed 38 days after cell injection. Data are means ± SEM = 15 xenografts; * P<0.05. (**B**) Representative IHC staining for CD31 and Masson's Trichrome staining on NDUFS3$^{-/-}$ xenograft samples removed 38 days after cell injection. Upon Masson's Trichrome staining, collagen I stained in blue, cytoplasm in pink, and nuclei are in dark brown (**C**) Representative IHC staining for pimonidazole adducts, **HIF1α** and CD31 on NDUFS3$^{+/+}$ removed 38 days after cell injection.*

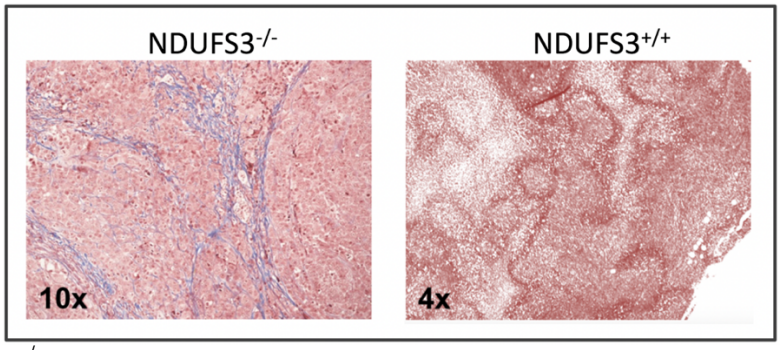

Figure 34: NDUFS3$^{-/-}$ xenografts present with stromal septa containing vessels. *Representative Masson's trichrome staining on xenograft samples removed* 38 days after cell injection. *Upon Masson's Trichrome staining, collagen I stained in blue, cytoplasm in pink, and nuclei are in dark brown.*

CI removal during tumor progression induces growth arrest

Lack of CI is associated to perturbation in oxygen, ROS and TCA cycle metabolite levels leading to HIF1α destabilization, impaired response to hypoxia, and to the trigger of alternative cell metabolic pathways and novel tumor architecture, which have most likely progressively settled during tumor progression. Despite the lack of a clear understanding of the mechanisms underlying cell metabolic and structural adaptation to both biochemical defects and environmental constraints in CI-defective xenografts, it can be expected that loss of CI during tumor progression may severely affect tumor biology, as cells may already display a specific architecture and metabolic landscape that are adapted to their bioenergetic capacity. Hence, and with the aim of reproducing better the patient situation and CI loss in oncocytomas, CI was targeted during xenografts progression.

The NDUFS3 gene, whose expression could be repressed by Dox, was reintroduced in 143B NDUFS3$^{-/-}$ clones (NDUFS3$^{-/- ind}$) (Figure 35). Re-inserting NDUFS3 in CI-deficient cells restored CI activity, which was instead suppressed upon treatment with 100ng.ml^{-1} of Dox (Figure 36). Importantly, treatment of NDUFS3$^{+/+}$ cells with Dox did not affect CI activity, confirming that the drug had no side-effect on CI assembly and activity (Figure 36).

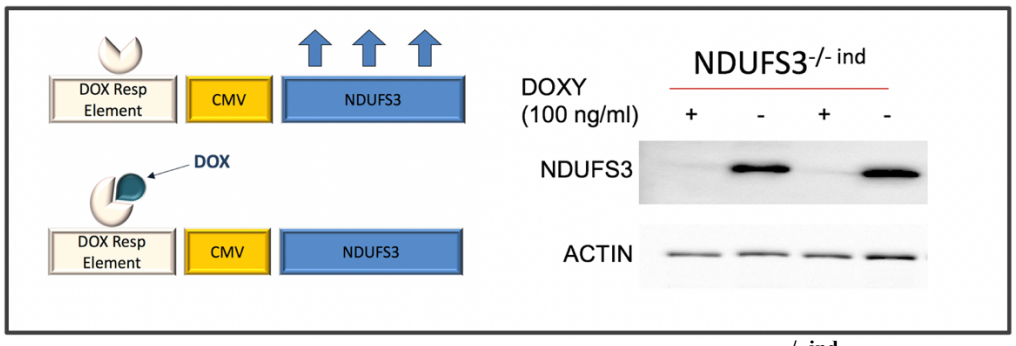

Figure 35: Doxycycline suppresses NDUFS3 expression in NDUFS3$^{-/- ind}$ cells

Simplified illustration of the vector containing NDUFS3 whose expression is mediated by a minimal CMV promoter that is under the control of a transactivator, inactivated in presence of Dox. The system is activated by Dox withdrawal (Left). SDS page followed by western blot analysis on 143B NDUFS3$^{-/- ind}$ clones incubated with or without Dox (100ng/mL) during 24hours (Right).

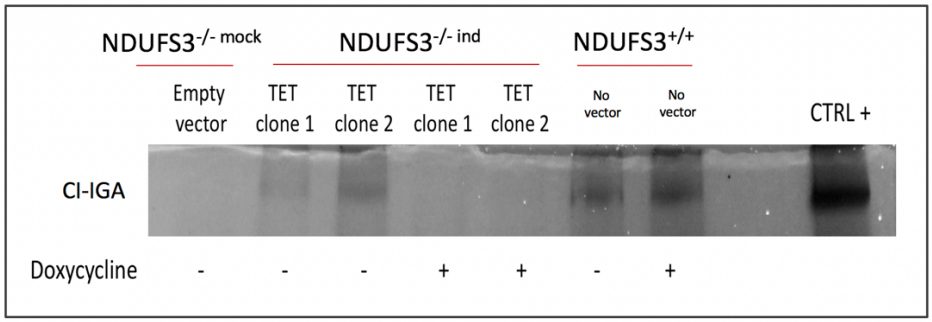

Figure 36: The reintroduction of dox-controlled NDUFS3 in NDUF3$^{-/-}$ 143B clones restores CI activity

Clear-Native PAGE followed by CI-in gel activity on NDUFS3$^{-/- mock}$ (containing an empty vector), NDUFS3$^{-/- ind}$ and NDUFS3$^{+/+}$ clones incubated without or without Dox during 9 days. Black bands appear only upon NADH oxidation by CI. Ctrl+ is a mitochondrial extract from bovin heart.

In vivo experiments without the utilization of Dox showed that the reintroduction of NDUFS3 restored the tumorigenic potential of 143B cells (Figure 37).

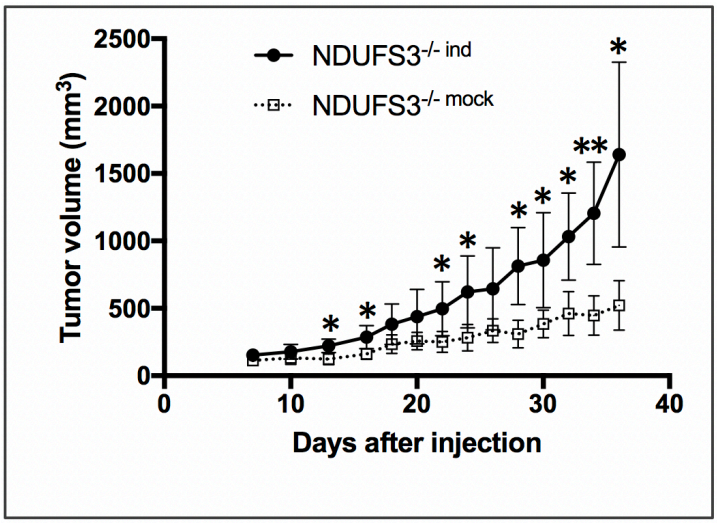

Figure 37: Re-introducing NDUFS3 restored the tumorigenic potential *in vivo*

*Xenograft growth after subcutaneous injection of NDUFS3$^{-/- ind}$ and NDUFS3$^{-/- mock}$ clones in nude mice. Data are means ± SEM ≥ 5 animals; * P<0.05; ** P<0.01.*

Contrariwise, when Dox was added to the drinking water of mice, NDUFS3$^{-/- ind}$ xenografts progressively stopped growing and mice survival was significantly increased (Figure 38A and B), while the treatment did not affect the survival of mice bearing NDUFS3$^{+/+}$ masses (Figure 38C). Immunohistochemical staining against NDUFS3 confirmed that only NDUFS3$^{-/- ind}$ showed loss of the CI subunit upon treatment with Dox (Figure 38D).

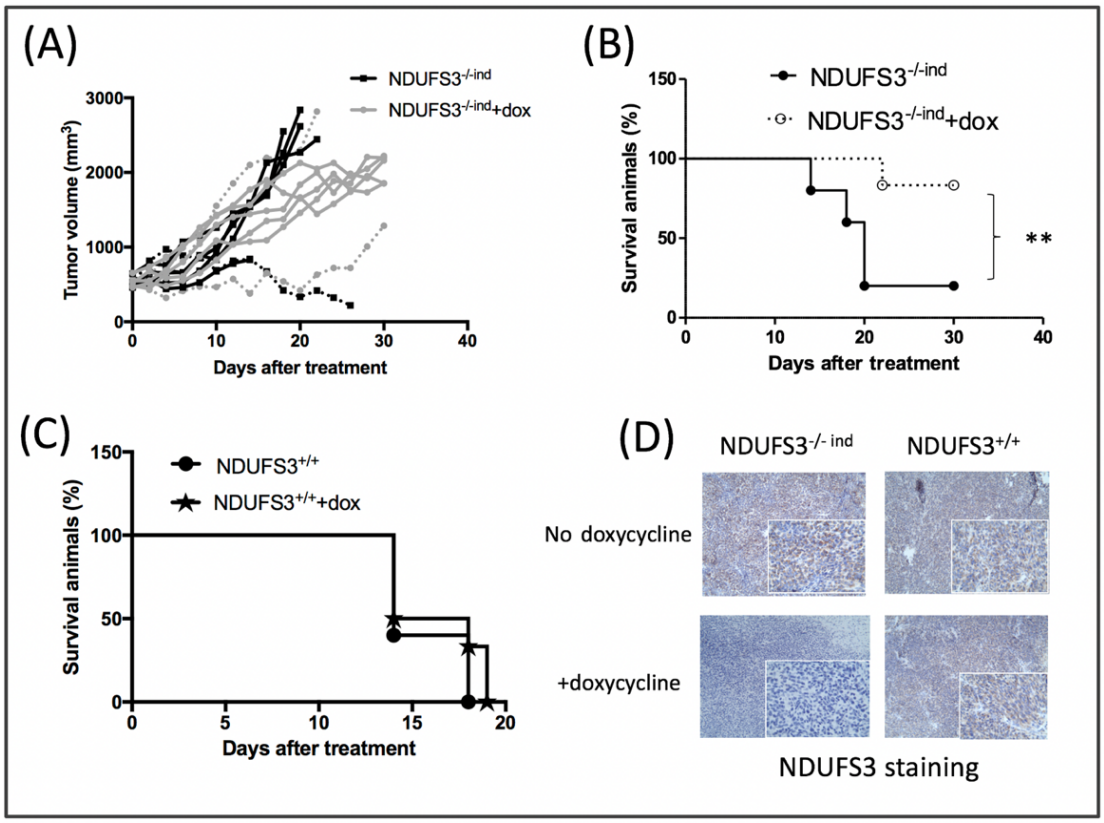

Figure 38: NDUFS3 removal induced growth arrest and increased mice survival
(A) *NDUFS3$^{-/-\ ind}$ xenografts growth and* ***(B)*** *mice survival after the addition of sucrose (3%) with or without Dox (1mg.ml^{-1}) into the drinking water of the animals.* ***(C)*** *Survival of mice bearing NDUFS3$^{+/+}$ xenografts after the addition of sucrose (3%) with or without Dox (1mg.ml^{-1}) into the drinking water of the animals.* ***(D)*** *Representative IHC staining of NDUFS3 at 10 and 40X magnification of the different xenograft samples.*

Altogether, these last data confirm the essential role of the multisubunit complex in cancer progression. While re-activating the enzyme in CI-deficient cancer cells rescued xenografts growth rate, suppressing its activity during tumor progression stopped tumor growth. In addition, the functional link between the respiratory complex and the transcription factor HIF1α is hereby demonstrated. In fact, western blot analysis on xenograft samples showed that re-inserting NDUFS3 in NDUFS3$^{-/-}$ clones rescued HIF1α stabilization, whereas its removal had the reverse effect (Figure 39). Finally, electron microscopy on xenograft samples revealed a strike difference in their ultrastructure. Tumor tissues that have lost NDUFS3 may have accumulated mitochondria with disrupted cristae and matrix rarefaction (Figure 40). The difficulty to obtain good quality samples for the ultrastructure analysis, however, did not permit to evidence any significance in the results. Overall, these data indicate that targeting NDUFS3 and thereby CI during tumor progression may

drive cancer cells to develop a more benign oncocytic phenotype, recapitulating HIF1α loss and impaired metabolic flexibility through perturbation in NADH/NAD$^+$ ratio, α-KG levels, oxygen consumption and ROS production.

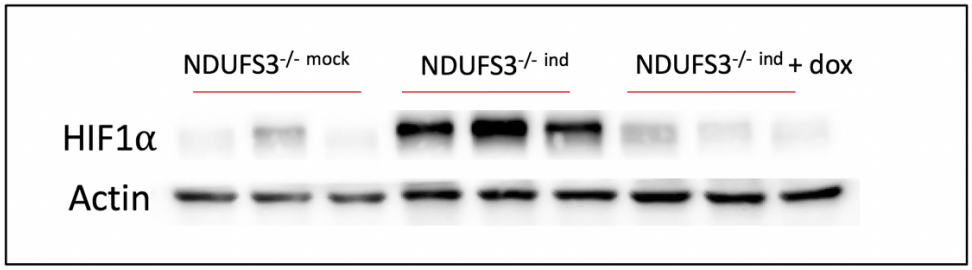

Figure 39: HIF1α stabilization strictly depends on CI activity *in vivo*
SDS page followed by western blot analysis on 3 representative xenograft samples for each group.

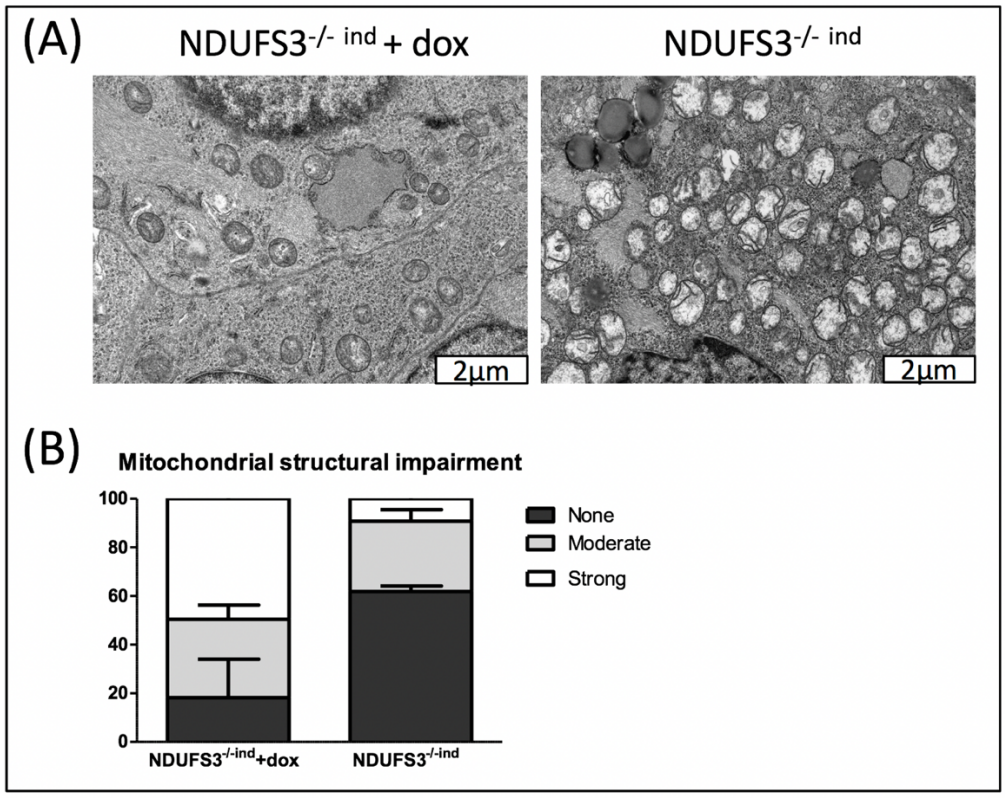

Figure 40: Loss of NDUF3 induces the accumulation of mitochondria with strong structural impairment
(A) Representative images of the ultrastructure of NDUFS3$^{-/-\ ind}$ xenograft samples treated or not with Dox. (B) Proportion of mitochondria that display moderate, strong or no mitochondrial defect. The latter was defined according to cristae morphology and matrix density. *Data are means ± SEM = 2 samples.*

DISCUSSION

Over the last two decades, the misconception that mitochondria are just bystanders in the processes of tumorigenesis has been progressively ruled out (DeBerardinis and Chandel, 2016). The unconventional case of oncocytomas offered an additional striking proof that is worthy of interest: high load of CI-disruptive mtDNA mutations are associated with a more benign tumor phenotype. Our group has previously showed that shifting mutation load from heteroplasmy towards homoplasmy resulted in a strong reduction of CI activity and a lower tumorigenic potential. Further, CI-deficient cancer cells lacked HIF1α and displayed impaired metabolic flexibility in hypoxia, while accumulating damaged mitochondria (Calabrese et al., 2013; Gasparre et al., 2011b).

In the present study, we dissected the biochemical and metabolic changes triggered upon CI loss in the osteosarcoma and intestinal cancer cell lines 143B and HCT116, respectively, with a focus on their capacity to recapitulate a benign phenotype such as the oncocytic features cited above.

Genome editing allowed us to target NDUFS3 successfully and to abolish CI and OXPHOS activity in 143B and HCT116 cells. Despite the severe respiratory deficit induced and a drop in aspartate levels, CI loss did not severely affect *in vitro* cell proliferation, nor it decreased ATP levels. Yet, this result could be obtained only when cells were cultured in nutrient rich condition, suggesting their ability to compensate CI loss by adjusting nutrient utilization. Accordingly, we observed a higher glucose consumption and the trigger of glutamine-dependent reductive carboxylation, which may have successfully permitted NDUFS3$^{-/-}$ clones to meet the anabolic and energetic requirements for proliferation. Conversely, *in vitro* and *in vivo* experiments showed that the tumorigenic potential of CI-defective cells was significantly reduced, indicating their inability to meet the metabolic requirements that support cell tumorigenic properties. Confirming our previous findings, the lack of CI was associated to an increase in the NADH/NAD^{+} ratio and to higher α-KG levels. Further, we showed that NDUFS3$^{-/-}$ clones also presented with a higher concentration of intracellular oxygen compared to NDUFS3$^{+/+}$ clones, even when cultured in condition of extracellular hypoxia. Hence, the accumulation of both α-KG and oxygen may have contributed to the significant reduction of stabilized HIF1α observed in cells and xenograft samples, which may have significantly participated

to limit cell tumorigenic potential. In line with this, we demonstrated that HIF1α redirection toward proteasomal degradation is greatly increased in CI-deficient cells. Furthermore, beside oxygen and α-KG accumulation, the inability of NDUFS3$^{-/-}$ cancer cells to generate ROS may have been one additional factor favouring PHD activation (Figure 41). Noticeably, the lack of CI and OXPHOS activity in NDUFS3$^{-/-}$ clones may have also prevented the hypoxia-mediated production of ROS. As expected, CI-deficient cells and tumors displayed a lower expression of HIF1-responsive genes compared to their WT counterparts, which indicates their inability to trigger the hypoxic response, even under low oxygen tension.

Altogether, these data revealed that although CI-deficient cells can adapt their metabolism to sustain proliferation, CI is however required to sustain cell tumorigenic properties.

Importantly, while several metabolic pathways are dispensable in mono-layer cell culture, increase evidence demonstrates that many cancer cell abilities such as cells capacity to grow anchorage-independently, to migrate and to survive their environment, may drastically modify their metabolic dependency (Davidson et al., 2016; Gui et al., 2016; Jiang et al., 2017; LeBleu et al., 2014). In this light, we do not exclude the involvement of limiting aspartate levels in the antitumorigenic effects observed in CI-defective clones. Indeed, increased nucleotide and amino acid synthesis, including aspartate, requires higher levels of NAD^+. Interestingly, upon CI inhibition, the latter may be provided through increased LDHA activity, which converts pyruvate into lactate, thereby compensating for the decrease in CI-mediated NADH oxidation (Gui et al., 2016; Vander Heiden and DeBerardinis, 2017). Hence, both the specific cell metabolic requirements and the environment may determine cancer cell dependence on NAD^+-driven metabolic routes, which may in turn determine cell sensibility to CI inhibition (Gui et al., 2016). We showed that the expression of the LDHA gene, target of HIF1, was significantly lower in CI-defective xenografts. The latter phenomenon may therefore represent an additional bioenergetic restriction that have contributed to the low xenograft growth rate observed *in vivo* (Figure 41).

Beside regulating the HIF1 pathway, it is important to note that α-KG is also a signal of amino acid availability (Durán et al., 2013). Dysregulated levels of the metabolite may have therefore further perturbed cell adaptation to nutrient limitation in CI-defective xenografts. In addition, α-KG and its derivatives may also affect the all family of Fe(II)/α-KG dependent dioxygenases, with important consequences at both metabolic and epigenetic levels. In this frame, we have recently discussed the role of α-KG in cancer progression, which can be dual, as it may promote both oncogenic and tumor suppressive functions (Vatrinet et al., 2017). Hence, the α-KG signal may contribute to the overall reprograming of cancer cell function to ensure their survival, or it may instead perturb cell response to internal and external pressures when dysregulated. Discriminating the role of the metabolite in modifying the tumorigenicity of CI-deficient cancer cells still ought to be understood more clearly.

Notwithstanding the decrease in xenografts growth rate, long term *in vivo* experiments have shown that the lack of CI did not prevent tumors formation and progression, suggesting that they have successfully met the metabolic requirements to sustain biomass production. The latter phenomenon could be explained by their ability to revise nutrient utilization, as observed *in vitro*, albeit it would have required abundant resources that are known to be limited *in vivo*. Furthermore, NDUFS3$^{-/-}$ cells displayed a lower expression of VEGF, master regulator of vascularization that is normally expressed upon HIF1 activation. Strikingly, however, CI-deficient xenografts presented with stromal invasion containing vessels, which were therefore likely to supply cells with nutrients. This finding shed light on a two-way relationship between the tumor environment and cancer cell metabolism, as each of the two may affect the other. CI-deficient cells may benefit from high levels of glucose and glutamine, the two major nutrients utilized by cancer cells, which are found in abundance in the blood (Hosios et al., 2016). Additionally, several studies have revealed the capacity of cancer cells to scavenge many extracellular molecules as proteins, acetate, fatty acids and lipids (Commisso et al., 2013; Michalopoulou et al., 2016; Palm et al., 2015). The latter mechanism is further favoured by the often poorly constructed and leaky vessels found in tumors, which may allow large complex and macromolecule as albumin and lipoprotein to feed the cells (Michalopoulou et al., 2016). Therefore,

it is plausible that CI-deficient xenografts may have rearranged their architecture to circumvent their poor metabolic flexibility. The mechanism through which CI-deficient xenografts have attracted host vessels remains to be investigated.

Finally, NDUFS3 was removed while xenograft already reached advanced development stage. In this context, we showed that xenografts arrested their growth and that CI loss induced HIF1α destabilization, hence confirming the functional link between the transcription factor and the enzymatic complex. In addition, removing NDUFS3 from xenografts have successfully recovered one key oncocytic feature that is the accumulation of defective mitochondria.

Overall, these findings indicate that targeting CI during tumor progression may redirect them towards a more benign oncocytic phenotype. While CI-deficient tumors developed tailored solution to sustain their growth, it is likely that the cell metabolic restriction induced by CI sudden loss induces cells incapacity to face the existent environmental condition, notably due to their inability to stabilize HIF1α. In the future, re-activating this transcription factor in CI-deficient xenografts and suppressing its stabilization in CI-competent ones will be useful strategies that will help to confirm the pivotal role of HIF1α loss in preventing tumor growth, together with discriminating the relative significance of CI disruption in carcinogenesis and cancer progression.

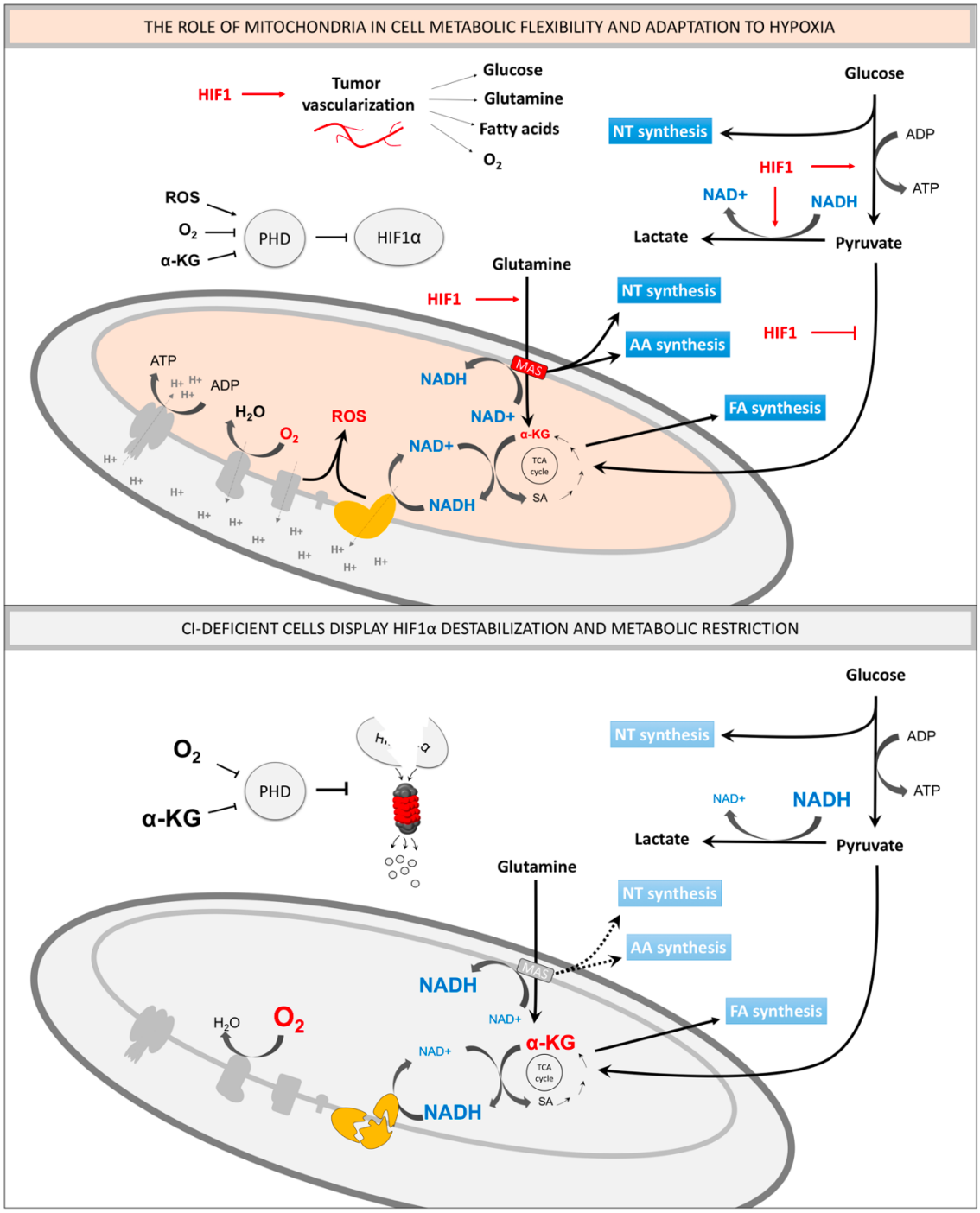

Figure 41: CI loss induces HIF1α destabilization and impair cell metabolic flexibility

ROS, O_2, and α-KG regulate HIF1α stabilization through PHD activity. The lack of ROS and the increase in the levels of O_2 and α-KG may induce HIF1α destabilization in CI-deficient cancer cells. HIF1 is a known enhancer of glycolysis, glutamine-dependant anaplerosis, and tumor vascularization, thus impaired upon CI loss. Homeostasis of NADH/NAD^+ ratio is required to drive essential biosynthetic pathways. Lack of CI may significantly reduce amino acids (AA) and NT (nucleotide) synthesis, which are dependent on mitochondrial metabolites exchange through the MAS shuttle, which is sensitive to high NADH/NAD^+ ratio. The latter may be further maintained at high levels due to limited HIF1-mediated pyruvate conversion in lactate that would partly restore NADH oxidation. Lack of OXPHOS activity may be responsible for reduced ATP levels and energetic crisis in condition of nutrient limitation.

REFERENCES

Adam-Vizi, V., and Chinopoulos, C. (2006). Bioenergetics and the formation of mitochondrial reactive oxygen species. Trends Pharmacol. Sci. *27*, 639–645.

Agarwal, N.R., Maurya, N., Pawar, J.S., and Ghosh, I. (2016). A combined approach against tumorigenesis using glucose deprivation and mitochondrial complex 1 inhibition by rotenone. Cell Biol. Int. *40*, 821–831.

Akatsuka, A., Kojima, N., Okamura, M., Dan, S., and Yamori, T. (2016). A novel thiophene-3-carboxamide analog of annonaceous acetogenin exhibits antitumor activity via inhibition of mitochondrial complex I. Pharmacol. Res. Perspect. *4*, e00246.

Alhazzazi, T.Y., Kamarajan, P., Verdin, E., and Kapila, Y.L. (2011a). SIRT3 and cancer: tumor promoter or suppressor? Biochim. Biophys. Acta *1816*, 80–88.

Alhazzazi, T.Y., Kamarajan, P., Joo, N., Huang, J.-Y., Verdin, E., D'Silva, N.J., and Kapila, Y.L. (2011b). Sirtuin-3 (SIRT3), a novel potential therapeutic target for oral cancer. Cancer *117*, 1670–1678.

Andrzejewski, S., Gravel, S.-P., Pollak, M., and St-Pierre, J. (2014). Metformin directly acts on mitochondria to alter cellular bioenergetics. Cancer Metab. *2*, 12.

Arany, Z., Huang, L.E., Eckner, R., Bhattacharya, S., Jiang, C., Goldberg, M.A., Bunn, H.F., and Livingston, D.M. (1996). An essential role for p300/CBP in the cellular response to hypoxia. Proc. Natl. Acad. Sci. U. S. A. *93*, 12969–12973.

Bastian, A., Matsuzaki, S., Humphries, K.M., Pharaoh, G.A., Doshi, A., Zaware, N., Gangjee, A., and Ihnat, M.A. (2017). AG311, a small molecule inhibitor of complex I and hypoxia-induced HIF-1α stabilization. Cancer Lett. *388*, 149–157.

Becker, C., Jick, S.S., Meier, C.R., and Bodmer, M. (2014). Metformin and the risk of head and neck cancer: a case-control analysis. Diabetes Obes. Metab. *16*, 1148–1154.

Bikas, A., Jensen, K., Patel, A., Costello, J., McDaniel, D., Klubo-Gwiezdzinska, J., Larin, O., Hoperia, V., Burman, K.D., Boyle, L., et al. (2015). Glucose-deprivation increases thyroid cancer cells sensitivity to metformin. Endocr. Relat. Cancer *22*, 919–932.

Birsoy, K., Possemato, R., Lorbeer, F.K., Bayraktar, E.C., Thiru, P., Yucel, B., Wang, T., Chen, W.W., Clish, C.B., and Sabatini, D.M. (2014). Metabolic determinants of cancer cell sensitivity to glucose limitation and biguanides. Nature *508*, 108–112.

Birsoy, K., Wang, T., Chen, W.W., Freinkman, E., Abu-Remaileh, M., and Sabatini, D.M. (2015). An Essential Role of the Mitochondrial Electron Transport Chain in Cell Proliferation Is to Enable Aspartate Synthesis. Cell *162*, 540–551.

Bradford, M.M. (1976). A rapid and sensitive method for the quantitation of microgram quantities of protein utilizing the principle of protein-dye binding. Anal. Biochem. *72*, 248–254.

Brandon, M., Baldi, P., and Wallace, D.C. (2006). Mitochondrial mutations in cancer. Oncogene *25*, 4647–4662.

Bridges, H.R., Jones, A.J.Y., Pollak, M.N., and Hirst, J. (2014). Effects of metformin and other biguanides on oxidative phosphorylation in mitochondria. Biochem. J. *462*, 475–487.

Calabrese, C., Iommarini, L., Kurelac, I., Calvaruso, M.A., Capristo, M., Lollini, P.-L., Nanni, P., Bergamini, C., Nicoletti, G., Giovanni, C.D., et al. (2013). Respiratory complex I is essential to induce a Warburg profile in mitochondria-defective tumor cells. Cancer Metab. *1*, 11.

Capecchi, M.R. (2005). Gene targeting in mice: functional analysis of the mammalian genome for the twenty-first century. Nat. Rev. Genet. *6*, 507–512.

Carossa, V., Ghelli, A., Tropeano, C.V., Valentino, M.L., Iommarini, L., Maresca, A., Caporali, L., La Morgia, C., Liguori, R., Barboni, P., et al. (2014). A novel in-frame 18-bp microdeletion in MT-CYB causes a multisystem disorder with prominent exercise intolerance. Hum. Mutat. *35*, 954–958.

Chandel, N.S., Maltepe, E., Goldwasser, E., Mathieu, C.E., Simon, M.C., and Schumacker, P.T. (1998). Mitochondrial reactive oxygen species trigger hypoxia-induced transcription. Proc. Natl. Acad. Sci. U. S. A. *95*, 11715–11720.

Chandel, N.S., McClintock, D.S., Feliciano, C.E., Wood, T.M., Melendez, J.A., Rodriguez, A.M., and Schumacker, P.T. (2000). Reactive oxygen species generated at mitochondrial complex III stabilize hypoxia-inducible factor-1alpha during hypoxia: a mechanism of O2 sensing. J. Biol. Chem. *275*, 25130–25138.

Chen, X., Qian, Y., and Wu, S. (2015). The Warburg effect: evolving interpretations of an established concept. Free Radic. Biol. Med. *79*, 253–263.

Cheong, J.-H., Park, E.S., Liang, J., Dennison, J.B., Tsavachidou, D., Nguyen-Charles, C., Wa Cheng, K., Hall, H., Zhang, D., Lu, Y., et al. (2011). Dual inhibition of tumor energy pathway by 2-deoxyglucose and metformin is effective against a broad spectrum of preclinical cancer models. Mol. Cancer Ther. *10*, 2350–2362.

Chiarugi, A., Dölle, C., Felici, R., and Ziegler, M. (2012). The NAD metabolome--a key determinant of cancer cell biology. Nat. Rev. Cancer *12*, 741–752.

Cho, H., and Kaelin, W.G. (2016). Targeting HIF2 in Clear Cell Renal Cell Carcinoma. Cold Spring Harb. Symp. Quant. Biol.

Collins, T.J. (2007). ImageJ for microscopy. BioTechniques *43*, 25–30.

Commisso, C., Davidson, S.M., Soydaner-Azeloglu, R.G., Parker, S.J., Kamphorst, J.J., Hackett, S., Grabocka, E., Nofal, M., Drebin, J.A., Thompson, C.B., et al. (2013). Macropinocytosis of protein is an amino acid supply route in Ras-transformed cells. Nature *497*, 633–637.

Conley, K.E., Kemper, W.F., and Crowther, G.J. (2001). Limits to sustainable muscle performance: interaction between glycolysis and oxidative phosphorylation. J. Exp. Biol. *204*, 3189–3194.

Crabtree, H.G. (1929). Observations on the carbohydrate metabolism of tumours. Biochem. J. *23*, 536–545.

Cuezva, J.M., Krajewska, M., de Heredia, M.L., Krajewski, S., Santamaría, G., Kim, H., Zapata, J.M., Marusawa, H., Chamorro, M., and Reed, J.C. (2002). The bioenergetic signature of cancer: a marker of tumor progression. Cancer Res. *62*, 6674–6681.

Dang, C.V. (2012). Links between metabolism and cancer. Genes Dev. *26*, 877–890.

Davar, D., Beumer, J.H., Hamieh, L., and Tawbi, H. (2012). Role of PARP Inhibitors in Cancer Biology and Therapy. Curr. Med. Chem. *19*, 3907–3921.

Davidson, S.M., Papagiannakopoulos, T., Olenchock, B.A., Heyman, J.E., Keibler, M.A., Luengo, A., Bauer, M.R., Jha, A.K., O'Brien, J.P., Pierce, K.A., et al. (2016). Environment Impacts the Metabolic Dependencies of Ras-Driven Non-Small Cell Lung Cancer. Cell Metab. *23*, 517–528.

De Luise, M., Girolimetti, G., Okere, B., Porcelli, A.M., Kurelac, I., and Gasparre, G. (2017). Molecular and metabolic features of oncocytomas: seeking the blueprints of indolent cancers. Biochim. Biophys. Acta.

DeBerardinis, R.J., and Chandel, N.S. (2016). Fundamentals of cancer metabolism. Sci. Adv. *2*, e1600200.

DeBerardinis, R.J., Mancuso, A., Daikhin, E., Nissim, I., Yudkoff, M., Wehrli, S., and Thompson, C.B. (2007). Beyond aerobic glycolysis: transformed cells can engage in glutamine metabolism that exceeds the requirement for protein and nucleotide synthesis. Proc. Natl. Acad. Sci. U. S. A. *104*, 19345–19350.

DeBerardinis, R.J., Sayed, N., Ditsworth, D., and Thompson, C.B. (2008). Brick by brick: metabolism and tumor cell growth. Curr. Opin. Genet. Dev. *18*, 54–61.

Denko, N.C. (2008). Hypoxia, HIF1 and glucose metabolism in the solid tumour. Nat. Rev. Cancer *8*, 705–713.

Depping, R., Steinhoff, A., Schindler, S.G., Friedrich, B., Fagerlund, R., Metzen, E., Hartmann, E., and Köhler, M. (2008). Nuclear translocation of hypoxia-inducible factors (HIFs): Involvement of the classical importin α/β pathway. Biochim. Biophys. Acta BBA - Mol. Cell Res. *1783*, 394–404.

Dulaney, C., Marcrom, S., Stanley, J., and Yang, E.S. (2017). Poly(ADP-ribose) polymerase activity and inhibition in cancer. Semin. Cell Dev. Biol.

Durán, R.V., MacKenzie, E.D., Boulahbel, H., Frezza, C., Heiserich, L., Tardito, S., Bussolati, O., Rocha, S., Hall, M.N., and Gottlieb, E. (2013). HIF-independent role of prolyl hydroxylases in the cellular response to amino acids. Oncogene *32*, 4549–4556.

Ellinger, J., Poss, M., Brüggemann, M., Gromes, A., Schmidt, D., Ellinger, N., Tolkach, Y., Dietrich, D., Kristiansen, G., and Müller, S.C. (2016). Systematic Expression Analysis of Mitochondrial Complex I Identifies NDUFS1 as a Biomarker in Clear-Cell Renal-Cell Carcinoma. Clin. Genitourin. Cancer.

Emerling, B.M., Platanias, L.C., Black, E., Nebreda, A.R., Davis, R.J., and Chandel, N.S. (2005). Mitochondrial reactive oxygen species activation of p38 mitogen-activated protein kinase is required for hypoxia signaling. Mol. Cell. Biol. *25*, 4853–4862.

Evans, J.M.M., Donnelly, L.A., Emslie-Smith, A.M., Alessi, D.R., and Morris, A.D. (2005). Metformin and reduced risk of cancer in diabetic patients. BMJ *330*, 1304–1305.

Farmer, R.E., Ford, D., Forbes, H.J., Chaturvedi, N., Kaplan, R., Smeeth, L., and Bhaskaran, K. (2016). Metformin and cancer in type 2 diabetes: a systematic review and comprehensive bias evaluation. Int. J. Epidemiol.

Faubert, B., Boily, G., Izreig, S., Griss, T., Samborska, B., Dong, Z., Dupuy, F., Chambers, C., Fuerth, B.J., Viollet, B., et al. (2013). AMPK is a negative regulator of the Warburg effect and suppresses tumor growth in vivo. Cell Metab. *17*, 113–124.

Favier, J., Lapointe, S., Maliba, R., and Sirois, M.G. (2007). HIF2 alpha reduces growth rate but promotes angiogenesis in a mouse model of neuroblastoma. BMC Cancer *7*, 139.

Fendt, S.-M., Bell, E.L., Keibler, M.A., Olenchock, B.A., Mayers, J.R., Wasylenko, T.M., Vokes, N.I., Guarente, L., Vander Heiden, M.G., and Stephanopoulos, G. (2013). Reductive glutamine metabolism is a function of the α-ketoglutarate to citrate ratio in cells. Nat. Commun. *4*, 2236.

Finley, L.W.S., Carracedo, A., Lee, J., Souza, A., Egia, A., Zhang, J., Teruya-Feldstein, J., Moreira, P.I., Cardoso, S.M., Clish, C.B., et al. (2011). SIRT3 opposes reprogramming of cancer cell metabolism through HIF1α destabilization. Cancer Cell *19*, 416–428.

Friedman, J.R., and Nunnari, J. (2014). Mitochondrial form and function. Nature *505*, 335–343.

Gaj, T., Gersbach, C.A., and Barbas, C.F. (2013). ZFN, TALEN and CRISPR/Cas-based methods for genome engineering. Trends Biotechnol. *31*, 397–405.

Galanis, A., Pappa, A., Giannakakis, A., Lanitis, E., Dangaj, D., and Sandaltzopoulos, R. (2008). Reactive oxygen species and HIF-1 signalling in cancer. Cancer Lett. *266*, 12–20.

Gallez, B., Neveu, M.-A., Danhier, P., and Jordan, B.F. (2017). Manipulation of tumor oxygenation and radiosensitivity through modification of cell respiration. A critical review of approaches and imaging biomarkers for therapeutic guidance. Biochim. Biophys. Acta.

Gasparre, G., Iommarini, L., Porcelli, A.M., Lang, M., Ferri, G.G., Kurelac, I., Zuntini, R., Mariani, E., Pennisi, L.F., Pasquini, E., et al. (2009). An inherited mitochondrial DNA disruptive mutation shifts to homoplasmy in oncocytic tumor cells. Hum. Mutat. *30*, 391–396.

Gasparre, G., Romeo, G., Rugolo, M., and Porcelli, A.M. (2011a). Learning from oncocytic tumors: Why choose inefficient mitochondria? Biochim. Biophys. Acta *1807*, 633–642.

Gasparre, G., Kurelac, I., Capristo, M., Iommarini, L., Ghelli, A., Ceccarelli, C., Nicoletti, G., Nanni, P., De Giovanni, C., Scotlandi, K., et al. (2011b). A mutation threshold distinguishes the antitumorigenic effects of the mitochondrial gene MTND1, an oncojanus function. Cancer Res. *71*, 6220–6229.

Gatenby, R.A., and Gillies, R.J. (2004). Why do cancers have high aerobic glycolysis? Nat. Rev. Cancer *4*, 891–899.

George, J., and Ahmad, N. (2016). Mitochondrial Sirtuins in Cancer: Emerging Roles and Therapeutic Potential. Cancer Res. *76*, 2500–2506.

Ghelli, A., Zanna, C., Porcelli, A.M., Schapira, A.H.V., Martinuzzi, A., Carelli, V., and Rugolo, M. (2003). Leber's hereditary optic neuropathy (LHON) pathogenic mutations induce mitochondrial-dependent apoptotic death in transmitochondrial cells incubated with galactose medium. J. Biol. Chem. *278*, 4145–4150.

Ghelli, A., Tropeano, C.V., Calvaruso, M.A., Marchesini, A., Iommarini, L., Porcelli, A.M., Zanna, C., De Nardo, V., Martinuzzi, A., Wibrand, F., et al. (2013). The cytochrome b p.278Y>C mutation causative of a multisystem disorder enhances superoxide production and alters supramolecular interactions of respiratory chain complexes. Hum. Mol. Genet. *22*, 2141–2151.

Giorgio, M., Trinei, M., Migliaccio, E., and Pelicci, P.G. (2007). Hydrogen peroxide: a metabolic by-product or a common mediator of ageing signals? Nat. Rev. Mol. Cell Biol. *8*, 722–728.

Griss, T., Vincent, E.E., Egnatchik, R., Chen, J., Ma, E.H., Faubert, B., Viollet, B., DeBerardinis, R.J., and Jones, R.G. (2015). Metformin Antagonizes Cancer Cell Proliferation by Suppressing Mitochondrial-Dependent Biosynthesis. PLOS Biol. *13*, e1002309.

Guerrero-Castillo, S., Baertling, F., Kownatzki, D., Wessels, H.J., Arnold, S., Brandt, U., and Nijtmans, L. (2017). The Assembly Pathway of Mitochondrial Respiratory Chain Complex I. Cell Metab. *25*, 128–139.

Gui, D.Y., Sullivan, L.B., Luengo, A., Hosios, A.M., Bush, L.N., Gitego, N., Davidson, S.M., Freinkman, E., Thomas, C.J., and Vander Heiden, M.G. (2016). Environment Dictates Dependence on Mitochondrial Complex I for NAD+ and Aspartate Production and Determines Cancer Cell Sensitivity to Metformin. Cell Metab. *24*, 716–727.

Guo, J.Y., Chen, H.-Y., Mathew, R., Fan, J., Strohecker, A.M., Karsli-Uzunbas, G., Kamphorst, J.J., Chen, G., Lemons, J.M.S., Karantza, V., et al. (2011). Activated Ras requires autophagy to maintain oxidative metabolism and tumorigenesis. Genes Dev. *25*, 460–470.

Guzy, R.D., Hoyos, B., Robin, E., Chen, H., Liu, L., Mansfield, K.D., Simon, M.C., Hammerling, U., and Schumacker, P.T. (2005). Mitochondrial complex III is required for hypoxia-induced ROS production and cellular oxygen sensing. Cell Metab. *1*, 401–408.

Hanahan, D., and Weinberg, R.A. (2000). The hallmarks of cancer. Cell *100*, 57–70.

Hanahan, D., and Weinberg, R.A. (2011). Hallmarks of cancer: the next generation. Cell *144*, 646–674.

Harbauer, A.B., Zahedi, R.P., Sickmann, A., Pfanner, N., and Meisinger, C. (2014). The protein import machinery of mitochondria-a regulatory hub in metabolism, stress, and disease. Cell Metab. *19*, 357–372.

Hardie, D.G., Ross, F.A., and Hawley, S.A. (2012). AMPK: a nutrient and energy sensor that maintains energy homeostasis. Nat. Rev. Mol. Cell Biol. *13*, 251–262.

Helbig, L., Koi, L., Brüchner, K., Gurtner, K., Hess-Stumpp, H., Unterschemmann, K., Baumann, M., Zips, D., and Yaromina, A. (2014). BAY 87-2243, a novel inhibitor of hypoxia-induced gene activation, improves local tumor control after fractionated irradiation in a schedule-dependent manner in head and neck human xenografts. Radiat. Oncol. Lond. Engl. *9*, 207.

Herranz, D., and Serrano, M. (2010). SIRT1: recent lessons from mouse models. Nat. Rev. Cancer *10*, 819–823.

Hirsch, H.A., Iliopoulos, D., Tsichlis, P.N., and Struhl, K. (2009). Metformin selectively targets cancer stem cells, and acts together with chemotherapy to block tumor growth and prolong remission. Cancer Res. *69*, 7507–7511.

Hirst, J. (2013). Mitochondrial complex I. Annu. Rev. Biochem. *82*, 551–575.

van Horssen, R., Willemse, M., Haeger, A., Attanasio, F., Güneri, T., Schwab, A., Stock, C.M., Buccione, R., Fransen, J.A.M., and Wieringa, B. (2013). Intracellular NAD(H) levels control motility and invasion of glioma cells. Cell. Mol. Life Sci. CMLS *70*, 2175–2190.

Hosios, A.M., Hecht, V.C., Danai, L.V., Johnson, M.O., Rathmell, J.C., Steinhauser, M.L., Manalis, S.R., and Vander Heiden, M.G. (2016). Amino Acids Rather than Glucose Account for the Majority of Cell Mass in Proliferating Mammalian Cells. Dev. Cell *36*, 540–549.

Huang, D., Li, T., Li, X., Zhang, L., Sun, L., He, X., Zhong, X., Jia, D., Song, L., Semenza, G.L., et al. (2014). HIF-1-Mediated Suppression of Acyl-CoA Dehydrogenases and Fatty Acid Oxidation Is Critical for Cancer Progression. Cell Rep. *8*, 1930–1942.

Iommarini, L., Calvaruso, M.A., Kurelac, I., Gasparre, G., and Porcelli, A.M. (2013). Complex I impairment in mitochondrial diseases and cancer: parallel roads leading to different outcomes. Int. J. Biochem. Cell Biol. *45*, 47–63.

Iommarini, L., Kurelac, I., Capristo, M., Calvaruso, M.A., Giorgio, V., Bergamini, C., Ghelli, A., Nanni, P., De Giovanni, C., Carelli, V., et al. (2014). Different mtDNA mutations modify tumor progression in dependence of the degree of respiratory complex I impairment. Hum. Mol. Genet. *23*, 1453–1466.

Ishikawa, K., Takenaga, K., Akimoto, M., Koshikawa, N., Yamaguchi, A., Imanishi, H., Nakada, K., Honma, Y., and Hayashi, J.-I. (2008). ROS-generating mitochondrial DNA mutations can regulate tumor cell metastasis. Science *320*, 661–664.

Jain, R.K., Munn, L.L., and Fukumura, D. (2002). Dissecting tumour pathophysiology using intravital microscopy. Nat. Rev. Cancer *2*, 266–276.

Jeong, S.M., Hwang, S., and Seong, R.H. (2016). SIRT4 regulates cancer cell survival and growth after stress. Biochem. Biophys. Res. Commun. *470*, 251–256.

Jiang, Z.-F., Wang, M., Xu, J.-L., and Ning, Y.-J. (2017). Hypoxia promotes mitochondrial glutamine metabolism through HIF1α-GDH pathway in human lung cancer cells. Biochem. Biophys. Res. Commun. *483*, 32–38.

Jones, D.P. (1981). Determination of pyridine dinucleotides in cell extracts by high-performance liquid chromatography. J. Chromatogr. *225*, 446–449.

Jones, R.G., and Thompson, C.B. (2009). Tumor suppressors and cell metabolism: a recipe for cancer growth. Genes Dev. *23*, 537–548.

Jose, C., Bellance, N., and Rossignol, R. (2011). Choosing between glycolysis and oxidative phosphorylation: a tumor's dilemma? Biochim. Biophys. Acta *1807*, 552–561.

Ju, Y.S., Alexandrov, L.B., Gerstung, M., Martincorena, I., Nik-Zainal, S., Ramakrishna, M., Davies, H.R., Papaemmanuil, E., Gundem, G., Shlien, A., et al. (2014). Origins and functional consequences of somatic mitochondrial DNA mutations in human cancer. eLife *3*.

Kirches, E. (2009). Mitochondrial and nuclear genes of mitochondrial components in cancer. Curr. Genomics *10*, 281–293.

Koopman, W.J.H., Nijtmans, L.G.J., Dieteren, C.E.J., Roestenberg, P., Valsecchi, F., Smeitink, J.A.M., and Willems, P.H.G.M. (2009). Mammalian Mitochondrial Complex I: Biogenesis, Regulation, and Reactive Oxygen Species Generation. Antioxid. Redox Signal. *12*, 1431–1470.

Kurelac, I., de Biase, D., Calabrese, C., Ceccarelli, C., Ng, C.K., Lim, R., MacKay, A., Weigelt, B., Porcelli, A.M., Reis-Filho, J.S., et al. (2015). High-resolution genomic profiling of thyroid lesions uncovers preferential copy number gains affecting mitochondrial biogenesis loci in the oncocytic variants. Am. J. Cancer Res. *5*, 1954–1971.

Lai, C.-C., Lin, P.-M., Lin, S.-F., Hsu, C.-H., Lin, H.-C., Hu, M.-L., Hsu, C.-M., and Yang, M.-Y. (2013). Altered expression of SIRT gene family in head and neck squamous cell carcinoma. Tumour Biol. J. Int. Soc. Oncodevelopmental Biol. Med. *34*, 1847–1854.

Lai, R.K.-H., Xu, I.M.-J., Chiu, D.K.-C., Tse, A.P.-W., Wei, L.L., Law, C.-T., Lee, D., Wong, C.-M., Wong, M.P., Ng, I.O.-L., et al. (2016). NDUFA4L2 Fine-tunes Oxidative Stress in Hepatocellular Carcinoma. Clin. Cancer Res. Off. J. Am. Assoc. Cancer Res. *22*, 3105–3117.

Lane, N., and Pariseau, K. (2016). The Vital Question: Energy, Evolution, and the Origins of Complex Life (Audible Studios on Brilliance Audio).

Larman, T.C., DePalma, S.R., Hadjipanayis, A.G., Cancer Genome Atlas Research Network, Protopopov, A., Zhang, J., Gabriel, S.B., Chin, L., Seidman, C.E., Kucherlapati, R., et al. (2012). Spectrum of somatic mitochondrial mutations in five cancers. Proc. Natl. Acad. Sci. U. S. A. *109*, 14087–14091.

LeBleu, V.S., O'Connell, J.T., Gonzalez Herrera, K.N., Wikman, H., Pantel, K., Haigis, M.C., de Carvalho, F.M., Damascena, A., Domingos Chinen, L.T., Rocha, R.M., et al. (2014). PGC-1α mediates mitochondrial biogenesis and oxidative phosphorylation in cancer cells to promote metastasis. Nat. Cell Biol. *16*, 992–1003, 1–15.

Lei, Y., Yi, Y., Liu, Y., Liu, X., Keller, E.T., Qian, C.-N., Zhang, J., and Lu, Y. (2017). Metformin targets multiple signaling pathways in cancer. Chin. J. Cancer *36*.

Liang, X.-J., Finkel, T., Shen, D.-W., Yin, J.-J., Aszalos, A., and Gottesman, M.M. (2008). SIRT1 contributes in part to cisplatin resistance in cancer cells by altering mitochondrial metabolism. Mol. Cancer Res. MCR *6*, 1499–1506.

Lim, J.-H., Lee, E.-S., You, H.-J., Lee, J.W., Park, J.-W., and Chun, Y.-S. (2004). Ras-dependent induction of HIF-1alpha785 via the Raf/MEK/ERK pathway: a novel mechanism of Ras-mediated tumor promotion. Oncogene *23*, 9427–9431.

Lim, S.C., Carey, K.T., and McKenzie, M. (2015). Anti-cancer analogues ME-143 and ME-344 exert toxicity by directly inhibiting mitochondrial NADH: ubiquinone oxidoreductase (Complex I). Am. J. Cancer Res. *5*, 689–701.

Liu, P., and Demple, B. (2010). DNA repair in mammalian mitochondria: Much more than we thought? Environ. Mol. Mutagen. *51*, 417–426.

Liu, L., Lan, G., Peng, L., Xie, X., Peng, F., Yu, S., Wang, Y., and Tang, X. (2016). NDUFA4L2 expression predicts poor prognosis in clear cell renal cell carcinoma patients. Ren. Fail. *38*, 1199–1205.

Loboda, A., Jozkowicz, A., and Dulak, J. (2010). HIF-1 and HIF-2 transcription factors--similar but not identical. Mol. Cells *29*, 435–442.

Lodish, H., Berk, A., Zipursky, S.L., Matsudaira, P., Baltimore, D., and Darnell, J. (2000). Proto-Oncogenes and Tumor-Suppressor Genes.

Loenarz, C., and Schofield, C.J. (2008). Expanding chemical biology of 2-oxoglutarate oxygenases. Nat. Chem. Biol. *4*, 152–156.

Lorendeau, D., Rinaldi, G., Boon, R., Spincemaille, P., Metzger, K., Jäger, C., Christen, S., Dong, X., Kuenen, S., Voordeckers, K., et al. (2016). Dual loss of succinate dehydrogenase (SDH) and complex I activity is necessary to recapitulate the metabolic phenotype of SDH mutant tumors. Metab. Eng.

Lu, C.-W., Lin, S.-C., Chen, K.-F., Lai, Y.-Y., and Tsai, S.-J. (2008). Induction of Pyruvate Dehydrogenase Kinase-3 by Hypoxia-inducible Factor-1 Promotes Metabolic Switch and Drug Resistance. J. Biol. Chem. *283*, 28106–28114.

Lu, W., Zuo, Y., Feng, Y., and Zhang, M. (2014). SIRT5 facilitates cancer cell growth and drug resistance in non-small cell lung cancer. Tumour Biol. J. Int. Soc. Oncodevelopmental Biol. Med. *35*, 10699–10705.

Lunt, S.Y., and Vander Heiden, M.G. (2011). Aerobic glycolysis: meeting the metabolic requirements of cell proliferation. Annu. Rev. Cell Dev. Biol. *27*, 441–464.

Lv, Y., Nie, S.-L., Zhou, J.-M., Liu, F., Hu, Y.-B., Jiang, J.-R., Li, N., and Liu, J.-S. (2016). Overexpression of NDUFA4L2 is associated with poor prognosis in patients with colorectal cancer. ANZ J. Surg.

MacKenzie, E.D., Selak, M.A., Tennant, D.A., Payne, L.J., Crosby, S., Frederiksen, C.M., Watson, D.G., and Gottlieb, E. (2007). Cell-permeating alpha-ketoglutarate derivatives alleviate pseudohypoxia in succinate dehydrogenase-deficient cells. Mol. Cell. Biol. *27*, 3282–3289.

Mannella, C.A., Lederer, W.J., and Jafri, M.S. (2013). The connection between inner membrane topology and mitochondrial function. J. Mol. Cell. Cardiol. *62*, 51–57.

Marin-Valencia, I., Yang, C., Mashimo, T., Cho, S., Baek, H., Yang, X.-L., Rajagopalan, K.N., Maddie, M., Vemireddy, V., Zhao, Z., et al. (2012). Analysis of tumor metabolism reveals mitochondrial glucose oxidation in genetically diverse human glioblastomas in the mouse brain in vivo. Cell Metab. *15*, 827–837.

Martin-Montalvo, A., and de Cabo, R. (2013). Mitochondrial metabolic reprogramming induced by calorie restriction. Antioxid. Redox Signal. *19*, 310–320.

Mayr, J.A., Meierhofer, D., Zimmermann, F., Feichtinger, R., Kögler, C., Ratschek, M., Schmeller, N., Sperl, W., and Kofler, B. (2008). Loss of complex I due to mitochondrial DNA mutations in renal oncocytoma. Clin. Cancer Res. Off. J. Am. Assoc. Cancer Res. *14*, 2270–2275.

McDonough, M.A., Loenarz, C., Chowdhury, R., Clifton, I.J., and Schofield, C.J. (2010). Structural studies on human 2-oxoglutarate dependent oxygenases. Curr. Opin. Struct. Biol. *20*, 659–672.

Metallo, C.M., Gameiro, P.A., Bell, E.L., Mattaini, K.R., Yang, J., Hiller, K., Jewell, C.M., Johnson, Z.R., Irvine, D.J., Guarente, L., et al. (2011). Reductive glutamine metabolism by IDH1 mediates lipogenesis under hypoxia. Nature *481*, 380–384.

Michalopoulou, E., Bulusu, V., and Kamphorst, J.J. (2016). Metabolic scavenging by cancer cells: when the going gets tough, the tough keep eating. Br. J. Cancer *115*, 635–640.

Minton, D.R., Fu, L., Mongan, N.P., Shevchuk, M.M., Nanus, D.M., and Gudas, L.J. (2016). Role of NADH Dehydrogenase (Ubiquinone) 1 Alpha Subcomplex 4-Like 2 in Clear Cell Renal Cell Carcinoma. Clin. Cancer Res. Off. J. Am. Assoc. Cancer Res. *22*, 2791–2801.

Morin, A., Letouzé, E., Gimenez-Roqueplo, A.-P., and Favier, J. (2014). Oncometabolites-driven tumorigenesis: From genetics to targeted therapy. Int. J. Cancer *135*, 2237–2248.

Morscher, R.J., Aminzadeh-Gohari, S., Feichtinger, R.G., Mayr, J.A., Lang, R., Neureiter, D., Sperl, W., and Kofler, B. (2015). Inhibition of Neuroblastoma Tumor Growth by Ketogenic Diet and/or Calorie Restriction in a CD1-Nu Mouse Model. PloS One *10*, e0129802.

Mottet, D., Dumont, V., Deccache, Y., Demazy, C., Ninane, N., Raes, M., and Michiels, C. (2003). Regulation of hypoxia-inducible factor-1alpha protein level during hypoxic conditions by the phosphatidylinositol 3-kinase/Akt/glycogen synthase kinase 3beta pathway in HepG2 cells. J. Biol. Chem. *278*, 31277–31285.

Mullen, A.R., Hu, Z., Shi, X., Jiang, L., Boroughs, L.K., Kovacs, Z., Boriack, R., Rakheja, D., Sullivan, L.B., Linehan, W.M., et al. (2014). Oxidation of alpha-ketoglutarate is required for reductive carboxylation in cancer cells with mitochondrial defects. Cell Rep. *7*, 1679–1690.

Murphy, M.P. (2009). How mitochondria produce reactive oxygen species. Biochem. J. *417*, 1–13.

Nelson, U.D.L., and Cox, U.M.M. (2017). Lehninger Principles of Biochemistry (W. H. Freeman).

Niehr, F., von Euw, E., Attar, N., Guo, D., Matsunaga, D., Sazegar, H., Ng, C., Glaspy, J.A., Recio, J.A., Lo, R.S., et al. (2011). Combination therapy with vemurafenib (PLX4032/RG7204) and metformin in melanoma cell lines with distinct driver mutations. J. Transl. Med. *9*, 76.

Palm, W., Park, Y., Wright, K., Pavlova, N.N., Tuveson, D.A., and Thompson, C.B. (2015). The Utilization of Extracellular Proteins as Nutrients Is Suppressed by mTORC1. Cell *162*, 259–270.

Palorini, R., Simonetto, T., Cirulli, C., and Chiaradonna, F. (2013). Mitochondrial complex I inhibitors and forced oxidative phosphorylation synergize in inducing cancer cell death. Int. J. Cell Biol. *2013*, 243876.

Park, J.S., Sharma, L.K., Li, H., Xiang, R., Holstein, D., Wu, J., Lechleiter, J., Naylor, S.L., Deng, J.J., Lu, J., et al. (2009). A heteroplasmic, not homoplasmic, mitochondrial DNA mutation promotes tumorigenesis via alteration in reactive oxygen species generation and apoptosis. Hum. Mol. Genet. *18*, 1578–1589.

Pereira, L., Soares, P., Máximo, V., and Samuels, D.C. (2012). Somatic mitochondrial DNA mutations in cancer escape purifying selection and high pathogenicity mutations lead to the oncocytic phenotype: pathogenicity analysis of reported somatic mtDNA mutations in tumors. BMC Cancer *12*, 53.

Pollard, P.J., Brière, J.J., Alam, N.A., Barwell, J., Barclay, E., Wortham, N.C., Hunt, T., Mitchell, M., Olpin, S., Moat, S.J., et al. (2005). Accumulation of Krebs cycle intermediates and over-expression of HIF1alpha in tumours which result from germline FH and SDH mutations. Hum. Mol. Genet. *14*, 2231–2239.

Pouysségur, J., and Mechta-Grigoriou, F. (2006). Redox regulation of the hypoxia-inducible factor. Biol. Chem. *387*, 1337–1346.

Ray, P.D., Huang, B.-W., and Tsuji, Y. (2012). Reactive oxygen species (ROS) homeostasis and redox regulation in cellular signaling. Cell. Signal. *24*, 981–990.

Rodríguez-Enríquez, S., Carreño-Fuentes, L., Gallardo-Pérez, J.C., Saavedra, E., Quezada, H., Vega, A., Marín-Hernández, A., Olín-Sandoval, V., Torres-Márquez, M.E., and Moreno-Sánchez, R. (2010). Oxidative phosphorylation is impaired by prolonged hypoxia in breast and possibly in cervix carcinoma. Int. J. Biochem. Cell Biol. *42*, 1744–1751.

Rose, N.R., McDonough, M.A., King, O.N.F., Kawamura, A., and Schofield, C.J. (2011). Inhibition of 2-oxoglutarate dependent oxygenases. Chem. Soc. Rev. *40*, 4364–4397.

Sánchez-Aragó, M., Chamorro, M., and Cuezva, J.M. (2010). Selection of cancer cells with repressed mitochondria triggers colon cancer progression. Carcinogenesis *31*, 567–576.

Schöckel, L., Glasauer, A., Basit, F., Bitschar, K., Truong, H., Erdmann, G., Algire, C., Hägebarth, A., Willems, P.H., Kopitz, C., et al. (2015). Targeting mitochondrial complex I using BAY 87-2243 reduces melanoma tumor growth. Cancer Metab. *3*, 11.

Selak, M.A., Armour, S.M., MacKenzie, E.D., Boulahbel, H., Watson, D.G., Mansfield, K.D., Pan, Y., Simon, M.C., Thompson, C.B., and Gottlieb, E. (2005). Succinate links TCA cycle dysfunction to oncogenesis by inhibiting HIF-alpha prolyl hydroxylase. Cancer Cell *7*, 77–85.

Semenza, G.L. (2007). Hypoxia-inducible factor 1 (HIF-1) pathway. Sci. STKE Signal Transduct. Knowl. Environ. *2007*, cm8.

Semenza, G.L. (2013). HIF-1 mediates metabolic responses to intratumoral hypoxia and oncogenic mutations. J. Clin. Invest. *123*, 3664–3671.

Sharma, L.K., Fang, H., Liu, J., Vartak, R., Deng, J., and Bai, Y. (2011). Mitochondrial respiratory complex I dysfunction promotes tumorigenesis through ROS alteration and AKT activation. Hum. Mol. Genet. *20*, 4605–4616.

Shen, H.-M., and Liu, Z. (2006). JNK signaling pathway is a key modulator in cell death mediated by reactive oxygen and nitrogen species. Free Radic. Biol. Med. *40*, 928–939.

Simonnet, H., Demont, J., Pfeiffer, K., Guenaneche, L., Bouvier, R., Brandt, U., Schägger, H., and Godinot, C. (2003). Mitochondrial complex I is deficient in renal oncocytomas. Carcinogenesis *24*, 1461–1466.

Smeitink, J., van den Heuvel, L., and DiMauro, S. (2001). The genetics and pathology of oxidative phosphorylation. Nat. Rev. Genet. *2*, 342–352.

Smolková, K., Bellance, N., Scandurra, F., Génot, E., Gnaiger, E., Plecitá-Hlavatá, L., Jezek, P., and Rossignol, R. (2010). Mitochondrial bioenergetic adaptations of breast cancer cells to aglycemia and hypoxia. J. Bioenerg. Biomembr. *42*, 55–67.

Smolková, K., Plecitá-Hlavatá, L., Bellance, N., Benard, G., Rossignol, R., and Ježek, P. (2011). Waves of gene regulation suppress and then restore oxidative phosphorylation in cancer cells. Int. J. Biochem. Cell Biol. *43*, 950–968.

Su, C.-Y., Chang, Y.-C., Yang, C.-J., Huang, M.-S., and Hsiao, M. (2016). The opposite prognostic effect of NDUFS1 and NDUFS8 in lung cancer reflects the oncojanus role of mitochondrial complex I. Sci. Rep. *6*, 31357.

Sullivan, L.B., Gui, D.Y., Hosios, A.M., Bush, L.N., Freinkman, E., and Vander Heiden, M.G. (2015). Supporting Aspartate Biosynthesis Is an Essential Function of Respiration in Proliferating Cells. Cell *162*, 552–563.

Sun, R.C., and Denko, N.C. (2014). Hypoxic regulation of glutamine metabolism through HIF1 and SIAH2 supports lipid synthesis that is necessary for tumor growth. Cell Metab. *19*, 285–292.

Szatrowski, T.P., and Nathan, C.F. (1991). Production of large amounts of hydrogen peroxide by human tumor cells. Cancer Res. *51*, 794–798.

Tello, D., Balsa, E., Acosta-Iborra, B., Fuertes-Yebra, E., Elorza, A., Ordóñez, Á., Corral-Escariz, M., Soro, I., López-Bernardo, E., Perales-Clemente, E., et al. (2011). Induction of the Mitochondrial NDUFA4L2 Protein by HIF-1α Decreases Oxygen Consumption by Inhibiting Complex I Activity. Cell Metab. *14*, 768–779.

Tennant, D.A., Frezza, C., MacKenzie, E.D., Nguyen, Q.D., Zheng, L., Selak, M.A., Roberts, D.L., Dive, C., Watson, D.G., Aboagye, E.O., et al. (2009). Reactivating HIF prolyl hydroxylases under hypoxia results in metabolic catastrophe and cell death. Oncogene *28*, 4009–4021.

Trachootham, D., Lu, W., Ogasawara, M.A., Valle, N.R.-D., and Huang, P. (2008). Redox Regulation of Cell Survival. Antioxid. Redox Signal. *10*, 1343–1374.

Trounce, I.A., Kim, Y.L., Jun, A.S., and Wallace, D.C. (1996). Assessment of mitochondrial oxidative phosphorylation in patient muscle biopsies, lymphoblasts, and transmitochondrial cell lines. Methods Enzymol. *264*, 484–509.

Urnov, F.D., Rebar, E.J., Holmes, M.C., Zhang, H.S., and Gregory, P.D. (2010). Genome editing with engineered zinc finger nucleases. Nat. Rev. Genet. *11*, 636–646.

Vander Heiden, M.G. (2011). Targeting cancer metabolism: a therapeutic window opens. Nat. Rev. Drug Discov. *10*, 671–684.

Vander Heiden, M.G., and DeBerardinis, R.J. (2017). Understanding the Intersections between Metabolism and Cancer Biology. Cell *168*, 657–669.

Vatrinet, R., Iommarini, L., Kurelac, I., De Luise, M., Gasparre, G., and Porcelli, A.M. (2015). Targeting respiratory complex I to prevent the Warburg effect. Int. J. Biochem. Cell Biol. *63*, 41–45.

Vatrinet, R., Leone, G., De Luise, M., Girolimetti, G., Vidone, M., Gasparre, G., and Porcelli, A.M. (2017). The α-ketoglutarate dehydrogenase complex in cancer metabolic plasticity. Cancer Metab. *5*, 3.

Villani, L.A., Smith, B.K., Marcinko, K., Ford, R.J., Broadfield, L.A., Green, A.E., Houde, V.P., Muti, P., Tsakiridis, T., and Steinberg, G.R. (2016). The diabetes medication Canagliflozin reduces cancer cell proliferation by inhibiting mitochondrial complex-I supported respiration. Mol. Metab. *5*, 1048–1056.

Wang, W., Fang, H., Groom, L., Cheng, A., Zhang, W., Liu, J., Wang, X., Li, K., Han, P., Zheng, M., et al. (2008). Superoxide flashes in single mitochondria. Cell *134*, 279–290.

Warburg, O., Wind, F., and Negelein, E. (1927). THE METABOLISM OF TUMORS IN THE BODY. J. Gen. Physiol. *8*, 519–530.

Wheaton, W.W., Weinberg, S.E., Hamanaka, R.B., Soberanes, S., Sullivan, L.B., Anso, E., Glasauer, A., Dufour, E., Mutlu, G.M., Budigner, G.S., et al. (2014). Metformin inhibits mitochondrial complex I of cancer cells to reduce tumorigenesis. eLife *3*, e02242.

Wise, D.R., Ward, P.S., Shay, J.E.S., Cross, J.R., Gruber, J.J., Sachdeva, U.M., Platt, J.M., DeMatteo, R.G., Simon, M.C., and Thompson, C.B. (2011). Hypoxia promotes isocitrate dehydrogenase-dependent carboxylation of α-ketoglutarate to citrate to support cell growth and viability. Proc. Natl. Acad. Sci. U. S. A. *108*, 19611–19616.

Wolf, D.A. (2014). Is reliance on mitochondrial respiration a “chink in the armor” of therapy-resistant cancer? Cancer Cell *26*, 788–795.

Xu, W., Yang, H., Liu, Y., Yang, Y., Wang, P., Kim, S.-H., Ito, S., Yang, C., Wang, P., Xiao, M.-T., et al. (2011). Oncometabolite 2-hydroxyglutarate is a competitive inhibitor of α-ketoglutarate-dependent dioxygenases. Cancer Cell *19*, 17–30.

Yang, B., Fu, X., Shao, L., Ding, Y., and Zeng, D. (2014). Aberrant expression of SIRT3 is conversely correlated with the progression and prognosis of human gastric cancer. Biochem. Biophys. Res. Commun. *443*, 156–160.

Yuan, H., Su, L., and Chen, W.Y. (2013a). The emerging and diverse roles of sirtuins in cancer: a clinical perspective. OncoTargets Ther. *6*, 1399–1416.

Yuan, P., Ito, K., Perez-Lorenzo, R., Guzzo, C.D., Lee, J.H., Shen, C.-H., Bosenberg, M.W., McMahon, M., Cantley, L.C., and Zheng, B. (2013b). Phenformin enhances the therapeutic benefit of BRAFV600E inhibition in melanoma. Proc. Natl. Acad. Sci. *110*, 18226–18231.

Zannella, V.E., Dal Pra, A., Muaddi, H., McKee, T.D., Stapleton, S., Sykes, J., Glicksman, R., Chaib, S., Zamiara, P., Milosevic, M., et al. (2013). Reprogramming metabolism with metformin improves tumor oxygenation and radiotherapy response. Clin. Cancer Res. Off. J. Am. Assoc. Cancer Res. *19*, 6741–6750.

Zhu, A., Lee, D., and Shim, H. (2011). Metabolic PET Imaging in Cancer Detection and Therapy Response. Semin. Oncol. *38*, 55–69.

Zhu, J., Vinothkumar, K.R., and Hirst, J. (2016). Structure of mammalian respiratory complex I. Nature *536*, 354–358.

Zimmermann, F.A., Mayr, J.A., Feichtinger, R., Neureiter, D., Lechner, R., Koegler, C., Ratschek, M., Rusmir, H., Sargsyan, K., Sperl, W., et al. (2011). Respiratory chain complex I is a mitochondrial tumor suppressor of oncocytic tumors. Front. Biosci. Elite Ed. *3*, 315–325.

Zu, X.L., and Guppy, M. (2004). Cancer metabolism: facts, fantasy, and fiction. Biochem. Biophys. Res. Commun. *313*, 459–465.

Vatrinet et al., The IJBCB, 2015 and Vatrinet et al., Cancer Metab, 2015

The International Journal of Biochemistry & Cell Biology 63 (2015) 41–45

Contents lists available at ScienceDirect

The International Journal of Biochemistry & Cell Biology

journal homepage: www.elsevier.com/locate/biocel

Organelles in focus

Targeting respiratory complex I to prevent the Warburg effect☆

Renaud Vatrinet[a,b,1], Luisa Iommarini[a,1], Ivana Kurelac[b], Monica De Luise[b], Giuseppe Gasparre[b], Anna Maria Porcelli[a,c,*]

[a] Dipartimento di Farmacia e Biotecnologie (FABIT), Università di Bologna, via Irnerio 42, 40126 Bologna, Italy
[b] Dipartimento di Scienze Mediche e Chirurgiche (DIMEC), U.O. Genetica Medica, Pol. Universitario S. Orsola-Malpighi, Università di Bologna, via Massarenti 9, 40138 Bologna, Italy
[c] Centro Interdipartimentale di Ricerca Industriale Scienze della Vita e Tecnologie per la Salute, Università di Bologna, 40100 Bologna, Italy

ARTICLE INFO

Article history:
Received 27 October 2014
Received in revised form 15 January 2015
Accepted 29 January 2015
Available online 7 February 2015

Keywords:
Respiratory complex I
OXPHOS
Tumor progression
Warburg effect
Metabolic reprogramming

ABSTRACT

In the last 10 years, studies of energetic metabolism in different tumors clearly indicate that the definition of Warburg effect, i.e. the glycolytic shift cells undergo upon transformation, ought to be revisited considering the metabolic plasticity of cancer cells. In fact, recent findings show that the shift from glycolysis to re-established oxidative metabolism is required for certain steps of tumor progression, suggesting that mitochondrial function and, in particular, respiratory complex I are crucial for metabolic and hypoxic adaptation. Based on these evidences, complex I can be considered a lethality target for potential anti-cancer strategies. In conclusion, in this mini review we summarize and discuss why it is not paradoxical to develop pharmacological and genome editing approaches to target complex I as novel adjuvant therapies for cancer treatment.

This article is part of a Directed Issue entitled: Energy Metabolism Disorders and Therapies.

1. Introduction

Metabolic reprogramming is currently recognized as one of the hallmarks of cancer (Hanahan and Weinberg, 2011). In particular, cancer cells are characterized by increased glycolytic metabolism regardless of the availability of O_2, as observed for the first time by Otto Warburg, who hypothesized that such metabolic preference was a consequence of dysfunctional mitochondria. Indeed, loss-of-function mutations have been identified in human cancers (Kirches, 2009) and it has been shown that carcinogenesis is associated with decreased levels of mitochondrial proteins and upregulation of glycolytic enzymes (Cuezva et al., 2002). However, Warburg's hypothesis has been somewhat revisited with time, since it has been found that certain tumors maintain oxidative metabolism during tumor progression (Bellance et al., 2009). In fact, oxidative phosphorylation (OXPHOS) and in particular respiratory complex I (CI) are crucial not only for energy generation, maintenance of redox homeostasis, and reactive oxygen species (ROS) production, but they are also indirectly involved in the regulation of biosynthetic pathways (DeBerardinis et al., 2008).

CI is a multi-subunit enzyme whose main function is to oxidize the NADH produced through glycolysis and tricarboxilic acid (TCA) cycle to NAD^+, and to transfer electrons to ubiquinone.

Key facts:

- Respiratory complex I impairment impinges on cancer progression.
- Complex I function is required for the induction of a Warburg profile.
- Targeting Complex I is a potential adjuvant anti-cancer strategy.

Abbreviations: OXPHOS, oxidative phosphorylation; CI, complex I; ROS, reactive oxygen species; TCA, tricarboxylic acid; PARP1, poly (ADP ribose) polymerase 1; AMPK, AMP activated kinase; mTORC1, mammalian target of rapamycin complex 1; HIF1α, hypoxia inducible factor 1α; PDC, pyruvate dehydrogenase complex; IDH, isocitrate dehydrogenase; αKG-DH, α-ketoglutarate dehydrogenase; αKG, α-ketoglutarate; SA, succinate; PHD, prolyl hydroxylase; ZNFs, zinc finger nucleases; TALENs, transcription activator-like effector nucleases; CRISPR, clustered regularly interspaced short palindromic repeats; Cas, CRISP-associated.

☆ This article is part of a Directed Issue entitled: Energy Metabolism Disorders and Therapies.

* Corresponding author: Anna Maria Porcelli, Dipartimento di Farmacia e Biotecnologie, Università di Bologna, Via Irnerio 42, 40126 Bologna, Italy.
Tel.: +39 051 2091282; fax: +39 051 242576.
E-mail address: annamaria.porcelli@unibo.it (A.M. Porcelli).
[1] Co-first authors.

http://dx.doi.org/10.1016/j.biocel.2015.01.017
1357-2725/

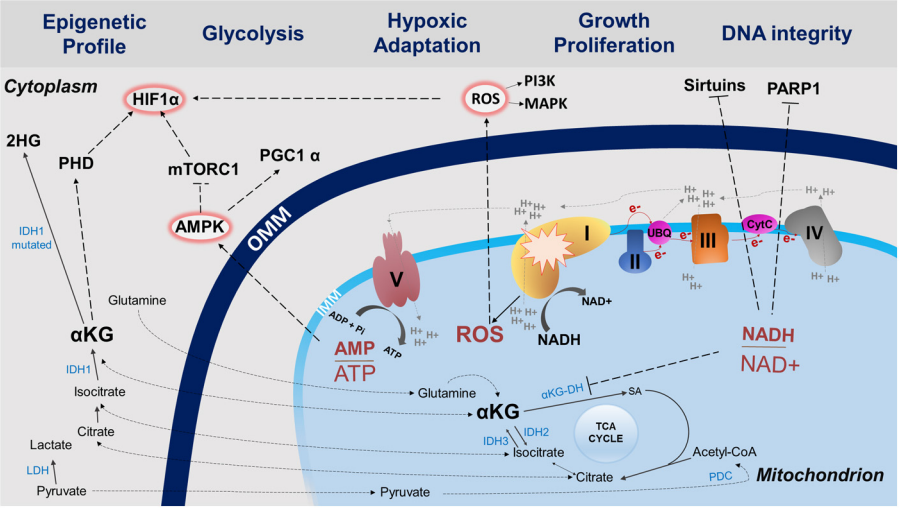

Fig. 1. Representation of the biochemical and molecular impact of CI dysfunction. Non functional CI leads to increased AMP/ATP ratio, decreased NAD^+/NADH balance, and potentially ROS levels alteration that directly impinge on several pathways involved in metabolic and hypoxic adaptation essential for tumor progression. NADH accumulation and ATP depletion slow down tricarboxylic acid (TCA) cycle, inhibiting the α-ketoglutarate dehydrogenase (αKG-DH), which in turn may result in an imbalance of αKG/SA toward αKG that promotes prolyl-hydroxylase (PHD) activity. Constitutive activation of PHD leads to HIF1α degradation regardless of O_2 tension. NADH accumulation and ATP depletion inhibit also pyruvate dehydrogenase complex (PDC) and isocitrate dehydrogenase 3 (IDH3), preventing the conversion of pyruvate to acetyl-CoA and promoting alternative metabolic strategies, such as glutaminolysis and reductive carboxylation, to feed biosynthetic pathways. Moreover, mutated forms of IDH1/2 produce the oncometabolite 2-hydroxyglutarate, known to induce epigenetic modifications. In pathological context such as cancer and/or OXPHOS impairment, the cytosolic LDH can convert pyruvate to lactate leading to extracellular environment acidification. NAD^+/NADH imbalance, energy depletion, and altered ROS levels due to CI impairment also regulate specific signaling cascades (*i.e.*, Sirtuins, AMPK/mTORC1, PGC-1α, PI3K) involved in metabolic reprogramming, hypoxic adaptation, DNA integrity, cell growth, and proliferation.

This process is coupled to the release of $4H^+$ from the mitochondrial matrix to the intermembrane space, providing the electrochemical gradient necessary for ATP production. As a by-product of these reactions, CI may generate ROS, especially under certain pathologic conditions. Therefore, it is not surprising that CI has been recently recognized as a key player in cancer development and progression (Iommarini et al., 2013). Interestingly, ours and other groups showed that severe CI dysfunctions can be disadvantageous to tumor growth (Gasparre et al., 2011; Park et al., 2009) and that a minimal CI function is required for the induction of a Warburg phenotype, disclosing this enzyme as a potential target for cancer therapy (Calabrese et al., 2013).

2. Respiratory complex I as a modulator of tumor progression

Several mechanisms have been proposed through which CI dysfunction may impinge on tumor progression, all of which may provide potential therapeutic targets. In particular, impairment of CI can be reflected on the cellular redox balance and energy charge, represented by ROS, NAD^+/NADH, and AMP/ATP, respectively (Fig. 1). Defective CI may increase ROS levels, which on one hand are known to activate pro-tumorigenic signaling (Ray et al., 2012), and on the other, may be toxic when chronically overproduced (Shen et al., 1998). It is noteworthy that oxidative stress can occur when CI is only partially defective (Ishikawa et al., 2008; Sharma et al., 2011), whereas no significant increase in ROS production has been observed in cancer models bearing severe CI dysfunction, most likely due to the lack of the CI sites where ROS are generated (Iommarini et al., 2014; Gasparre et al., 2011). The maintenance of the redox and energetic homeostasis is essential to determine cell fate, and when these balances are altered cells attempt to respond by re-routing metabolic reactions and triggering different signaling pathways. In particular, the NAD^+/NADH balance regulates the Sirtuins-dependent signaling pathway and poly (ADP ribose) polymerase 1 (PARP1) mediated control of DNA integrity and cell proliferation. Those pathways have been widely linked to neoplasia, highlighting the relevance of the NAD metabolome in cancer (Chiarugi et al., 2012). Interestingly, we have previously demonstrated that cancer cells carrying severe CI defect show decreased NAD^+/NADH ratio due to NADH accumulation associated with reduced tumorigenic potential (Calabrese et al., 2013), indicating that CI dysfunction may generate an inhibitory signal for Sirtuins and trigger adaptive responses (Fig. 1). All the seven human Sirtuins (SIRT1-7) have been involved in cancer in some way, but whether they play a tumor suppressor or oncogenic role seems to depend on the cellular and molecular context. For example, SIRT1 overexpression reduces the spontaneous formation of carcinomas and sarcomas (Herranz et al., 2010), but it has also been found highly expressed in different human cancers (Yuan et al., 2013a,b), where it promotes carcinogenesis and resistance to chemotherapy (Herranz et al., 2013; Liang et al., 2008; Chen et al., 2012). Similarly, mitochondrial SIRT3 and SIRT5 have been found overexpressed in some types of cancer (Alhazzazi et al., 2011; Yan et al., 2014; Lu et al., 2014) and their knock down represses cell proliferation and tumor formation. Nonetheless, they have been also found down-regulated in other tumors (Yang et al., 2014; Lai et al., 2013) and they may act as tumor suppressors by regulating ROS production and hypoxic response (Finley et al., 2011). Conversely, SIRT4 seems to act exclusively as a tumor suppressor by restricting glutamine utilization and repressing Myc-induced B cells lymphomagenesis (Jeong et al., 2013; Jeong et al., 2014). Owing to a crucial role in energy production, CI dysfunctions have been also associated with altered AMP/ATP ratio and increasing evidences demonstrate that cellular energetic crisis may impact on tumor progression despite the enhanced glycolysis (Guo et al., 2011; Jones et al., 2005). Nutrient deprivation commonly experienced by cancer cells during tumor progression triggers the activation of the energy sensor AMP activated kinase (AMPK), which inhibits biosynthetic pathways and supports catabolic events in order to restore intracellular energetic balance (Hardie et al., 2012). Moreover, AMPK

down-regulates the mTORC1 signaling, preventing cell growth and proliferation, and suppresses the translation and therefore the transcriptional activity of Hypoxia Inducible Factor 1α (HIF1α), the master regulator of hypoxic adaptation (Faubert et al., 2013). Interestingly, lack of AMPK induced a metabolic shift toward aerobic glycolysis in a HIF1α-dependent mechanism, suggesting that AMPK acts as a tumor suppressor by down-modulating the HIF1α-mediated Warburg effect (Faubert et al., 2013). We recently showed that malignant cells carrying severe CI defects displayed a striking increase in AMP/ATP ratio and AMPK activation under metabolic stress conditions (Iommarini et al., 2014), meaning that CI targeting could affect AMPK activation (Fig. 1). However, such compensatory strategy to energy depletion did not influence cell proliferation, which was rather controlled by HIF1α in an AMPK-independent mechanism, at least *in vitro* under normoxic conditions (Iommarini et al., 2014). Hence, the intricate molecular events linking CI to Sirtuins and AMPK pathways in tumor progression seem to be context- and environment-dependent, highlighting the plasticity of metabolic reprogramming in modulating cell adaptation to stress stimuli.

It is well known that CI controls the rate of glycolysis and TCA cycle, allosterically regulating their main checkpoints, namely the pyruvate dehydrogenase complex (PDC), isocitrate dehydrogenase (IDH) and α-ketoglutarate dehydrogenase (αKG-DH). In order to sustain high glycolytic metabolism and regenerate the NAD^+ pool, cancer cells preferentially convert pyruvate to lactate, thus uncoupling the mitochondrial metabolism from glycolysis and causing extracellular environment acidification (DeBerardinis et al., 2008). In such context, it is not surprising that the TCA gatekeeper PDC has been found critical for cancer cell proliferation, since it reduces oncogene-induced senescence (Kaplon et al., 2013) and promotes the Warburg effect (Fan et al., 2014). Nonetheless, CI defective cells showed low levels of PDC subunits E1β and E3, and decreased activity under metabolic stress conditions (Musicco et al., 2014). These findings suggest that TCA cycle checkpoints may be regulated in a non-canonical manner under unusual metabolic states, such as NADH accumulation accompanied with ATP depletion, found in CI-deficient cells. In fact, to sustain cell proliferation, cancer cells can bypass PDC inactivation by converting pyruvate to oxaloacetate *via* pyruvate carboxylase (Cheng et al., 2011) or by using reductive carboxylation of glutamine as an alternative carbon source for citrate biosynthesis (Mullen et al., 2011). Interestingly, reductive carboxylation involves IDHs and αKG-DH, which are the other two enzymatic TCA cycle checkpoints regulated by CI function, directly (IDH3) or indirectly (IDH1/2) *via* NADH accumulation. Despite the fact that IDH1 and IDH2 have been found mutated in different types of cancer (Yan et al., 2009; Mardis et al., 2009), they acquire a neomorphic function through the production of the oncometabolite 2-hydroxyglutarate, indicating that their effects on tumor growth are not exclusively exerted through a CI-related mechanism. Lastly, NADH accumulation and ATP depletion caused by CI defects may allosterically inhibit αKG-DH with subsequent unbalance of αKG/succinate (SA) ratio, leading to HIF1α destabilization and in turn to progression toward malignancy. In fact, αKG/SA ratio controls HIF1α degradation by regulating the prolyl-hydroxylases (PHDs) activity and αKG is also required for reductive carboxylation in mitochondrial defective cancer cells (Mullen et al., 2014). Regardless of the oxygen tension level, cells exposed to permeable derivatives of αKG displayed increased HIF1α degradation (Tennant et al., 2009), whereas high SA levels promote HIF1α chronic stabilization (Pollard et al., 2005). Interestingly, CI-defective cells displayed an unbalance in αKG/SA ratio and constitutive destabilization of HIF1α (Gasparre et al., 2011; Calabrese et al., 2013; Iommarini et al., 2014) (Fig. 1). These cells were unable to induce a glycolytic shift during hypoxic adaptation and to generate a Warburg profile *in vitro* and *in vivo*, thus hampering tumor growth (Calabrese et al., 2013). These data indicate that respiratory CI is essential for the induction of the Warburg effect and adaptation to hypoxia of cancer cells.

Overall, considering the above mentioned metabolic plasticity and the essential role of CI in controlling metabolism, hypoxic adaptation and cell proliferation, this enzyme may be envisioned as an intriguing target for development of new anticancer agents. In particular, these compounds may be considered for adjuvant therapies in combination with other drugs targeting peculiar features of cancer cells such as metabolic and proliferative pathways (Cairns et al., 2011).

3. Targeting complex I as an anticancer strategy

A large panel of pharmacological compounds affecting CI has been proposed and studied as anticancer drugs (Table 1). Specific CI inhibitors, such as the plant alkaloid rotenone, piericidin A and capsaicin have been shown to be selectively cytotoxic for cancer cells under metabolic stress conditions (Palorini et al., 2013). Recently, biguanides have been recognized as a new class of CI inhibitors, preventing ubiquinone reduction in a non-competitive manner and stimulating ROS production (Bridges et al., 2014). In particular, the widely used anti-diabetic drug metformin has been found to exert anti-neoplastic effects, as documented by clinical studies which highlighted a potential reduction of risk of cancer in patients treated with the drug (Evans et al., 2005; Becker et al., 2014). Accordingly, several studies *in vitro* and *in vivo* provided a body of evidence for metformin-mediated anti-neoplastic effects (Wheaton et al., 2014; Andrzejewski et al., 2014). In particular, cancer cells with OXPHOS defects or glucose utilization impairment were found to be more prone to respond to CI inhibition by biguanides (Birsoy et al., 2014). Moreover, metformin and phenformin have been already shown to enhance the anti-proliferative effect of BRAF inhibitors in BRAF-mutated melanoma cell lines (Niehr et al., 2011; Yuan et al., 2013a,b). Therefore, CI may be envisioned as a lethality target for potential adjuvant anticancer strategies, in combination with anti-proliferative or anti-glycolytic drugs. Such targeting of both oxidative and glycolytic cells might prevent tumor relapse due to cancer heterogeneity and its constant metabolic adaptability.

The molecular mechanisms by which biguanides affect cancer cell metabolism and proliferation are still unclear. In fact, biguanides may influence other enzymes, such as ATP synthase [Bridges et al., 2014), and they contribute to the regulation of insulin-like growth factor signaling (Xie et al., 2014). Since specific CI inhibitors displayed adverse effects and biguanides have been shown to have wide-spread response, the druggability of CI results weakened, highlighting the necessity of a step forward in drug design and in molecular approaches. An alternative strategy would be to envisage the use of emerging genome editing technologies, such as Zinc Finger Nucleases (ZFNs), transcription activator-like effector nucleases (TALENs) and clustered regularly interspaced short palindromic repeats/CRISP-associated (CRISPR/Cas). These are site-specific nucleases that efficiently induce DNA modifications, such as insertions and deletions, at user-defined genetic locations, leading to gene disruption. Indeed, such molecular approaches have been already tested to target nuclear and mitochondrially-encoded CI genes (Bacman et al., 2013; Stroud et al., 2013) and represent promising implements for functional studies on CI, meeting the capability to dissect the molecular and biochemical mechanisms underlying the potential anti-tumorigenic effect of its disruption, in CI-free engineered models.

Table 1
Respiratory complex I inhibitors used as anticancer molecules.

Inhibitor (class)[#]	Family of compounds	Mechanism of action	References
Piericidin A (I/A)	Piericidins	-Induces cell death in association with glucose starvation -Synergistic effect with Forskolin	Hwang et al., 2008; Palorini et al., 2013
Rotenone (II/B)	Rotenoids	-Induces cell death in association with glucose starvation -Synergistic effect with Forskolin	Palorini et al., 2013; Wheaton et al., 2014
Capsaicin (C)	Vanilloids	-Induces cell death in association with glucose starvation -Synergistic effect with Forskolin -Stimulates ROS production and promotes apoptosis	Pramanik et al., 2011; Palorini et al., 2013
Rolliniastatin-1 (I/A)	Annonaceus acetogenins	-Induces the mitochondrial apoptotic pathway	de Pedro et al., 2013
Metformin	Biguanides	-Reduces HIF1α stabilization under hypoxia -Activates AMPK pathway -Modulates IGF pathway	Wheaton et al., 2014; Andrzejewski et al., 2014; Birsoy et al., 2014
Phenformin	Biguanides	-Reduces HIF1α stabilization under hypoxia -Activates AMPK pathway -Modulates IGF pathway	Wheaton et al., 2014; Birsoy et al., 2014
BAY 87-2243	Aminoalkyl pyrimidine	-Prevents HIF1α stabilization under hypoxia	Ellinghaus et al., 2013

[#] Classification by mechanism of inhibition is available only for canonical respiratory complex I inhibitors.

4. Conclusions and perspectives

Based on the evidences here discussed that respiratory complex I is a modulator of cancer metabolism, it can be stated that targeting CI to prevent the Warburg effect is not paradoxical. In fact, recent advances demonstrated that the Warburg hypothesis must be reinterpreted considering that cancer cells need a functional OXPHOS to progress toward malignancy. Owing to the crucial role of CI in the regulation of hypoxic and metabolic adaptation and to its ability to determine cell fate under selective tumor microenvironment, this enzyme can be envisioned as a lethality target for novel potential anticancer strategies. New advances in drug design and genome editing techniques will represent valuable tools to improve the development of adjuvant therapies for cancer treatment.

Conflict of interest statement

The authors declare that there are no conflicts of interest.

Acknowledgements

This work was supported by Associazione Italiana Ricerca sul Cancro - AIRC grant IG 14242; EU FP7 Marie Curie project MEET-317433; I.K. is supported by a triennial fellowship "Borromeo" from Associazione Italiana Ricerca sul Cancro - AIRC.

References

Alhazzazi TY, Kamarajan P, Joo N, Huang JY, Verdin E, D'Silva NJ, Kapila YL. Sirtuin-3 (SIRT3), a novel potential therapeutic target for oral cancer. Cancer 2011;117(April (8)):1670–8, http://dx.doi.org/10.1002/cncr.25676.

Andrzejewski S, Gravel SP, Pollak M, St-Pierre J. Metformin directly acts on mitochondria to alter cellular bioenergetics. Cancer Metab 2014;2(August):12, http://dx.doi.org/10.1186/2049-3002-2-12.

Bacman SR, Williams SL, Pinto M, Peralta S, Moraes CT. Specific elimination of mutant mitochondrial genomes in patient-derived cells by mitoTALENs. Nat Med 2013;19(September (9)):1111–3, http://dx.doi.org/10.1038/nm.3261.

Becker C, Jick SS, Meier CR, Bodmer M. Metformin and the risk of head and neck cancer: a case-control analysis. Diabetes Obes Metab 2014;16(November (11)):1148–54, http://dx.doi.org/10.1111/dom.12351.

Bellance N, Benard G, Furt F, Begueret H, Smolková K, Passerieux E, Delage JP, Baste JM, Moreau P, Rossignol R. Bioenergetics of lung tumors: alteration of mitochondrial biogenesis and respiratory capacity. Int J Biochem Cell Biol 2009;41(December (12)):2566–77, http://dx.doi.org/10.1016/j.biocel.2009.08.012.

Birsoy K, Possemato R, Lorbeer FK, Bayraktar EC, Thiru P, Yucel B, Wang T, Chen WW, Clish CB, Sabatini DM. Metabolic determinants of cancer cell sensitivity to glucose limitation and biguanides. Nature 2014;508(April (7494)):108–12, http://dx.doi.org/10.1038/nature13110.

Bridges HR, Jones AJ, Pollak MN, Hirst J. Effects of metformin and other biguanides on oxidative phosphorylation in mitochondria. Biochem J 2014;462(September (3)):475–87, http://dx.doi.org/10.1042/BJ20140620.

Cairns RA, Harris IS, Mak TW. Regulation of cancer cell metabolism. Nat Rev Cancer 2011;11(February (2)):85–95, http://dx.doi.org/10.1038/nrc2981.

Calabrese C, Iommarini L, Kurelac I, Calvaruso MA, Capristo M, Lollini PL, Nanni P, Bergamini C, Nicoletti G, Giovanni CD, Ghelli A, Giorgio V, Caratozzolo MF, Marzano F, Manzari C, Betts CM, Carelli V, Ceccarelli C, Attimonelli M, Romeo G, Fato R, Rugolo M, Tullo A, Gasparre G, Porcelli AM. Respiratory complex I is essential to induce a Warburg profile in mitochondria-defective tumor cells. Cancer Metab 2013;1(March (1)):11, http://dx.doi.org/10.1186/2049-3002-1-11.

Chen HC, Jeng YM, Yuan RH, Hsu HC, Chen YL. SIRT1 promotes tumorigenesis and resistance to chemotherapy in hepatocellular carcinoma and its expression predicts poor prognosis. Ann Surg Oncol 2012;19(June (6)):2011–9, http://dx.doi.org/10.1245/s10434-011-2159-4.

Cheng T, Sudderth J, Yang C, Mullen AR, Jin ES, Matés JM, DeBerardinis RJ. Pyruvate carboxylase is required for glutamine-independent growth of tumor cells. Proc Natl Acad Sci U S A 2011;108(May (21)):8674–9, http://dx.doi.org/10.1073/pnas.1016627108.

Chiarugi A, Dölle C, Felici R, Ziegler M. The NAD metabolome–a key determinant of cancer cell biology. Nat Rev Cancer 2012;12(November (11)):741–52, http://dx.doi.org/10.1038/nrc3340.

Cuezva JM, Krajewska M, de Heredia ML, Krajewski S, Santamaría G, Kim H, Zapata JM, Marusawa H, Chamorro M, Reed JC. The bioenergetic signature of cancer: a marker of tumor progression. Cancer Res 2002;62(November (22)):6674–81.

de Pedro N, Cautain B, Melguizo A, Vicente F, Genilloud O, Peláez F, Tormo JR. Mitochondrial complex I inhibitors, acetogenins, induce HepG2 cell death through the induction of the complete apoptotic mitochondrial pathway. J Bioenerg Biomembr 2013;45(February (1–2)):153–64, http://dx.doi.org/10.1007/s10863-012-9489-1.

DeBerardinis RJ, Lum JJ, Hatzivassiliou G, Thompson CB. The biology of cancer: metabolic reprogramming fuels cell growth and proliferation. Cell Metab 2008;7(January (1)):11–20, http://dx.doi.org/10.1016/j.cmet.2007.10.002.

Ellinghaus P, Heisler I, Unterschemmann K, Haerter M, Beck H, Greschat S, Ehrmann A, Summer H, Flamme I, Oehme F, Thierauch K, Michels M, Hess-Stumpp H, Ziegelbauer K. BAY 87-2243, a highly potent and selective inhibitor of hypoxia-induced gene activation has antitumor activities by inhibition of mitochondrial complex I. Cancer Med 2013;2(October (5)):611–24, http://dx.doi.org/10.1002/cam4.112.

Evans JM, Donnelly LA, Emslie-Smith AM, Alessi DR, Morris AD. Metformin and reduced risk of cancer in diabetic patients. BMJ 2005;330(June (7503)):1304–5.

Fan J, Kang HB, Shan C, Elf S, Lin R, Xie J, Gu TL, Aguiar M, Lonning S, Chung TW, Arellano M, Khoury HJ, Shin DM, Khuri FR, Boggon TJ, Kang S, Chen J. Tyr-301 phosphorylation inhibits pyruvate dehydrogenase by blocking substrate binding and promotes the warburg effect. J Biol Chem 2014;289(September (38)):26533–41, http://dx.doi.org/10.1074/jbc.M114.593970.

Faubert B, Boily G, Izreig S, Griss T, Samborska B, Dong Z, Dupuy F, Chambers C, Fuerth BJ, Viollet B, Mamer OA, Avizonis D, DeBerardinis RJ, Siegel PM, Jones RG. AMPK is a negative regulator of the Warburg effect and suppresses tumor growth in vivo. Cell Metab 2013;17(January (1)):113–24, http://dx.doi.org/10.1016/j.cmet.2012.12.001.

Finley LW, Carracedo A, Lee J, Souza A, Egia A, Zhang J, Teruya-Feldstein J, Moreira PI, Cardoso SM, Clish CB, Pandolfi PP, Haigis MC. SIRT3 opposes reprogramming of cancer cell metabolism through HIF1α destabilization. Cancer Cell 2011;19(March (3)):416–28, http://dx.doi.org/10.1016/j.ccr.2011.02.014.

Gasparre G, Kurelac I, Capristo M, Iommarini L, Ghelli A, Ceccarelli C, Nicoletti G, Nanni P, De Giovanni C, Scotlandi K, Betts CM, Carelli V, Lollini PL, Romeo G, Rugolo M, Porcelli AM. A mutation threshold distinguishes the antitumorigenic effects of the mitochondrial gene MTND1, an oncojanus function. Cancer Res 2011;71(October (19)):6220–9, http://dx.doi.org/10.1158/0008-5472.CAN-11-1042.

Guo JY, Chen HY, Mathew R, Fan J, Strohecker AM, Karsli-Uzunbas G, Kamphorst JJ, Chen G, Lemons JM, Karantza V, Coller HA, Dipaola RS, Gelinas C,

Rabinowitz JD, White E. Activated Ras requires autophagy to maintain oxidative metabolism and tumorigenesis. Genes Dev 2011;25(March (5)):460–70, http://dx.doi.org/10.1101/gad.2016311.

Hanahan D, Weinberg RA. Hallmarks of cancer: the next generation. Cell 2011;144(March (5)):646–74, http://dx.doi.org/10.1016/j.cell.2011.02.013.

Hardie DG, Ross FA, Hawley SA, AMPK:. a nutrient and energy sensor that maintains energy homeostasis. Nat Rev Mol Cell Biol 2012;13(March (4)):251–62, http://dx.doi.org/10.1038/nrm3311.

Herranz D, Maraver A, Cañamero M, Gómez-López G, Inglada-Pérez L, Robledo M, Castelblanco E, Matias-Guiu X, Serrano M. SIRT1 promotes thyroid carcinogenesis driven by PTEN deficiency. Oncogene 2013;32(August (34)):4052–6, http://dx.doi.org/10.1038/onc.2012.407.

Herranz D, Muñoz-Martin M, Cañamero M, Mulero F, Martinez-Pastor B, Fernandez-Capetillo O, Serrano M. Sirt1 improves healthy ageing and protects from metabolic syndrome-associated cancer. Nat Commun 2010;1(April):3, http://dx.doi.org/10.1038/ncomms1001.

Hwang JH, Kim JY, Cha MR, Ryoo IJ, Choo SJ, Cho SM, Tsukumo Y, Tomida A, Shin-Ya K, Hwang YI, Yoo ID, Park HR. Etoposide-resistant HT-29 human colon carcinoma cells during glucose deprivation are sensitive to piericidin A, a GRP78 down-regulator. J Cell Physiol 2008;215(April (1)):243–50.

Iommarini L, Calvaruso MA, Kurelac I, Gasparre G, Porcelli AM, Complex I. impairment in mitochondrial diseases and cancer: parallel roads leading to different outcomes. Int J Biochem Cell Biol 2013;45(January (1)):47–63, http://dx.doi.org/10.1016/j.biocel.2012.05.016.

Iommarini L, Kurelac I, Capristo M, Calvaruso MA, Giorgio V, Bergamini C, Ghelli A, Nanni P, De Giovanni C, Carelli V, Fato R, Lollini PL, Rugolo M, Gasparre G, Porcelli AM. Different mtDNA mutations modify tumor progression in dependence of the degree of respiratory complex I impairment. Hum Mol Genet 2014;23(March (6)):1453–66, http://dx.doi.org/10.1093/hmg/ddt533.

Ishikawa K, Takenaga K, Akimoto M, Koshikawa N, Yamaguchi A, Imanishi H, Nakada K, Honma Y, Hayashi J. ROS-generating mitochondrial DNA mutations can regulate tumor cell metastasis. Science 2008;320(May (5876)):661–4, http://dx.doi.org/10.1126/science.1156906.

Jeong SM, Lee A, Lee J, Haigis MC. SIRT4 protein suppresses tumor formation in genetic models of Myc-induced B cell lymphoma. J Biol Chem 2014;289(February (7)):4135–44, http://dx.doi.org/10.1074/jbc.M113.525949.

Jeong SM, Xiao C, Finley LW, Lahusen T, Souza AL, Pierce K, Li YH, Wang X, Laurent G, German NJ, Xu X, Li C, Wang RH, Lee J, Csibi A, Cerione R, Blenis J, Clish CB, Kimmelman A, Deng CX, Haigis MC. SIRT4 has tumor-suppressive activity and regulates the cellular metabolic response to DNA damage by inhibiting mitochondrial glutamine metabolism. Cancer Cell 2013;23(April (4)):450–63, http://dx.doi.org/10.1016/j.ccr.2013.02.024.

Jones RG, Plas DR, Kubek S, Buzzai M, Mu J, Xu Y, Birnbaum MJ, Thompson CB. AMP-activated protein kinase induces a p53-dependent metabolic checkpoint. Mol Cell 2005;18(April (3)):283–93.

Kaplon J, Zheng L, Meissl K, Chaneton B, Selivanov VA, Mackay G, van der Burg SH, Verdegaal EM, Cascante M, Shlomi T, Gottlieb E, Peeper DS. A key role for mitochondrial gatekeeper pyruvate dehydrogenase in oncogene-induced senescence. Nature 2013;498(June (7452)):109–12, http://dx.doi.org/10.1038/nature12154.

Kirches E. Mitochondrial and nuclear genes of mitochondrial components in cancer. Curr Genomics 2009;10(June (4)):281–93, http://dx.doi.org/10.2174/138920209788488517..

Lai CC, Lin PM, Lin SF, Hsu CH, Lin HC, Hu ML, Hsu CM, Yang MY. Altered expression of SIRT gene family in head and neck squamous cell carcinoma. Tumour Biol 2013;34(June (3)):1847–54, http://dx.doi.org/10.1007/s13277-013-0726-y.

Liang XJ, Finkel T, Shen DW, Yin JJ, Aszalos A, Gottesman MM. SIRT1 contributes in part to cisplatin resistance in cancer cells by altering mitochondrial metabolism. Mol Cancer Res 2008;6(September (9)):1499–506, http://dx.doi.org/10.1158/1541-7786.MCR-07-2130.

Lu W, Zuo Y, Feng Y, Zhang M. SIRT5 facilitates cancer cell growth and drug resistance in non-small cell lung cancer. Tumour Biol 2014;35(November (11)):10699–705, http://dx.doi.org/10.1007/s13277-014-2372-4.

Mardis ER, Ding L, Dooling DJ, Larson DE, McLellan MD, Chen K, Koboldt DC, Fulton RS, Delehaunty KD, McGrath SD, Fulton LA, Locke DP, Magrini VJ, Abbott RM, Vickery TL, Reed JS, Robinson JS, Wylie T, Smith SM, Carmichael L, Eldred JM, Harris CC, Walker J, Peck JB, Du F, Dukes AF, Sanderson GE, Brummett AM, Clark E, McMichael JF, Meyer RJ, Schindler JK, Pohl CS, Wallis JW, Shi X, Lin L, Schmidt H, Tang Y, Haipek C, Wiechert ME, Ivy JV, Kalicki J, Elliott G, Ries RE, Payton JE, Westervelt P, Tomasson MH, Watson MA, Baty J, Heath S, Shannon WD, Nagarajan R, Link DC, Walter MJ, Graubert TA, DiPersio JF, Wilson RK, Ley TJ. Recurring mutations found by sequencing an acute myeloid leukemia genome. N Engl J Med 2009;361(September (11)):1058–66, http://dx.doi.org/10.1056/NEJMoa0903840.

Mullen AR, Hu Z, Shi X, Jiang L, Boroughs LK, Kovacs Z, Boriack R, Rakheja D, Sullivan LB, Linehan WM, Chandel NS, DeBerardinis RJ. Oxidation of alpha-ketoglutarate is required for reductive carboxylation in cancer cells with mitochondrial defects. Cell Rep 2014;7(June (5)):1679–90, http://dx.doi.org/10.1016/j.celrep.2014.04.037.

Mullen AR, Wheaton WW, Jin ES, Chen PH, Sullivan LB, Cheng T, Yang Y, Linehan WM, Chandel NS, DeBerardinis RJ. Reductive carboxylation supports growth in tumour cells with defective mitochondria. Nature 2011;481(November (7381)):385–8, http://dx.doi.org/10.1038/nature10642.

Musicco C, Cormio A, Calvaruso MA, Iommarini L, Gasparre G, Porcelli AM, Timperio AM, Zolla L, Gadaleta MN. Analysis of the mitochondrial proteome of cybrid cells harbouring a truncative mitochondrial DNA mutation in respiratory complex I. Mol Biosyst 2014;10(June (6)):1313–9, http://dx.doi.org/10.1039/c3mb70542k.

Niehr F, von Euw E, Attar N, Guo D, Matsunaga D, Sazegar H, Ng C, Glaspy JA, Recio JA, Lo RS, Mischel PS, Comin-Anduix B, Ribas A. Combination therapy with vemurafenib (PLX4032/RG7204) and metformin in melanoma cell lines with distinct driver mutations. J Transl Med 2011;9(May):76, http://dx.doi.org/10.1186/1479-5876-9-76.

Palorini R, Simonetto T, Cirulli C, Chiaradonna F. Mitochondrial complex I inhibitors and forced oxidative phosphorylation synergize in inducing cancer cell death. Int J Cell Biol 2013;2013:243876, http://dx.doi.org/10.1155/2013/243876.

Park JS, Sharma LK, Li H, Xiang R, Holstein D, Wu J, Lechleiter J, Naylor SL, Deng JJ, Lu J, Bai Y. A heteroplasmic, not homoplasmic, mitochondrial DNA mutation promotes tumorigenesis via alteration in reactive oxygen species generation and apoptosis. Hum Mol Genet 2009;18(May (9)):1578–89, http://dx.doi.org/10.1093/hmg/ddp069.

Pollard PJ, Brière JJ, Alam NA, Barwell J, Barclay E, Wortham NC, Hunt T, Mitchell M, Olpin S, Moat SJ, Hargreaves IP, Heales SJ, Chung YL, Griffiths JR, Dalgleish A, McGrath JA, Gleeson MJ, Hodgson SV, Poulsom R, Rustin P, Tomlinson IP. Accumulation of Krebs cycle intermediates and over-expression of HIF1alpha in tumours which result from germline FH and SDH mutations. Hum Mol Genet 2005;14(August (15)):2231–9.

Pramanik KC, Boreddy SR, Srivastava SK. Role of mitochondrial electron transport chain complexes in capsaicin mediated oxidative stress leading to apoptosis in pancreatic cancer cells. PLoS One 2011;6(5):e20151, http://dx.doi.org/10.1371/journal.pone.0020151.

Ray PD, Huang BW, Tsuji Y. Reactive oxygen species (ROS) homeostasis and redox regulation in cellular signaling. Cell Signal 2012;24(May (5)):981–90, http://dx.doi.org/10.1016/j.cellsig.2012.01.008.

Sharma LK, Fang H, Liu J, Vartak R, Deng J, Bai Y. Mitochondrial respiratory complex I dysfunction promotes tumorigenesis through ROS alteration and AKT activation. Hum Mol Genet 2011;20(December (23)):4605–16, http://dx.doi.org/10.1093/hmg/ddr395.

Shen YH, Wang XL, Wilcken DE. Nitric oxide induces and inhibits apoptosis through different pathways. FEBS Lett 1998;433(August (1–2)):125–31.

Stroud DA, Formosa LE, Wijeyeratne XW, Nguyen TN, Ryan MT. Gene knockout using transcription activator-like effector nucleases (TALENs) reveals that human NDUFA9 protein is essential for stabilizing the junction between membrane and matrix arms of complex I. J Biol Chem 2013;288(January (3)):1685–90, http://dx.doi.org/10.1074/jbc.C112.436766.

Tennant DA, Frezza C, MacKenzie ED, Nguyen QD, Zheng L, Selak MA, Roberts DL, Dive C, Watson DG, Aboagye EO, Gottlieb E. Reactivating HIF prolyl hydroxylases under hypoxia results in metabolic catastrophe and cell death. Oncogene 2009;28(November (45)):4009–21, http://dx.doi.org/10.1038/onc.2009.250.

Wheaton WW, Weinberg SE, Hamanaka RB, Soberanes S, Sullivan LB, Anso E, Glasauer A, Dufour E, Mutlu GM, Budigner GS, Chandel NS. Metformin inhibits mitochondrial complex I of cancer cells to reduce tumorigenesis. Elife 2014;May (3):e02242, http://dx.doi.org/10.7554/eLife.02242.

Xie Y, Wang JL, Ji M, Yuan ZF, Peng Z, Zhang Y, Wen JG, Shi HR. Regulation of insulin-like growth factor signaling by metformin in endometrial cancer cells. Oncol Lett 2014;8(November (5)):1993–9.

Yan H, Parsons DW, Jin G, McLendon R, Rasheed BA, Yuan W, Kos I, Batinic-Haberle I, Jones S, Riggins GJ, Friedman H, Friedman A, Reardon D, Herndon J, Kinzler KW, Velculescu VE, Vogelstein B, Bigner DD. IDH1 and IDH2 mutations in gliomas. N Engl J Med 2009;360(February (8)):765–73, http://dx.doi.org/10.1056/NEJMoa0808710.

Yan SM, Han X, Han PJ, Chen HM, Huang LY, Li Y. SIRT3 is a novel prognostic biomarker for esophageal squamous cell carcinoma. Med Oncol 2014;31(August (8)):103, http://dx.doi.org/10.1007/s12032-014-0103-8.

Yang B, Fu X, Shao L, Ding Y, Zeng D. Aberrant expression of SIRT3 is conversely correlated with the progression and prognosis of human gastric cancer. Biochem Biophys Res Commun 2014;443(January (1)):156–60, http://dx.doi.org/10.1016/j.bbrc.2013.11.068.

Yuan H, Su L, Chen WY. The emerging and diverse roles of sirtuins in cancer: a clinical perspective. Onco Targets Ther 2013a;October (6):1399–416, http://dx.doi.org/10.2147/OTT.S37750.

Yuan P, Ito K, Perez-Lorenzo R, Del Guzzo C, Lee JH, Shen CH, Bosenberg MW, McMahon M, Cantley LC, Zheng B. Phenformin enhances the therapeutic benefit of BRAF(V600E) inhibition in melanoma. Proc Natl Acad Sci U S A 2013b;110(November (45)):18226–31, http://dx.doi.org/10.1073/pnas.1317577110.

Vatrinet et al. Cancer & Metabolism (2017) 5:3
DOI 10.1186/s40170-017-0165-0

Cancer & Metabolism

REVIEW Open Access

The α-ketoglutarate dehydrogenase complex in cancer metabolic plasticity

Renaud Vatrinet[1,2], Giulia Leone[1], Monica De Luise[2], Giulia Girolimetti[2], Michele Vidone[2], Giuseppe Gasparre[2*] and Anna Maria Porcelli[1*]

Abstract

Deregulated metabolism is a well-established hallmark of cancer. At the hub of various metabolic pathways deeply integrated within mitochondrial functions, the α-ketoglutarate dehydrogenase complex represents a major modulator of electron transport chain activity and tricarboxylic acid cycle (TCA) flux, and is a pivotal enzyme in the metabolic reprogramming following a cancer cell's change in bioenergetic requirements. By contributing to the control of α-ketoglutarate levels, dynamics, and oxidation state, the α-ketoglutarate dehydrogenase is also essential in modulating the epigenetic landscape of cancer cells. In this review, we will discuss the manifold roles that this TCA enzyme and its substrate play in cancer.

Keywords: α-Ketoglutarate dehydrogenase complex, α-Ketoglutarate, Mitochondrial function, Metabolic stresses, Cancer plasticity, Cell signaling, Oncometabolite, Epigenetics

Background

Cancer cells must acquire several biological properties in order to survive, proliferate, and disseminate. These functional features, or "hallmarks of cancer", comprise sustaining proliferative signaling, evading growth suppressors, escaping cell death, and activating invasion/metastasis, all of which conspire to lead to pathologically high levels of cell survival and growth, and ultimately tumorigenesis [1]. In the last 10 years, an increasing number of studies suggests that cancer cells reprogram their metabolism in order to most effectively support growth and proliferation. Thus, metabolic rewiring has become an additional hallmark of cancer [1]. Increased aerobic glycolysis, as initially described by Otto Warburg [2], is observed in the majority of neoplasms in vivo, where it is believed to confer advantages to cancer cells for the production of energy, biomass, and reducing equivalents [3]. Although Warburg hypothesized that such a biochemical phenotype arises from the accumulation of mitochondrial defects, it is now known that, upon nutrient deprivation, oxidative metabolism can be promptly re-established, and a significant level of OXPHOS is maintained both in vitro and in vivo [4–9]. A common feature of solid tumors is that cells rapidly accumulate in bulks, with limited blood supply, and will hence cope with fluctuations in oxygen and nutrients, which will inevitably force them to modulate mitochondrial function consequently. Interestingly, it has been shown that neither hypoxia nor OXPHOS defects imply a complete shutoff of mitochondrial metabolism, and in either case the tricarboxylic acid (TCA) cycle may adjust metabolic fluxes to promote a glutamine-dependent biosynthetic pathway that sustains tumor progression [10]. Hence, the TCA cycle represents a metabolic hub that drives substrate utilization upon changes in resources availability. With respect to this, the discovery of mutations in genes encoding key enzymes of the TCA cycle has brought into light the importance of intracellular TCA cycle metabolite levels in modifying both the metabolic and the epigenetic landscape of cancer cells. Modification of TCA metabolic fluxes and metabolites levels in response to environmental pressures might therefore account for tumor adaptation and plasticity in the changing environment. In this frame, the α-ketoglutarate dehydrogenase complex (α-KGDC) stands out as being deeply interconnected

* Correspondence: giuseppe.gasparre@gmail.com; annamaria.porcelli@unibo.it
[2]Dipartimento Scienze Mediche e Chirurgiche (DIMEC), U.O. Genetica Medica, Pol. Universitario S. Orsola-Malpighi, Università di Bologna, Via Massarenti 9, 40138 Bologna, Italy
[1]Dipartimento Farmacia e Biotecnologie (FABIT), Università di Bologna, Via Selmi 3, 40126 Bologna, Italy

with the respiratory chain, tightly regulated upon tumor microenvironmental changes, a modulator of the level of the signaling metabolite α-ketoglutarate (α-KG), a regulator of cellular redox state, and at the crossroads of numerous metabolic routes. In this review, we will discuss the manifold roles this enzymatic complex and its substrate α-KG play in cancer.

Main text

The α-KGDC in cell metabolism

The TCA cycle is fueled by substrates entering at different gateways to convey the carbon source for both energy production and biosynthesis. In the canonical view, acetyl CoA is provided by the oxidation of carbohydrates, mostly glucose and fatty acids, and is then condensed with oxaloacetate to form citrate. The subsequent series of oxidative reactions leads to the production of the reducing equivalents NADH and $FADH_2$ that feed respiratory complex I (CI) and respiratory complex II (CII), respectively, to generate the mitochondrial membrane potential ($\Delta\psi_m$) required for ATP production. Glutamine, the most abundant amino acid in the plasma, has been widely described as an additional key source of both carbon and nitrogen, especially for fast proliferating cells [11]. Glutaminolysis results in the production of α-KG, either following dehydrogenation of glutamate or through a transamination reaction. In turn, α-KG can fuel both energetic and anabolic pathways: it may be oxidized by the α-KGDC inside the mitochondria or it may be reduced, thereby pushing the TCA cycle towards citrate [10, 12–14]. The latter may be extruded to the cytosol, where it may be converted back into acetyl CoA, and thereby used for lipid biosynthesis.

Hence, the manifold mitochondrial functions allow cells to rely on different sources of nutrients for energetic and anabolic purposes. How cells balance the utilization of these nutrients depends on key metabolic enzymes, whose activities are modulated in response to genetics and environmental pressures. In this light, the α-KGDC lies at the very hub of metabolic pathways and its activity is finely regulated by the levels of ATP, ADP, inorganic phosphate (Pi), and by the $NADH/NAD^+$ ratio, which are tightly dependent on the respiratory chain activity and on the rate of the glycolytic flux. The product of the α-KGDC reaction, succinyl CoA (Succ-CoA), has been shown to exert a direct control on the enzyme activity along with calcium (Ca^{2+}) and reactive oxygen species (ROS) (Fig. 1). Further, variations of mitochondrial pH and oxygen levels also

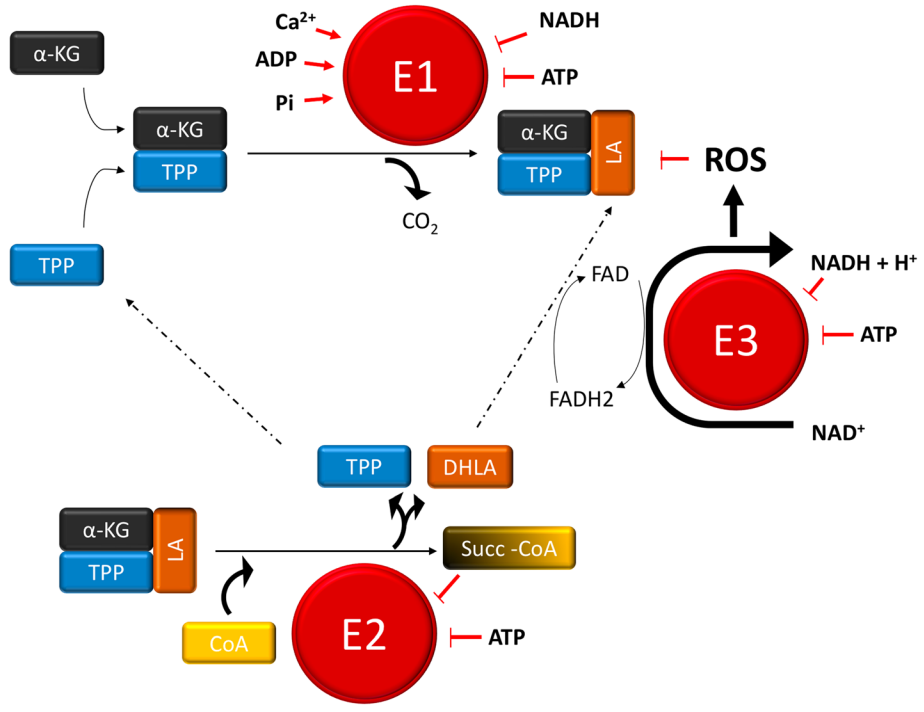

Fig. 1 Regulation mechanisms of α-KGDC. α-KGDC is a complex consisting of multiple copies of three enzymes: α-ketoglutarate dehydrogenase (E1), dihydrolipoamide succinyltransferase (E2), and dihydrolipoamide dehydrogenase (E3). α-KG reacts with the TPP that binds E1, and is thereby a decarboxylated-generating hydroxyethyl compound. E1 also catalyzes the transfer of two electrons and the acetyl group of the TPP on lipoic acid (LA), which is bound to the E2 subunit. The reaction performed by E2 is a transesterification in which the thiol group of the Coenzyme A (CoA) replaces the thiol group of E2, producing Succ-CoA and the reduced form of the lipoic group, the dihydrolipoic acid (DHLA). The subunit E3 catalyzes the transfer of two atoms of hydrogens from DHLA to its prosthetic group FAD, restoring oxidized LA. The reduced $FADH_2$ of the E3 enzyme transfer H^+ to NAD^+ to form NADH.

appear to be involved in the regulation of the enzyme. Hence, the multifactorial modulation of α-KGDC function may reflect its key role in orchestrating the responses to the ever-changing metabolic requirements of a cancer cell.

How the α-KGDC contributes to adapt mitochondrial metabolism to bioenergetic requirements

Structure and energetic regulation of the α-KGDC

In the TCA cycle, the α-KGDC catalyzes the reaction between α-KG and CoA, using thiamine pyrophosphate (TPP) as a cofactor and reducing the pyridine nucleotide NAD^+ to NADH, finally generating succ-CoA and CO_2. The α-KGDC is a multienzyme complex composed of three subunits (Fig. 1). The E1 subunit, encoded by the human *OGDH* gene, is a dehydrogenase that catalyzes the decarboxylation of α-KG, the first step required to produce succ-CoA. The second step is the reductive succinylation of the dihydrolipoyl groups, a reaction carried out by the E2 subunit, i.e., the dihydrolipoamide succinyltransferase, encoded by the human *DLST* gene. The E3 subunit, encoded by the human *DLD* gene, is the dihydrolipoamide dehydrogenase, which catalyzes the reoxidation of the E2 dihydrolipoyl groups, eventually reducing the final acceptor NAD^+ to NADH [15]. The regulation of the α-KGDC highlights a dynamic interplay between the enzyme and the OXPHOS to adjust mitochondrial metabolism through cell energy status sensing. Both the E1 and the E3 subunits are inhibited by NADH [16], which accumulates following a decrease of CI function [17]. Indeed, the latter complex is the first and the largest of the respiratory chain and catalyzes NADH oxidation to transfer electrons to flavin mononucleotide, which are used to reduce coenzyme Q to ubiquinol (QH_2). The latter is subsequently used by complex III to reduce cytochrome *c* in the mitochondrial intermembrane space (IMS), and complex IV uses cytochrome *c* to reduce molecular oxygen, which is the final electron acceptor [18]. Hence, CI actively participates to the generation of the electrochemical gradient by feeding the ETC to generate ATP, which makes NADH an essential substrate for oxidative metabolism. Interestingly, evidence is given for the existence of a direct interaction between CI and α-KGDC, which not only would provide an effective NADH oxidation mechanism via substrate channeling compared to free diffusion [19–21] but also implicates a higher sensitivity of α-KGDC to NADH levels, placing the enzyme on the front line to adapt to variations in ETC efficiency. In addition, a high ADP/ATP ratio and a high concentration of Pi independently enhance the activity of the α-KGDC, with a low ADP/ATP ratio having opposite effects [22, 23]. The levels of Pi and ADP are indicators of a low energetic condition, and both molecules act as positive effectors by increasing the affinity of the enzyme for its substrate. Conversely, higher ATP levels increase the amount of substrate necessary to reach the half-maximum rate of the enzyme, therefore reducing its activity [22, 24]. The regulation of α-KGDC by both the adenine nucleotide phosphorylation state and the NADH/NAD^+ ratio is tightly dependent on the $\Delta\psi_m$: on the one side, ATP extrusion from the mitochondria to the cytosol is controlled by the ADP/ATP carrier that is regulated by high $\Delta\psi_m$ and exchanges ATP with ADP in a 1:1 ratio [25]. On the other side, in cases when the ETC is damaged, the production of mitochondrial NADH, driven by cytosolic reductive power, is decreased [26]. This implies that the energetic control on the α-KGDC might be exclusively mitochondrial, and that a feedback loop relying on both substrate and energy availability is triggered between the OXPHOS and the enzyme, thereby ensuring an optimal cooperation. In this light, it may be envisioned that a decrease in mitochondrial respiration, or a significant ATP accumulation, may be associated with a decrease in α-KGDC activity. Changes in the enzyme function would in turn balance mitochondrial NADH levels, thus modulating CI activity and thereby ATP production. However, it has been observed in human neuroblastoma cells that decreasing α-KGDC activity up to half its maximum decreases neither $\Delta\psi_m$ nor mitochondrial ATP levels [27]. In line with this, the existence of a threshold for the α-KGDC capacity has been demonstrated, which can be greatly inhibited before affecting the maximal mitochondrial oxygen consumption rate [28]. NADH levels can therefore vary broadly before becoming a limiting factor for cellular respiration, suggesting that any reduction of α-KGDC activity might represent a first attempt to adapt metabolism by modulating TCA flux, before impinging on ETC function.

Calcium-mediated regulation of the α-KGDC

The relationship between α-KGDC and Ca^{2+} further emphasizes the pivotal role of the enzyme in regulating cell metabolism. The mitochondria have long been thought to be a Ca^{2+} sink, with the main scope of regulating this cation homeostasis in cells. Cytosolic Ca^{2+} has been shown to foster NADH oxidation by the glycerol dehydrogenase to ultimately produce and import $FADH_2$ within the mitochondria as a substrate for CII [29]. Furthermore, Ca^{2+} stimulates NADH production through the reactions of the TCA enzymes pyruvate dehydrogenase (PDH), isocitrate dehydrogenase (IDH) and α-KGDC [16, 30]. Among these three enzymes, α-KGDC has been shown to be the most responsive to Ca^{2+}, as the cation lowers the enzyme K_M for α-KG [22, 25, 29, 31]. Interestingly, the sensibility of α-KGDC to Ca^{2+} depends on the concentration of NADH, and on the ATP/ADP ratio, again highlighting a regulatory role of the ETC on the enzyme activity. Indeed, an increase in both cofactors lowers α-KGDC

stimulation by Ca^{2+} [24]. Also, calcium enters the mitochondria through a uniporter, a process driven by the negative potential across the IMM [32]. With respect to this, cancer cells have been shown to be particularly sensitive to an arrest of mitochondrial metabolism through the inhibition of Ca^{2+} transfer into the mitochondria. Indeed, while normal cells slow down proliferation when Ca^{2+} import is inhibited, cancer cells proceed through mitosis and end up necrotic, a route that may be rescued through dimethyl-α-KG supplementation [33]. This finding indicates that cancer cells ought to rely on a functional TCA cycle to sustain successful proliferation, and that α-KG may help overcome calcium shortage and sustain a minimal OXPHOS activity, or may drive adaptive responses to oxidative metabolism impairment.

pH-mediated regulation of the α-KGDC

A tight link between α-KGDC and OXPHOS is further exemplified when considering the role of pH in α-KGDC regulation. It has been widely shown that cytosolic Ca^{2+} elevation leads to rapid mitochondrial acidification, boosting oxidative metabolism. A range of pH between 6.6 and 7.4 has been demonstrated to increase α-KGDC activity [22]. Nonetheless, cytosolic pH is ~7.6 whereas in the mitochondrial matrix it ranges between 7.5 and 8.2 [34, 35]. The α-KGDC activity would thus be promoted upon environment acidification. In agreement with this, α-KG concentration in acidotic rat kidneys significantly decreases due to an increase of α-KGDC activity [36], which raises the question of whether changes in pH affect mitochondrial function in cancers, since they mostly rely on aerobic glycolysis and undergo a prominent acidosis [2]. However, cancer cells secrete lactate/H^+ to maintain intracellular pH at physiological values, leading to the acidification of the extracellular microenvironment [37]. Noticeably, pH in the mitochondria is inherently related to the activity of the ETC that is driven by the proton motive force and $\Delta\psi_m$ [18]. Thus, the pH of the mitochondrial matrix would rather reflect the equilibrium between proton extrusion and entry into the matrix, mainly driven by OXPHOS activity [38]. It may be easily argued that a low OXPHOS activity is associated with a decrease of pH in the mitochondrial matrix due to proton accumulation, at least around the inner membrane. In this respect, the subsequent induction of α-KGDC activity and of the subsequent NADH generation might help maintaining a proper chemical gradient by fostering CI proton pumping in the IMS. Hence, beside the adenine nucleotide phosphorylation state, the NADH/NAD^+ ratio and calcium levels, the OXPHOS might exert an additional control on the α-KGDC through the modulation of pH in the matrix of mitochondria.

ROS and α-KGDC activity

ROS are by-products of mitochondrial oxidative metabolism and their levels are a reliable indicator of ETC damage [39]. Noteworthy, α-KGDC can both sense and generate ROS (Fig. 1). An increase in ROS levels may decrease or completely inhibit α-KGDC function via two different mechanisms involving the modification of LA. While a post-translational modification may lead to the partial and reversible inhibition of the enzyme, the generation of a thiyl radical on the cofactor precedes its complete inactivation [40–42]. On the other hand, in response to NADH accumulation, stimulated by increased α-KG levels, the E3 subunit may generate H_2O_2 [43, 44] (Fig. 1) at much higher levels than CI [45]. Although physiological amounts of ROS are essential for cell survival, their excess fosters cancer initiation and progression through the induction of genomic instability, gene expression modifications, and the activation of signaling pathways [46, 47]. The aconitase is the most ROS-sensitive TCA cycle enzyme [48], and its inhibition in cells may therefore limit NADH production by interrupting the cycle from pyruvate to α-KG, and thus electron flux through the respiratory chain, ultimately reducing ROS in a negative loop. Conversely, cancer cells' high reliance on glutamine metabolism may allow the α-KGDC to fully sustain NADH-linked respiration [49], even upon a great reduction of aconitase activity. However, unlike the latter, high ROS levels are required to inhibit the α-KGDC [42]. In this light, the elevated threshold might play a prominent role in the progression of tumors with ETC defects. Similarly, prolonged metabolic perturbations such as NADH and α-KG accumulation may lead to α-KGDC-dependent oxidative stress, which in turn may profoundly affect cancer cell redox state and metabolism through a ROS-mediated self-inactivation of the enzyme [50]. Based on these characteristics, with the aim of proposing potential anti-cancer treatment, Stuart and co-workers described a member of anti-cancer lipoate derivatives, CPI-613, which induces an E3-mediated burst of ROS leading to E2 inactivation in cancer cells [51]. Although CPI-613 is known to be implicated in cell death, whether this is due to α-KGDC inhibition, ROS overproduction, or to the reduction of the activity of other lipoate-dependent mitochondrial metabolic enzymes remains unclear [51, 52].

The α-KGDC in cancer metabolic reprogramming

Glucose and glutamine are the two primary nutrients utilized by cancer cells [11]. However, unlike glucose, which only provides carbon for biosynthesis, glutamine can provide both carbon and nitrogen for anabolic reactions, thereby conferring substantial additional benefits [53]. Cancer cells also depend on lipid biosynthesis for biomass increase [54–56]. A crucial precursor of fatty acids biosynthesis is the citrate that is canonically

provided by glucose and glutamine metabolism through a forward running TCA cycle [10]. Instead, in neoplastic cells under hypoxic condition or in the presence of ETC defects, citrate is generated from reductive carboxylation of glutamine-derived α-KG, by cytosolic and mitochondrial NADPH-dependent IDH1 and 2, respectively [12, 13]. The α-KG conversion to isocitrate implies a lower α-KGDC activity and the unbalance of the α-KG/citrate ratio, leading to a TCA cycle functioning in a reverse mode, ultimately supporting de novo fatty acids synthesis and favoring tumor growth [13, 56, 57] (Fig. 2). It is worth noting that the activity of the α-KGDC is reduced via the hypoxia inducible factor 1 (HIF1)-mediated degradation of a splice variant of the E1 subunit, whose prevention renders cancer cells dependent on citrate or exogenous lipids to proliferate, and impedes tumor growth in vivo [56]. HIF1, the master regulator of the hypoxic response in malignant cancer cells [58], might also contribute to increase the α-KG/citrate ratio by inhibiting the activity of PDH and therefore citrate generation [59, 60] (Fig. 2a). These findings highlight an important role for HIF1 in modulating TCA metabolites levels and in the rewiring of α-KG fate from oxidative to reductive metabolism. In line with this, it has been shown that, in normoxia, constitutive activation of HIF1 alone is able to promote the reductive carboxylation of α-KG [12, 57]. Nevertheless, HIF1 is not essential in

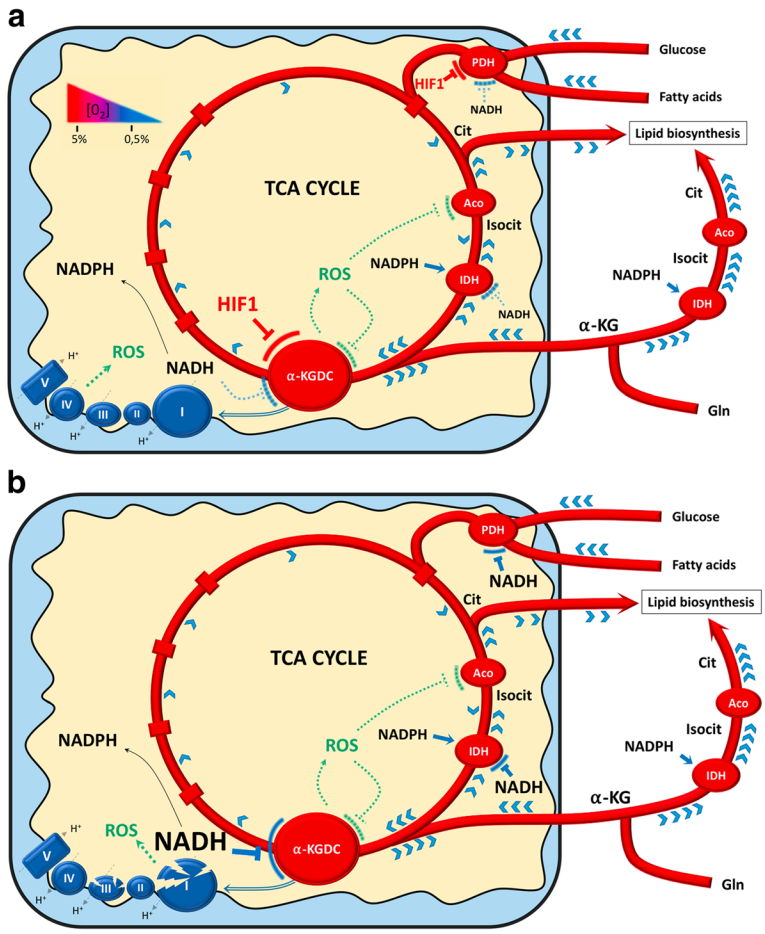

Fig. 2 Scheme of the molecular actors driving α-KG reductive carboxylation in mitochondria upon hypoxia (**a**) and in cancer cells with ETC defects (**b**). Reductive carboxylation requires the elevation of the α-KG/citrate ratio and reduces α-KG to isocitrate that is subsequently converted to citrate. This latter is shuttled to the cytosol where it is used for the biosynthesis of lipids. Noteworthy, in both cases (**a-b**), ROS production by ETC and α-KGDC may induce the inhibition of aconitase and α-KGDC, thereby preventing citrate and α-KG oxidation, respectively. **a** Upon hypoxia (5–0.5% O_2 tension), HIF1 can participate to the increase of the α-KG/citrate ratio, by preventing both PDH and α-KGDC activity, in turn limiting citrate production and α-KG oxidation, respectively. (**b**) In cancer cells with ETC defects, the accumulation of NADH may lead to the inhibition of mitochondrial NADH-dehydrogenases (PDH, IDH, and α-KGDC), thus decreasing citrate production/oxidation and α-KG oxidation. Further, NADH increase may also promote NADPH-dependent IDH1/2 activity. Finally, it is important to note that NADH accumulation might also foster reductive carboxylation under low oxygen tension. The TCA metabolic flux is represented by *blue arrows* (), and () indicate the specific enzyme for each TCA cycle step. *Ac-CoA (Acetyl-Coenzyme A*; Aco (aconitase); Cit (citrate); Isocit (Isocitrate); Gln (Glutamine); α-KG (α-ketoglutarate)

driving the reduction of α-KG since any conditions leading to a high α-KG to citrate ratio might promote it, by mass action on the TCA cycle flux [14]. For instance, in hypoxia and in cancer cells with ETC defects, the decrease of α-KG oxidation may be driven by changes in the levels of reducing equivalents. In this scenario, modifications of the mitochondrial redox state might account for the inhibition of the TCA dehydrogenases α-KGDC and PDH and for the promotion of the NADPH-dependent IDHs [12, 14, 61, 62] (Fig. 2b). Furthermore, ETC defects or hypoxia often lead to increase in ROS [63], which may contribute to the reduction of α-KGDC and aconitase activity. In this condition, the ROS-mediated inhibition of α-KGDC might foster α-KG accumulation and its diversion towards lipid biosynthesis, while the inactivation of aconitase might contribute to the accumulation and the extrusion of citrate from mitochondria [64] (Fig. 2).

Silencing *OGDH* in cancer cells with mitochondrial defects has been shown to prevent the production of sufficient levels of NADH, ultimately increasing the $NADP^+$/NADPH ratio and preventing the NADPH-dependent IDHs to reduce α-KG [13]. This observation demonstrates that a minimal activity of α-KGDC is essential for the occurrence of reductive carboxylation and that this enzyme may operate even in the presence of respiration defects. Accordingly, HIF1 does not mediate a complete inhibition of α-KGDC activity, but only up to approximately 60% [56]. Moreover, accumulation of α-KG represses HIF1α stabilization and its downstream pathway by fostering the activity of the metabolic sensor prolyl hydroxylases (PHDs). This may represent a feedback control to keep the enzyme under the stringent regulation required for metabolic adaptation to hypoxia. To the same extent, the NADH and ROS-mediated regulation of α-KGDC activity represents additional feedback mechanisms that prevent complete enzyme inactivation. Since the forward and reverse modes of the TCA cycle are not exclusive, a fine-tuning of α-KGDC activity is required to balance α-KG fate in both energetic and anabolic pathways, according to oxygen levels and to ETC status.

In great contrast with impaired respiration, conditions of nutrient deprivation lead to OXPHOS enhancement and increase the NAD^+/NADH ratio in the matrix, hence promoting mitochondrial biogenesis, fatty acids oxidation, and preventing oxidative stress [65, 66]. Surprisingly, a decrease in α-KGDC activity and thereby of mitochondrial ATP synthesis, due to the accumulation of α-KG and subsequent inhibition of the ATP synthase, has been shown to mimic calorie restriction in *Caenorhabditis elegans* [67]. This mechanism is proposed to ensure energetic efficiency in response to nutrient deprivation [67] and suggests that decreasing α-KGDC activity is not in contradiction with optimal cellular respiration. However, the accumulation of α-KG in starved animals appears to come from an increase in glutamine metabolism to sustain anaplerotic gluconeogenesis from amino acids catabolism and not from a decrease in α-KGDC activity [68]. Thus, the relevance of this mechanism has yet to be proven in cancer cells, where nutrient requirements and metabolic networks are known to be drastically different from non-malignant cells. In cancer cells, glutaminolysis exceeds the cellular requirement for glutamine in the production of amino acids, nucleotides, and energy [69]. Duràn and co-workers have shown that α-KG levels are a crucial sign of amino acids availability status. In this scenario, high cytosolic levels of α-KG may promote mammalian target of rapamycin 1 (mTORC1) signaling, which in turn blocks autophagy, the housekeeping mechanism to survive nutrient deprivation stress, and increases anabolism in neoplastic cells. On the other hand, low levels of α-KG have opposite effects and correlate with reduced mitochondrial respiration and ATP levels [70, 71]. In this light, it might be hypothesized that the high α-KG production due to enhanced glutamine metabolism might be beneficial for cancer cells by promoting proliferation while inhibiting autophagy [72]. However, the complex interplay between glutamine metabolism and the regulation of mTOR and autophagic processes in cancer cells makes an uncertainty whether α-KG plays a pivotal role in this respect [73]. In addition, upon glucose deprivation, treatment with α-KG derivatives and its reduced form 2-hydroxyglutarate (2-HG) has revealed the ability to inhibit the ATP synthase, resulting in mTOR signaling reduction and autophagy blockage in cancer cells [74]. Overall, these findings suggest that α-KG levels variation may differently affect autophagy regulation according to nutrient availability and compartmentalization of the metabolite (i.e., cytosolic versus mitochondrial), whose regulation still warrants investigation.

Is α-KG an oncometabolite?

Mutations in fumarate hydratase (*FH*), succinate dehydrogenase (*SDH*), and *IDH1* and *IDH2* are associated to specific human neoplasms that hence accumulate succinate, fumarate, and (*R*)-2-HG, respectively, all conveying broad oncogenic signals [75]. Mutations in *FH* and *SDH* follow the classic Knudson "two-hit" model, with somatic loss of gene function leading to the accumulation of their substrates. In a non-canonic fashion, a single allele mutation in *IDH1/2* creates a neomorphic enzyme with increased affinity for α-KG, from which an excess of the (*R*)-2-HG metabolite is produced [75, 76]. The prime mechanism of action of these so-called "oncometabolites" lies within the fact that they are structurally and metabolically similar to α-KG and retain the

capacity to regulate a family of more than 60 enzymes involved in fatty acid metabolism, collagen biosynthesis, nutrient sensing, oxygen sensing, and epigenome editing [77, 78]. These enzymes are the Fe(II)/α-KG-dependent dioxygenases, and they include the PHDs introduced earlier. They are ubiquitously expressed and catalyze hydroxylation reactions on several targets. Moreover, they all use α-KG and O_2 as co-substrates and require Fe(II) as a cofactor to produce succinate and CO_2 [79]. Additionally, ascorbate is required to induce the reduction of Fe(III) to Fe(II), thus restoring enzyme activity [80, 81]. Noticeably, even in the absence of O_2, α-KG alone is sufficient to promote the activity of a subset of Fe(II)/α-KG-dependent dioxygenases, [82], which are instead inhibited by succinate and fumarate [83]. (*R*)-2-HG occupies the same binding site of α-KG and thereby acts as a competitive inhibitor [84]. Since the K_M of dioxygenases for α-KG is close to the metabolite physiological concentration, any condition causing even a modest variation in the cytosolic levels of α-KG may profoundly modify dioxygenases-mediated signals.

Understanding α-KG dynamics and their effect on its downstream targets

A comprehensive identification of enzymes that use α-KG to carry out their reactions will help to better define the metabolite role in bridging mitochondrial function to metabolic reprogramming in cancer cells. In this frame, PHDs have been extensively studied, in particular for their role in the response to hypoxia by determining HIF1α stabilization (Fig. 3). The transcription factor HIF1 consists of an α- and a β-subunit, which are both constitutively produced. Under normoxic conditions, HIF1α is degraded following the hydroxylation of two specific prolyl residues in its oxygen-dependent degradation domain (ODDD), operated by three different enzymes, namely PDH1, 2, and 3. This in turn recruits an E3 ubiquitin ligase complex containing the Von Hippel Lindau protein (pVHL), resulting in HIF1α ubiquitylation and subsequent degradation by the proteasome. Conversely, in hypoxia, the PHDs low affinity for oxygen does not allow them to hydroxylate HIF1α, which cannot be degraded and becomes stabilized. Although the three PHDs have been reported to be competitively inhibited by several TCA metabolites and pyruvate [83, 85–88], the most consistent effects are observed with fumarate and succinate [88] (Fig. 3). Accordingly, chronic inhibition of PHDs in both SDH-deficient and FH-deficient tumors is associated with the stabilization of HIF1α and activation of downstream hypoxic pathways even in normoxia (i.e., pseudohypoxia) [87]. Nevertheless, it is yet unclear whether the pseudohypoxic response caused by TCA cycle defects is sufficient *per se* to promote tumorigenesis or to support tumor progression [75]. Accumulation of α-KG, on the other hand, may have an opposite effect and rather lead to the constitutive destabilization of HIF1α. Accordingly, Gottlieb and his group have shown that the increase in α-KG alone is sufficient to oppose succinate, fumarate, and hypoxia-mediated activation of HIF1α. This resulted in the reversal of enhanced glycolysis and cell death [82, 89]. Hence, the levels of α-KG, even in hypoxia, may be sufficient to foster PHD activity and prevent the hypoxic response. In line with this, our group has

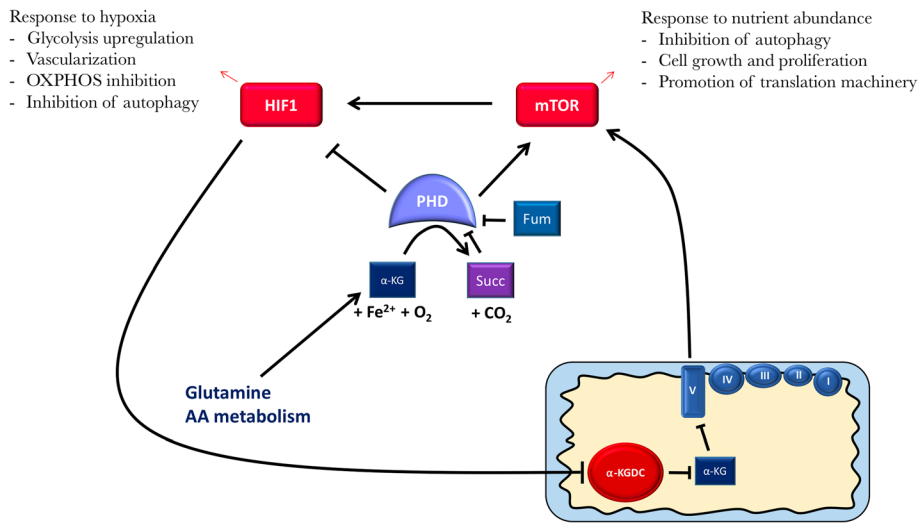

Fig. 3 Schematic representation of the influence of α-KG levels and compartmentalization on PHDs and ATP synthase. PHDs have a dual role in the context of cell response to resources availability. PHDs control both adaptations to reduced oxygen levels, through HIF1α destabilization, and to nutrient availability via mTOR promotion. Cytosolic accumulation of α-KG may promote both PHDs and mTOR pathway and may inhibit HIF1 signaling. Conversely, mitochondrial accumulation of α-KG may prevent mTOR activation through the ATP synthase inhibition

demonstrated that cancer cells with severe mitochondrial CI impairment display an increase of α-KG/succinate ratio, likely due to an inhibition of α-KGDC resulting from an increased NADH/NAD^+ ratio. This accumulation is associated to a constitutive destabilization of HIF1α even in a hypoxic environment (i.e., pseudonormoxia), together with a reduction of the tumorigenic potential in vivo [62, 90–92]. Importantly, both mitochondrial impairment and hypoxia can lead to the overproduction of L-(*R*)-2-HG, which is mostly generated by the conversion of glutamine-derived α-KG and competes with the latter [12, 61, 93–95]. Thus, dioxygenases would respond to the (*L*)-2-HG/α-KG ratio rather than to α-KG levels. Unlike (*R*)-2-HG, the L enantiomer does not stem from *IDH1* or *IDH2* mutations, but via a promiscuous activity of lactate dehydrogenase A (LDHA), MDH1 and PHGDH in the cytosol, and via MDH2 activity in the mitochondria, in a NADH-dependent manner [93, 96–98]. Hence, changes in the redox state as NADH accumulation and the subsequent modification of enzymatic functions associated to impaired respiration would foster α-KG conversion into (*L*)-2-HG. It has recently been remarked that an essential role of the respiratory chain is to transfer electrons from reduced substrate to oxygen, thereby maintaining an adequate redox state to allow aspartate synthesis and sustain cancer proliferation [26, 99]. In this context, it is plausible to envision that the α-KG may alternatively accept electrons and become reduced to (*L*)-2-HG, behaving as a *de facto* substitute of the ETC to support cancer growth. Consistently with this, supplementation with α-KG or inhibition of α-KGDC in normoxia causes a slight increase in (*L*)-2-HG levels, whereas in hypoxia the increase is far higher [93]. In the presence of respiration defects, on the other hand, the subsequent accumulation of α-KG might have different effects depending on its conversion rate into (*L*)-2-HG, as the enantiomer may inactivate PHDs over a certain threshold. It appears unlikely that the reduction of OXPHOS alone is sufficient to drive the (*L*)-2-HG-mediated HIF1 response, since, as shown by our group, a severe CI impairment rather prevents HIF1α stabilization. Additional factors would thus be required (Fig. 4). Besides low PHD activity due to the oxygen shortage, additional mechanisms may be envisioned. For instance, in physiological situations, the (*L*)-2-HG dehydrogenase (L2HGDH) converts (*L*)-2-HG back to α-KG [100], whereas in hypoxia *L2HGDH* expression is decreased by 50% and is therefore important to maintain a high (*L*)-2-HG/α-KG ratio (Fig. 4). Furthermore, a low L2HGDH activity would promote the production of ROS [93] with consequent HIF1α stabilization [101] (Fig. 4). It is remarkable that the regulation of *L2HGDH* expression is HIF1-independent, thus suggesting a potential upstream role in the initiation of the hypoxic response. Strikingly however, a recent study carried out by Burr and coworkers has shown that disruption of OGDH leads to HIF1α accumulation in normoxia via a ROS-independent PHD2-mediated mechanism that relies on (*L*)-2-HG production through both MDH1/2 and LDHA [102]. Hence, while cell response to hypoxia is mediated by multiple signals, including O_2, reductive equivalents, α-KG, (*L*)-2-HG and ROS, the modulation of α-KGDC activity alone may have a great impact on HIF1α stabilization. To support this, it was shown that decreasing PHD activity does not inevitably promote the HIF1-signaling pathway, even in hypoxia. This seems to depend on a diminished HIF1α translation, due to a decreased mTOR signaling that follows O2 and amino acids deprivation, and hence, low levels of cytosolic α-KG, as PHDs are enhancers of mTOR activity (Fig. 3) [71]. Both low and high levels of α-KG may therefore impede the hypoxic response, suggesting that the maintenance of a certain α-KG amount is essential for HIF1 activation. In this light, it is possible to speculate that maintaining α-KGDC activity in an appropriate range would not only permit cells to meet metabolic requirements in hypoxia but it would also accurately control α-KG and (*L*)-2-HG levels in order to provide cells with a tailored signal for HIF1 activation.

Besides mTOR, autophagy is also modulated by HIF1 [103], making PHDs and thereby α-KG levels pivotal in organelles catabolism. Accumulation of α-KG may also promote mTOR function via ATP synthase inhibition in the mitochondrion, without involving PHDs [67] (Fig. 3). Hence, while cytosolic accumulation of α-KG might prevent autophagy by activating PHDs, the elevation of its levels in the mitochondria would instead promote it, via ATP synthase inhibition. Nonetheless, cytosolic Fe(II)/α-KG-dependent dioxygenases respond to the ratio between α-KG and its various competitors, whereas α-KG mediates the inhibition of ATP synthase in a non-competitive manner [67]. Consequently, the former mechanism is sensitive to high cytosolic α-KG/2-HG ratio, generated by an increase in amino acids metabolism or a decrease in OXPHOS. The latter may instead be triggered by both α-KG and its reduced forms in the mitochondrial matrix with respect to ATP synthase abundance, and would serve to optimize cell respiration according to substrate availability, thereby contributing to caloric restriction adaptation.

In conclusion, the response to fluctuations of α-KG levels in cells is multifactorial and remains an open area of research. The α-KG signaling is likely to be defined by the metabolite abundance, its oxidation state, and dynamics, which are determined by ETC status and oxygen levels, perhaps among other yet unknown mechanisms. Based on these considerations, it is plausible to argue that fluctuations of α-KG levels may be an intrinsic

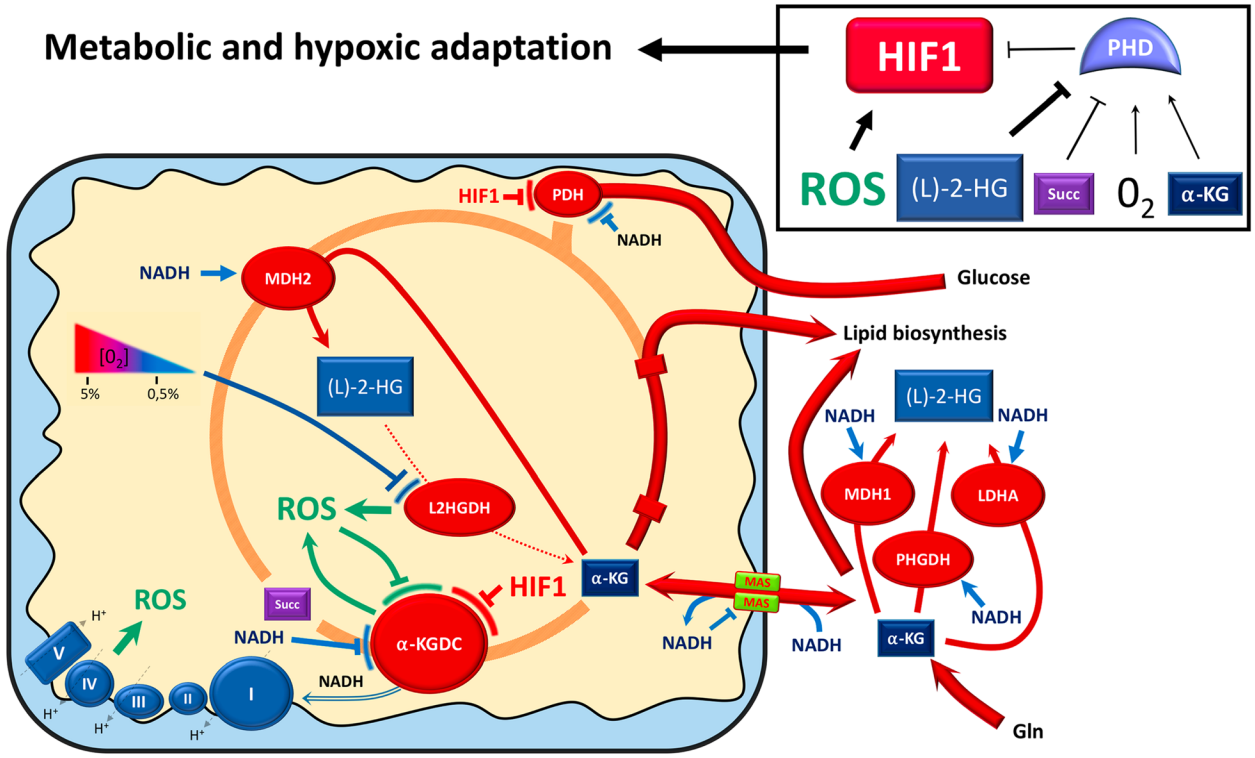

Fig. 4 Mitochondrial signals that shape the HIF1-mediated metabolic and hypoxic adaptation in cancer cells. The hypoxic response may originate both from HIF1α stabilization, via the decrease in oxygen levels and the increase in the (*L*)-2-HG/α-KG ratio that lower PHDs activity, and from HIF1 activation, due to high ROS levels. In the first instance, reduced oxygen levels may inhibit the L2HGDH activity thereby decreasing (*L*)-2-HG conversion into α-KG, together with fostering ROS production. Additionally, the elevation of NADH levels in the mitochondria that stems from decreased respiration inhibits the malate-aspartate shuttle (MAS) and therefore mitochondrial NADH production from cytosolic reductive power. Both mitochondrial and cytosolic NADH accumulation foster the activity of the NADH-dependent enzymes MDH1/2, PHGDH and LDHA that convert α-KG into (*L*)-2-HG. Furthermore, the potential production of ROS by the ETC and α-KGDC might further promote HIF1 activation. Finally, both NADH and HIF1 may inhibit α-KGDC and PDH, further promoting α-KG accumulation, in turn converted into (*L*)-2-HG or utilized for lipid biosynthesis

characteristic of tumor progression, useful to trigger the bioenergetic changes in response to selective pressures. In this light, the role of α-KG remains dual as it may promote both oncogenic and tumor suppressive functions, paralleling the oncojanus function of mitochondrial genes, as we have previously proposed [91].

Impact of α-ketoglutarate on cancer cell epigenetics

Epigenetics alterations at both DNA and histone levels are increasingly being recognized as modifiers of tumorigenesis [104]. CpG islands are widely hypermethylated in many cancer types compared to the corresponding normal tissue, while the rest of the genome is rather subject to demethylation. The hypermethylation of CpG islands has been utilized as a criterion to distinguish different tumor types from non-malignant tissue [105], and tumors characterized by high levels of DNA methylation have been classified as having a CpG island methylator phenotype and are predominantly associated with worse prognosis, potentially due to a silencing of tumor suppressor genes. In many cases, this phenotype originates in early phases of tumorigenesis of many tumor types such as glioblastomas, acute myeloid leukemias, gastric cancer, and ependymomas [106–111], where drugs targeting the DNA methylation machinery are a promising strategy.

The large family of α-KG-dependent dioxygenases includes two classes of enzymes involved in demethylation and hydroxylation reactions of DNA and histones. The ten-eleven translocation hydroxylases (TET 1 to 3) catalyze DNA demethylation, whereas the Jumonji C domain containing lysine demethylases (KDM 2 to 7) is the largest family of histone demethylases [112–114]. Both (*L*)-2-HG and (*R*)-2-HG are competitive inhibitors of TETs and KDMs, and are thus important modifiers of the epigenetic landscape of cancer cells [84, 94, 115, 116]. Accordingly, accumulation of (*L*)-2-HG and (*R*)-2-HG has been associated to several types of cancers [96, 117–119]. Similarly, recent studies have revealed that together with 2HGs, succinate and fumarate can also induce alterations in DNA and histones methylation, thus enhancing cancer formation [84, 120–125]. These findings suggest that

different cytosolic concentrations of α-KG affect the methylation status of both histones and DNA and thereby trigger epigenetic changes. Accordingly, Thompson's group has demonstrated how maintenance of a proper α-KG to succinate ratio is fundamental to determine the identity and the fate of embryonic stem cells (ESC) [126]. In particular, a high α-KG/succinate ratio promotes the activity of DNA and histone demethylases, and modifying this ratio is sufficient to regulate multiple chromatin modifications. Indeed, treatment with α-KG supports ESC self-renewal, which is known to display an unusual "open" chromatin structure, associated to hypertranscription [127]. In this light, high cytosolic levels of α-KG would promote high energy-consuming processes, a hypothesis that is supported by the existence of the PHD-driven mTOR activation mediated by α-KG, which fosters anabolic processes. Conversely, in cancer cells facing hypoxia, it is plausible that α-KG conversion into (*L*)-2-HG most likely helps in reducing the energetic demand while promoting HIF1α stabilization for hypoxic adaptation. Consistent with this, hypoxia induces a global increase in trimethylation of histone H3 at lysine 9 (H3K9me3) marks, known to repress gene expression, through the accumulation of (*L*)-2-HG that inhibits the activity of the demethylase KDM4C [94]. Furthermore, oxygen shortage has recently been shown to directly cause DNA hypermethylation by reducing TET activity in cancer cells, predominantly at the level of gene promoters [128]. Notwithstanding this, both TETs and KDMs may stimulate the transcription of specific HIF1-targeted genes, while being themselves transcriptional targets of HIF1 [125, 128–133], a mechanism that most likely compensates for their lower enzymatic activity. Hence, while oncometabolites and low oxygen availability can promote a closed chromatin state and a drop in global gene expression through α-KG-dependent dioxygenases activity, it is plausible that retaining a minimal activity of these enzymes would induce a specific genetic response in cells by restraining transcription machinery to HIF1-targeted genes.

Similarly, given the role of α-KG as an indicator of amino acids availability, it is plausible to speculate the occurrence of an epigenetic remodeling upon glutamine deprivation, which may be faced by solid cancers. Accordingly, a recent study has demonstrated that glutamine deficiency is associated to low α-KG levels, which may in turn determine the inhibition of KDMs in the core regions of the tumor. In this context, the increase in histone methylation induces cancer cells dedifferentiation and may cause therapy resistance [134].

The consequence of epigenetics modifications is the transduction of external stimuli into a transcriptional response, thus adjusting cells phenotype without affecting their genotype [135]. It is most likely that cell bioenergetic changes driven by external and internal selective pressures promote an intricate epigenetic remodeling through α-KG signaling.

Conclusions

A revisited role of mitochondria highlights that they are not mere bystanders during carcinogenesis. The ever-changing tumor microenvironment may force cells to rely on fluctuating levels of oxygen, as well as varying availability and types of nutrients, whereby optimization of substrates utilization and a continuous restructuring of both metabolic and genetic signatures becomes mandatory for survival. In this review, we have highlighted a hub role for the TCA cycle enzyme α-KGDC as a front-line player in the adaptation of cancer cells to a demanding environment in vivo. This enzyme may be considered a gatekeeper of the OXPHOS system and one of the major regulators of mitochondrial metabolism. Indeed, α-KGDC responds to OXPHOS activity fluctuations, controls the mitochondrial redox status through NADH and ROS levels balance, and directs the TCA metabolite fluxes towards energetic, anabolic, and signaling pathways. Changes in α-KGDC activity, and consequently in overall mitochondrial bioenergetics, may impact not only on TCA cycle fluxes but may become amplified and eventually drive an intricate metabolic and epigenetic remodeling. Overall, NADH/NAD^+ and AMP/ATP ratio, oxidative stress, membrane potential, and oxygen levels are pivotal players in the translation of the α-KG signal. In turn, α-KG and its reduced forms may influence the activity of dioxygenases to shape cells metabolic and epigenetic landscape according to oxygen and nutrient availability and ETC efficiency. In this light, the α-KGDC and its substrate appear to be inescapable actors in cancer cells plasticity. It is remarkable that genetic and metabolic modifications within a tumor mass are likely to differ from cell to cell thereby contributing to a phenotypic heterogeneity, thus accounting for therapy resistance and disease progression [134, 136]. Several studies have considered the anti-tumorigenic properties of α-KG but its mechanisms of action are still not fully understood. The anti-tumorigenic effect observed upon in vivo treatment with derivatives of α-KG has been shown not only to depend on impaired HIF1 signaling pathway but also to a much greater extent on multiple unknown side effects of α-KG on tumor growth [94]. In this frame, it has been reported that α-KG antagonizes the effect of other oncometabolites, and might therefore be considered a tumor suppressor metabolite. Nevertheless, α-KG supplementation leads to the risk of feeding oncogenic pathways not only due to its conversion into (*L*)-2-HG in respiratory deficient cells but also into succinate and fumarate, on a long-term treatment [137]. On the other hand, several human Fe(II)/α-KG-dependent

dioxygenases have been investigated as possible therapeutic targets and might represent an interesting alternative strategy to render tumors more sensitive to radiotherapy and chemotherapy [90]. A complete understanding of the α-KG-mediated interplay between metabolic and genetic reprogramming will help us to disclose a new therapeutic window in which cancer progression can be restrained. While cancer is defined as a genetic disease, there is nowadays a growing and legitimate interest in its metabolic dimension. In particular, these two aspects are increasingly recognized as being so interconnected that they are likely to represent the two edges of the same sword.

Abbreviations

2-HG: 2-Hydroxyglutarate; Ca^{2+}: Calcium; CI: Complex I; CoA: Coenzyme A; CS: Citrate synthase; DHLA: Dihydrolipoic acid; E1: α-Ketoglutarate dehydrogenase; E2: Dihydrolipoamide succinyltransferase; E3: Dihydrolipoamide dehydrogenase; ETC: Electron transport chain; FH: Fumarate hydratase; H3K9me3: Trimethylation of histone H3 at lysine 9; HIF1: Hypoxia inducible factor 1; IMM: Inner mitochondrial membrane; IMS: Mitochondrial intermembrane space; KDM: Lysine demethylases; K_M: Michaelis constant; L2HGDH: (*L*)-2-HG dehydrogenase; LA: Lipoic acid; MAS: Malate-aspartate shuttle; mtDNA: Mitochondrial DNA; mTORC1: Mammalian target of rapamycin 1; ODDD: Oxygen-dependent degradation domain; OGC: 2-Oxoglutarate carrier; OXPHOS: Oxidative phosphorylation; PDH: Pyruvate dehydrogenase; PHDs: Prolyl hydroxylases; Pi: Inorganic phosphate; pVHL: Von Hippel Lindau protein; ROS: Reactive oxygen species; Succ-CoA: Succinyl coenzyme A; TCA: Tricarboxylic acid ; TET: Ten-eleven translocation hydroxylases; TOR: Target of rapamycin; TPP: Thiamine pyrophosphate; α-KG: α-Ketoglutarate; α-KGDC: α-Ketoglutarate dehydrogenase complex; $\Delta\psi_m$: Membrane potential

Acknowledgements

We would like to thank Dr. Rosanna Clima from the University of Bari (Italy) for her bioinformatics support.

Funding

This paper was supported by the European Commission FP7 Marie Curie ITN-317433 MEET and the Italian Ministry of Health project GR-2013-02356666 DISCO TRIP to G.Gasparre. It was also supported by the Italian Association for Cancer Research (AIRC) grants IG14242 JANEUTICS to G.Gasparre and IG17387 TOUCHME to A.M.Porcelli. G.Girolimetti is supported by a triennial AIRC fellowship "Livia Perotti".

Availability of data and materials

Not applicable

Authors' contributions

RV wrote the manuscript and prepared the figures. GL, MDL, GGirolimetti, and MV have all supported this work by carrying out the literature search and summarizing the key information. GGasparre and AM Porcelli supervised the design of the review and wrote the manuscript. All authors read and approved the final manuscript.

Competing interests

The authors declare that they have no competing interests.

Consent for publication

Not applicable

Ethics approval and consent to participate

Not applicable

Received: 21 December 2016 Accepted: 18 January 2017
Published online: 02 February 2017

References

1. Hanahan D, Weinberg RA. Hallmarks of cancer: the next generation. Cell. 2011;144:646–74.
2. Warburg O, Wind F, Negelein E. The metabolism of tumors in the body. J Gen Physiol. 1927;8:519–30.
3. Chen X, Qian Y, Wu S. The Warburg effect: evolving interpretations of an established concept. Free Radic Biol Med. 2015;79:253–63.
4. Marin-Valencia I, Yang C, Mashimo T, Cho S, Baek H, Yang X-L, et al. Analysis of tumor metabolism reveals mitochondrial glucose oxidation in genetically diverse human glioblastomas in the mouse brain in vivo. Cell Metab. 2012;15:827–37.
5. Smolková K, Plecitá-Hlavatá L, Bellance N, Benard G, Rossignol R, Ježek P. Waves of gene regulation suppress and then restore oxidative phosphorylation in cancer cells. Int J Biochem Cell Biol. 2011;43:950–68.
6. Jose C, Bellance N, Rossignol R. Choosing between glycolysis and oxidative phosphorylation: a tumor's dilemma? Biochim Biophys Acta. 2011;1807:552–61.
7. Tan AS, Baty JW, Berridge MV. The role of mitochondrial electron transport in tumorigenesis and metastasis. Biochim Biophys Acta. 2014;1840:1454–63.
8. Birsoy K, Possemato R, Lorbeer FK, Bayraktar EC, Thiru P, Yucel B, et al. Metabolic determinants of cancer cell sensitivity to glucose limitation and biguanides. Nature. 2014;508:108–12.
9. Wolf DA. Is reliance on mitochondrial respiration a "chink in the armor" of therapy-resistant cancer? Cancer Cell. 2014;26:788–95.
10. DeBerardinis RJ, Mancuso A, Daikhin E, Nissim I, Yudkoff M, Wehrli S, et al. Beyond aerobic glycolysis: transformed cells can engage in glutamine metabolism that exceeds the requirement for protein and nucleotide synthesis. Proc Natl Acad Sci U S A. 2007;104:19345–50.
11. Hosios AM, Hecht VC, Danai LV, Johnson MO, Rathmell JC, Steinhauser ML, et al. Amino acids rather than glucose account for the majority of cell mass in proliferating mammalian cells. Dev Cell. 2016;36:540–9.
12. Wise DR, Ward PS, Shay JES, Cross JR, Gruber JJ, Sachdeva UM, et al. Hypoxia promotes isocitrate dehydrogenase-dependent carboxylation of α-ketoglutarate to citrate to support cell growth and viability. Proc Natl Acad Sci U S A. 2011;108:19611–6.
13. Mullen AR, Wheaton WW, Jin ES, Chen P-H, Sullivan LB, Cheng T, et al. Reductive carboxylation supports growth in tumour cells with defective mitochondria. Nature. 2011;481:385–8.
14. Fendt S-M, Bell EL, Keibler MA, Olenchock BA, Mayers JR, Wasylenko TM, et al. Reductive glutamine metabolism is a function of the α-ketoglutarate to citrate ratio in cells. Nat Commun. 2013;4:2236.
15. Reed LJ, Hackert ML. Structure-function relationships in dihydrolipoamide acyltransferases. J Biol Chem. 1990;265:8971–4.
16. Strumilo S. Short-term regulation of the alpha-ketoglutarate dehydrogenase complex by energy-linked and some other effectors. Biochem Biokhimiia. 2005;70:726–9.
17. Robinson BH. Use of fibroblast and lymphoblast cultures for detection of respiratory chain defects. Methods Enzymol. 1996;264:454–64.
18. Nelson UDL, Cox UMM. Lehninger Principles of Biochemistry. New York: 7th edition. W. H. Freeman; 2017.
19. Porpaczy Z, Sumegi B, Alkonyi I. Interaction between NAD-dependent isocitrate dehydrogenase, alpha-ketoglutarate dehydrogenase complex, and NADH: ubiquinone oxidoreductase. J Biol Chem. 1987;262:9509–14.
20. Fukushima T, Decker RV, Anderson WM, Spivey HO. Substrate channeling of NADH and binding of dehydrogenases to complex I. J Biol Chem. 1989;264:16483–8.
21. Maas E, Bisswanger H. Localization of the alpha-oxoacid dehydrogenase multienzyme complexes within the mitochondrion. FEBS Lett. 1990;277:189–90.
22. McCormack JG, Denton RM. The effects of calcium ions and adenine nucleotides on the activity of pig heart 2-oxoglutarate dehydrogenase complex. Biochem J. 1979;180:533–44.
23. Lawlis VB, Roche TE. Inhibition of bovine kidney alpha-ketoglutarate dehydrogenase complex by reduced nicotinamide adenine dinucleotide in the presence or absence of calcium ion and effect of adenosine 5'-diphosphate on reduced nicotinamide adenine dinucleotide inhibition. Biochemistry (Mosc). 1981;20:2519–24.
24. Armstrong CT, Anderson JLR, Denton RM. Studies on the regulation of the human E1 subunit of the 2-oxoglutarate dehydrogenase complex, including the identification of a novel calcium-binding site. Biochem J. 2014;459:369–81.
25. Klingenberg M. The ADP, and ATP transport in mitochondria and its carrier. Biochim Biophys Acta. 2008;1778:1978–2021.

26. Birsoy K, Wang T, Chen WW, Freinkman E, Abu-Remaileh M, Sabatini DM. An essential role of the mitochondrial electron transport chain in cell proliferation is to enable aspartate synthesis. Cell. 2015;162:540–51.
27. Banerjee K, Munshi S, Xu H, Frank DE, Chen H-L, Chu CT, et al. Mild mitochondrial metabolic deficits by α-ketoglutarate dehydrogenase inhibition cause prominent changes in intracellular autophagic signaling: potential role in the pathobiology of Alzheimer's disease. Neurochem Int. 2016;96:32–45.
28. Kumar MJ, Nicholls DG, Andersen JK. Oxidative alpha-ketoglutarate dehydrogenase inhibition via subtle elevations in monoamine oxidase B levels results in loss of spare respiratory capacity: implications for Parkinson's disease. J Biol Chem. 2003;278:46432–9.
29. Denton RM. Regulation of mitochondrial dehydrogenases by calcium ions. Biochim Biophys Acta. 2009;1787:1309–16.
30. Tarasov AI, Griffiths EJ, Rutter GA. Regulation of ATP production by mitochondrial Ca(2+). Cell Calcium. 2012;52:28–35.
31. McCormack JG, Halestrap AP, Denton RM. Role of calcium ions in regulation of mammalian intramitochondrial metabolism. Physiol Rev. 1990;70:391–425.
32. Santo-Domingo J, Demaurex N. Calcium uptake mechanisms of mitochondria. Biochim Biophys Acta. 2010;1797:907–12.
33. Cárdenas C, Müller M, McNeal A, Lovy A, Jaňa F, Bustos G, et al. Selective vulnerability of cancer cells by inhibition of Ca(2+) transfer from endoplasmic reticulum to mitochondria. Cell Rep. 2016;15:219–20.
34. Rottenberg H, Lee CP. Energy dependent hydrogen ion accumulation in submitochondrial particles. Biochemistry (Mosc). 1975;14:2675–80.
35. Porcelli AM, Ghelli A, Zanna C, Pinton P, Rizzuto R, Rugolo M. pH difference across the outer mitochondrial membrane measured with a green fluorescent protein mutant. Biochem Biophys Res Commun. 2005;326:799–804.
36. Lowry M, Ross BD. Activation of oxoglutarate dehydrogenase in the kidney in response to acute acidosis. Biochem J. 1980;190:771–80.
37. Damaghi M, Wojtkowiak JW, Gillies RJ. pH sensing and regulation in cancer. Front Physiol. 2013;4:370.
38. Santo-Domingo J, Demaurex N. Perspectives on: SGP symposium on mitochondrial physiology and medicine: the renaissance of mitochondrial pH. J Gen Physiol. 2012;139:415–23.
39. Murphy MP. How mitochondria produce reactive oxygen species. Biochem J. 2009;417:1–13.
40. Nulton-Persson AC, Starke DW, Mieyal JJ, Szweda LI. Reversible inactivation of alpha-ketoglutarate dehydrogenase in response to alterations in the mitochondrial glutathione status. Biochemistry (Mosc). 2003;42:4235–42.
41. Applegate MAB, Humphries KM, Szweda LI. Reversible inhibition of alpha-ketoglutarate dehydrogenase by hydrogen peroxide: glutathionylation and protection of lipoic acid. Biochemistry (Mosc). 2008;47:473–8.
42. McLain AL, Szweda PA, Szweda LI. α-Ketoglutarate dehydrogenase: a mitochondrial redox sensor. Free Radic Res. 2011;45:29–36.
43. Starkov AA, Fiskum G, Chinopoulos C, Lorenzo BJ, Browne SE, Patel MS, et al. Mitochondrial alpha-ketoglutarate dehydrogenase complex generates reactive oxygen species. J Neurosci Off J Soc Neurosci. 2004;24:7779–88.
44. Tretter L, Adam-Vizi V. Generation of reactive oxygen species in the reaction catalyzed by alpha-ketoglutarate dehydrogenase. J Neurosci Off J Soc Neurosci. 2004;24:7771–8.
45. Quinlan CL, Goncalves RLS, Hey-Mogensen M, Yadava N, Bunik VI, Brand MD. The 2-oxoacid dehydrogenase complexes in mitochondria can produce superoxide/hydrogen peroxide at much higher rates than complex I. J Biol Chem. 2014;289:8312–25.
46. Szatrowski TP, Nathan CF. Production of large amounts of hydrogen peroxide by human tumor cells. Cancer Res. 1991;51:794–8.
47. Ray PD, Huang B-W, Tsuji Y. Reactive oxygen species (ROS) homeostasis and redox regulation in cellular signaling. Cell Signal. 2012;24:981–90.
48. Nulton-Persson AC, Szweda LI. Modulation of mitochondrial function by hydrogen peroxide. J Biol Chem. 2001;276:23357–61.
49. Coloff JL, Murphy JP, Braun CR, Harris IS, Shelton LM, Kami K, et al. Differential glutamate metabolism in proliferating and quiescent mammary epithelial cells. Cell Metab. 2016;23:867–80.
50. Bunik VI. 2-Oxo acid dehydrogenase complexes in redox regulation. Eur J Biochem. 2003;270:1036–42.
51. Stuart SD, Schauble A, Gupta S, Kennedy AD, Keppler BR, Bingham PM, et al. A strategically designed small molecule attacks alpha-ketoglutarate dehydrogenase in tumor cells through a redox process. Cancer Metab. 2014;2:4.
52. Zachar Z, Marecek J, Maturo C, Gupta S, Stuart SD, Howell K, et al. Non-redox-active lipoate derivates disrupt cancer cell mitochondrial metabolism and are potent anticancer agents in vivo. J Mol Med Berl Ger. 2011;89:1137–48.
53. Hensley CT, Wasti AT, DeBerardinis RJ. Glutamine and cancer: cell biology, physiology, and clinical opportunities. J Clin Invest. 2013;123:3678–84.
54. Kuhajda FP, Jenner K, Wood FD, Hennigar RA, Jacobs LB, Dick JD, et al. Fatty acid synthesis: a potential selective target for antineoplastic therapy. Proc Natl Acad Sci U S A. 1994;91:6379–83.
55. Hatzivassiliou G, Zhao F, Bauer DE, Andreadis C, Shaw AN, Dhanak D, et al. ATP citrate lyase inhibition can suppress tumor cell growth. Cancer Cell. 2005;8:311–21.
56. Sun RC, Denko NC. Hypoxic regulation of glutamine metabolism through HIF1 and SIAH2 supports lipid synthesis that is necessary for tumor growth. Cell Metab. 2014;19:285–92.
57. Metallo CM, Gameiro PA, Bell EL, Mattaini KR, Yang J, Hiller K, et al. Reductive glutamine metabolism by IDH1 mediates lipogenesis under hypoxia. Nature. 2011;481:380–4.
58. Semenza GL. Hypoxia-inducible factor 1 (HIF-1) pathway. Sci STKE Signal Transduct Knowl Environ. 2007;2007:cm8.
59. Kim J, Tchernyshyov I, Semenza GL, Dang CV. HIF-1-mediated expression of pyruvate dehydrogenase kinase: a metabolic switch required for cellular adaptation to hypoxia. Cell Metab. 2006;3:177–85.
60. Gameiro PA, Yang J, Metelo AM, Pérez-Carro R, Baker R, Wang Z, et al. In vivo HIF-mediated reductive carboxylation is regulated by citrate levels and sensitizes VHL-deficient cells to glutamine deprivation. Cell Metab. 2013;17:372–85.
61. Mullen AR, Hu Z, Shi X, Jiang L, Boroughs LK, Kovacs Z, et al. Oxidation of alpha-ketoglutarate is required for reductive carboxylation in cancer cells with mitochondrial defects. Cell Rep. 2014;7:1679–90.
62. Calabrese C, Iommarini L, Kurelac I, Calvaruso MA, Capristo M, Lollini P-L, et al. Respiratory complex I is essential to induce a Warburg profile in mitochondria-defective tumor cells. Cancer Metab. 2013;1:11.
63. Sullivan LB, Chandel NS. Mitochondrial reactive oxygen species and cancer. Cancer Metab. 2014;2:17. doi:10.1186/2049-3002-2-17.
64. Armstrong JS, Whiteman M, Yang H, Jones DP. The redox regulation of intermediary metabolism by a superoxide-aconitase rheostat. BioEssays News Rev Mol Cell Dev Biol. 2004;26:894–900.
65. Smolková K, Bellance N, Scandurra F, Génot E, Gnaiger E, Plecitá-Hlavatá L, et al. Mitochondrial bioenergetic adaptations of breast cancer cells to aglycemia and hypoxia. J Bioenerg Biomembr. 2010;42:55–67.
66. Martin-Montalvo A, de Cabo R. Mitochondrial metabolic reprogramming induced by calorie restriction. Antioxid Redox Signal. 2013;19:310–20.
67. Chin RM, Fu X, Pai MY, Vergnes L, Hwang H, Deng G, et al. The metabolite α-ketoglutarate extends lifespan by inhibiting ATP synthase and TOR. Nature. 2014;510:397–401.
68. Brugnara L, Vinaixa M, Murillo S, Samino S, Rodriguez MA, Beltran A, et al. Metabolomics approach for analyzing the effects of exercise in subjects with type 1 diabetes mellitus. PLoS One. 2012;7:e40600.
69. Zu XL, Guppy M. Cancer metabolism: facts, fantasy, and fiction. Biochem Biophys Res Commun. 2004;313:459–65.
70. Durán RV, Oppliger W, Robitaille AM, Heiserich L, Skendaj R, Gottlieb E, et al. Glutaminolysis activates Rag-mTORC1 signaling. Mol Cell. 2012;47:349–58.
71. Durán RV, MacKenzie ED, Boulahbel H, Frezza C, Heiserich L, Tardito S, et al. HIF-independent role of prolyl hydroxylases in the cellular response to amino acids. Oncogene. 2013;32:4549–56.
72. Durán RV, Hall MN. Glutaminolysis feeds mTORC1. Cell Cycle (Georgetown, Texas). 2012;11:4107–8.
73. Altman BJ, Stine ZE, Dang CV. From Krebs to clinic: glutamine metabolism to cancer therapy. Nat Rev Cancer. 2016;16:619–34.
74. Fu X, Chin RM, Vergnes L, Hwang H, Deng G, Xing Y, et al. 2-Hydroxyglutarate inhibits ATP synthase and mTOR signaling. Cell Metab. 2015;22:508–15.
75. Morin A, Letouzé E, Gimenez-Roqueplo A-P, Favier J. Oncometabolites-driven tumorigenesis: from genetics to targeted therapy. Int J Cancer. 2014;135:2237–48.
76. Dang L, White DW, Gross S, Bennett BD, Bittinger MA, Driggers EM, et al. Cancer-associated IDH1 mutations produce 2-hydroxyglutarate. Nature. 2009;462:739–44.
77. Loenarz C, Schofield CJ. Expanding chemical biology of 2-oxoglutarate oxygenases. Nat Chem Biol. 2008;4:152–6.
78. Rose NR, McDonough MA, King ONF, Kawamura A, Schofield CJ. Inhibition of 2-oxoglutarate dependent oxygenases. Chem Soc Rev. 2011;40:4364–97.
79. McDonough MA, Loenarz C, Chowdhury R, Clifton IJ, Schofield CJ. Structural studies on human 2-oxoglutarate dependent oxygenases. Curr Opin Struct Biol. 2010;20:659–72.

80. Pan Y, Mansfield KD, Bertozzi CC, Rudenko V, Chan DA, Giaccia AJ, et al. Multiple factors affecting cellular redox status and energy metabolism modulate hypoxia-inducible factor prolyl hydroxylase activity in vivo and in vitro. Mol Cell Biol. 2007;27:912–25.
81. Flashman E, Hoffart LM, Hamed RB, Bollinger JM, Krebs C, Schofield CJ. Evidence for the slow reaction of hypoxia-inducible factor prolyl hydroxylase 2 with oxygen. FEBS J. 2010;277:4089–99.
82. Tennant DA, Frezza C, MacKenzie ED, Nguyen QD, Zheng L, Selak MA, et al. Reactivating HIF prolyl hydroxylases under hypoxia results in metabolic catastrophe and cell death. Oncogene. 2009;28:4009–21.
83. Selak MA, Armour SM, MacKenzie ED, Boulahbel H, Watson DG, Mansfield KD, et al. Succinate links TCA cycle dysfunction to oncogenesis by inhibiting HIF-alpha prolyl hydroxylase. Cancer Cell. 2005;7:77–85.
84. Xu W, Yang H, Liu Y, Yang Y, Wang P, Kim S-H, et al. Oncometabolite 2-hydroxyglutarate is a competitive inhibitor of α-ketoglutarate-dependent dioxygenases. Cancer Cell. 2011;19:17–30.
85. Dalgard CL, Lu H, Mohyeldin A, Verma A. Endogenous 2-oxoacids differentially regulate expression of oxygen sensors. Biochem J. 2004;380(Pt 2):419–24.
86. Hewitson KS, Liénard BMR, McDonough MA, Clifton IJ, Butler D, Soares AS, et al. Structural and mechanistic studies on the inhibition of the hypoxia-inducible transcription factor hydroxylases by tricarboxylic acid cycle intermediates. J Biol Chem. 2007;282:3293–301.
87. Pollard PJ, Brière JJ, Alam NA, Barwell J, Barclay E, Wortham NC, et al. Accumulation of Krebs cycle intermediates and over-expression of HIF1alpha in tumours which result from germline FH and SDH mutations. Hum Mol Genet. 2005;14:2231–9.
88. Koivunen P, Hirsilä M, Remes AM, Hassinen IE, Kivirikko KI, Myllyharju J. Inhibition of hypoxia-inducible factor (HIF) hydroxylases by citric acid cycle intermediates: possible links between cell metabolism and stabilization of HIF. J Biol Chem. 2007;282:4524–32.
89. MacKenzie ED, Selak MA, Tennant DA, Payne LJ, Crosby S, Frederiksen CM, et al. Cell-permeating alpha-ketoglutarate derivatives alleviate pseudohypoxia in succinate dehydrogenase-deficient cells. Mol Cell Biol. 2007;27:3282–9.
90. Porcelli AM, Ghelli A, Ceccarelli C, Lang M, Cenacchi G, Capristo M, et al. The genetic and metabolic signature of oncocytic transformation implicates HIF1alpha destabilization. Hum Mol Genet. 2010;19:1019–32.
91. Gasparre G, Kurelac I, Capristo M, Iommarini L, Ghelli A, Ceccarelli C, et al. A mutation threshold distinguishes the antitumorigenic effects of the mitochondrial gene MTND1, an oncojanus function. Cancer Res. 2011;71:6220–9.
92. Iommarini L, Kurelac I, Capristo M, Calvaruso MA, Giorgio V, Bergamini C, et al. Different mtDNA mutations modify tumor progression in dependence of the degree of respiratory complex I impairment. Hum Mol Genet. 2014;23:1453–66.
93. Oldham WM, Clish CB, Yang Y, Loscalzo J. Hypoxia-mediated increases in L-2-hydroxyglutarate coordinate the metabolic response to reductive stress. Cell Metab. 2015;22:291–303.
94. Intlekofer AM, Dematteo RG, Venneti S, Finley LWS, Lu C, Judkins AR, et al. Hypoxia induces production of L-2-hydroxyglutarate. Cell Metab. 2015;22:304–11.
95. Worth AJ, Gillespie KP, Mesaros C, Guo L, Basu SS, Snyder NW, et al. Rotenone stereospecifically increases (S)-2-hydroxyglutarate in SH-SY5Y neuronal cells. Chem Res Toxicol. 2015;28:948–54.
96. Koivunen P, Lee S, Duncan CG, Lopez G, Lu G, Ramkissoon S, et al. Transformation by the (R)-enantiomer of 2-hydroxyglutarate linked to EGLN activation. Nature. 2012;483:484–8.
97. Harris AL. A new hydroxy metabolite of 2-oxoglutarate regulates metabolism in hypoxia. Cell Metab. 2015;22:198–200.
98. Fan J, Teng X, Liu L, Mattaini KR, Looper RE, Vander Heiden MG, et al. Human phosphoglycerate dehydrogenase produces the oncometabolite D-2-hydroxyglutarate. ACS Chem Biol. 2015;10:510–6.
99. Sullivan LB, Gui DY, Hosios AM, Bush LN, Freinkman E, Vander Heiden MG. Supporting aspartate biosynthesis is an essential function of respiration in proliferating cells. Cell. 2015;162:552–63.
100. Linster CL, Van Schaftingen E, Hanson AD. Metabolite damage and its repair or pre-emption. Nat Chem Biol. 2013;9:72–80.
101. Chandel NS, McClintock DS, Feliciano CE, Wood TM, Melendez JA, Rodriguez AM, et al. Reactive oxygen species generated at mitochondrial complex III stabilize hypoxia-inducible factor-1alpha during hypoxia: a mechanism of O2 sensing. J Biol Chem. 2000;275:25130–8.
102. Burr SP, Costa ASH, Grice GL, Timms RT, Lobb IT, Freisinger P, et al. Mitochondrial protein lipoylation and the 2-oxoglutarate dehydrogenase complex controls HIF1α stability in aerobic conditions. Cell Metab. 2016;24:740-52. doi:10.1016/j.cmet.2016.09.015.
103. Mazure NM, Pouysségur J. Atypical BH3-domains of BNIP3 and BNIP3L lead to autophagy in hypoxia. Autophagy. 2009;5:868–9.
104. Feinberg AP, Koldobskiy MA, Göndör A. Epigenetic modulators, modifiers and mediators in cancer aetiology and progression. Nat Rev Genet. 2016;17:284–99.
105. Christensen BC, Marsit CJ, Houseman EA, Godleski JJ, Longacker JL, Zheng S, et al. Differentiation of lung adenocarcinoma, pleural mesothelioma, and nonmalignant pulmonary tissues using DNA methylation profiles. Cancer Res. 2009;69:6315–21.
106. Toyota M, Ahuja N, Ohe-Toyota M, Herman JG, Baylin SB, Issa JP. CpG island methylator phenotype in colorectal cancer. Proc Natl Acad Sci U S A. 1999;96:8681–6.
107. Weisenberger DJ, Siegmund KD, Campan M, Young J, Long TI, Faasse MA, et al. CpG island methylator phenotype underlies sporadic microsatellite instability and is tightly associated with BRAF mutation in colorectal cancer. Nat Genet. 2006;38:787–93.
108. Figueroa ME, Abdel-Wahab O, Lu C, Ward PS, Patel J, Shih A, et al. Leukemic IDH1 and IDH2 mutations result in a hypermethylation phenotype, disrupt TET2 function, and impair hematopoietic differentiation. Cancer Cell. 2010;18:553–67.
109. Noushmehr H, Weisenberger DJ, Diefes K, Phillips HS, Pujara K, Berman BP, et al. Identification of a CpG island methylator phenotype that defines a distinct subgroup of glioma. Cancer Cell. 2010;17:510–22.
110. Zouridis H, Deng N, Ivanova T, Zhu Y, Wong B, Huang D, et al. Methylation subtypes and large-scale epigenetic alterations in gastric cancer. Sci Transl Med. 2012;4:156ra140.
111. Mack SC, Witt H, Piro RM, Gu L, Zuyderduyn S, Stütz AM, et al. Epigenomic alterations define lethal CIMP-positive ependymomas of infancy. Nature. 2014;506:445–50.
112. Adam J, Yang M, Soga T, Pollard PJ. Rare insights into cancer biology. Oncogene. 2014;33:2547–56.
113. Loenarz C, Schofield CJ. Physiological and biochemical aspects of hydroxylations and demethylations catalyzed by human 2-oxoglutarate oxygenases. Trends Biochem Sci. 2011;36:7–18.
114. Kaelin WG, McKnight SL. Influence of metabolism on epigenetics and disease. Cell. 2013;153:56–69.
115. Chowdhury R, Yeoh KK, Tian Y-M, Hillringhaus L, Bagg EA, Rose NR, et al. The oncometabolite 2-hydroxyglutarate inhibits histone lysine demethylases. EMBO Rep. 2011;12:463–9.
116. Lu C, Ward PS, Kapoor GS, Rohle D, Turcan S, Abdel-Wahab O, et al. IDH mutation impairs histone demethylation and results in a block to cell differentiation. Nature. 2012;483:474–8.
117. Losman J-A, Kaelin WG. What a difference a hydroxyl makes: mutant IDH, (R)-2-hydroxyglutarate, and cancer. Genes Dev. 2013;27:836–52.
118. Moroni I, Bugiani M, D'Incerti L, Maccagnano C, Rimoldi M, Bissola L, et al. L-2-hydroxyglutaric aciduria and brain malignant tumors: a predisposing condition? Neurology. 2004;62:1882–4.
119. Shim E-H, Livi CB, Rakheja D, Tan J, Benson D, Parekh V, et al. L-2-Hydroxyglutarate: an epigenetic modifier and putative oncometabolite in renal cancer. Cancer Discov. 2014;4:1290–8.
120. Cervera AM, Bayley J-P, Devilee P, McCreath KJ. Inhibition of succinate dehydrogenase dysregulates histone modification in mammalian cells. Mol Cancer. 2009;8:89.
121. Xiao M, Yang H, Xu W, Ma S, Lin H, Zhu H, et al. Inhibition of α-KG-dependent histone and DNA demethylases by fumarate and succinate that are accumulated in mutations of FH and SDH tumor suppressors. Genes Dev. 2012;26:1326–38.
122. Letouzé E, Martinelli C, Loriot C, Burnichon N, Abermil N, Ottolenghi C, et al. SDH mutations establish a hypermethylator phenotype in paraganglioma. Cancer Cell. 2013;23:739–52.
123. Mason EF, Hornick JL. Succinate dehydrogenase deficiency is associated with decreased 5-hydroxymethylcytosine production in gastrointestinal stromal tumors: implications for mechanisms of tumorigenesis. Mod Pathol Off J U S Can Acad Pathol Inc. 2013;26:1492–7.
124. Sciacovelli M, Gonçalves E, Johnson TI, Zecchini VR, da Costa ASH, Gaude E, et al. Fumarate is an epigenetic modifier that elicits epithelial-to-mesenchymal transition. Nature. 2016;537:544–7.
125. Laukka T, Mariani CJ, Ihantola T, Cao JZ, Hokkanen J, Kaelin WG, et al. Fumarate and succinate regulate expression of hypoxia-inducible genes via TET enzymes. J Biol Chem. 2016;291:4256–65.

126. Carey BW, Finley LWS, Cross JR, Allis CD, Thompson CB. Intracellular α-ketoglutarate maintains the pluripotency of embryonic stem cells. Nature. 2015;518:413–6.
127. Turner BM. Open chromatin and hypertranscription in embryonic stem cells. Cell Stem Cell. 2008;2:408–10.
128. Thienpont B, Steinbacher J, Zhao H, D'Anna F, Kuchnio A, Ploumakis A, et al. Tumour hypoxia causes DNA hypermethylation by reducing TET activity. Nature. 2016;537:63–8.
129. Beyer S, Kristensen MM, Jensen KS, Johansen JV, Staller P. The histone demethylases JMJD1A and JMJD2B are transcriptional targets of hypoxia-inducible factor HIF. J Biol Chem. 2008;283:36542–52.
130. Pollard PJ, Loenarz C, Mole DR, McDonough MA, Gleadle JM, Schofield CJ, et al. Regulation of Jumonji-domain-containing histone demethylases by hypoxia-inducible factor (HIF)-1alpha. Biochem J. 2008;416:387–94.
131. Luo W, Chang R, Zhong J, Pandey A, Semenza GL. Histone demethylase JMJD2C is a coactivator for hypoxia-inducible factor 1 that is required for breast cancer progression. Proc Natl Acad Sci U S A. 2012;109:E3367–76.
132. Mimura I, Nangaku M, Kanki Y, Tsutsumi S, Inoue T, Kohro T, et al. Dynamic change of chromatin conformation in response to hypoxia enhances the expression of GLUT3 (SLC2A3) by cooperative interaction of hypoxia-inducible factor 1 and KDM3A. Mol Cell Biol. 2012;32:3018–32.
133. Mariani CJ, Vasanthakumar A, Madzo J, Yesilkanal A, Bhagat T, Yu Y, et al. TET1-mediated hydroxymethylation facilitates hypoxic gene induction in neuroblastoma. Cell Rep. 2014;7:1343–52.
134. Pan M, Reid MA, Lowman XH, Kulkarni RP, Tran TQ, Liu X, et al. Regional glutamine deficiency in tumours promotes dedifferentiation through inhibition of histone demethylation. Nat Cell Biol. 2016;18:1090–101.
135. Xu W, Wang F, Yu Z, Xin F. Epigenetics and cellular metabolism. Genet Epigenet. 2016;8:43–51.
136. Meacham CE, Morrison SJ. Tumour heterogeneity and cancer cell plasticity. Nature. 2013;501:328–37.
137. Kuo C-Y, Cheng C-T, Hou P, Lin Y-P, Ma H, Chung Y, et al. HIF-1-alpha links mitochondrial perturbation to the dynamic acquisition of breast cancer tumorigenicity. Oncotarget. 2016;7:34052–69.

ASSESSMENT OF THESIS

Prof. Gyorgy Szabadkai, University College of London, UK

Dr Nathalie Mazure, CNRS, Nice, France

UCL RESEARCH DEPARTMENT OF
CELL AND DEVELOPMENTAL BIOLOGY

PROF. GYORGY SZABADKAI, MD, PHD

London, 19th March, 2017

RE: Evaluation of the thesis by Renaud Vatrinet, entitled: TARGETING MITOCHONDRIAL RESPIRATORY COMPLEX I: A NOVEL ANTICANCER STRATEGY; DOTTORATO DI RICERCA IN BIOLOGIA CELLULARE E MOLECOLARE, Ciclo 29, University of Bologna, 2017.

The thesis of Renoud Vatrinet gives account of his experimental project to characterise the role of respiratory complex I in tumorigenesis. It explores the hypothesis arising from previous studies of the group, is that complex I deficiency inhibits tumour growth. While the association of complex I deficiency was previously observed to be associated with reduced tumorigenicity in clinical samples and in vitro experiments, the primary aim of the thesis was to generate in vivo experimental models to directly test the hypothesis.
The first part of the thesis gives a broad overview of the topic, starting from summarising the recently rediscovered role of tumour energy metabolism in tumour formation and progression, then focusing on the specific topic of the thesis: the role of mitochondria and in particular complex I in tumour cells. The introduction properly covers all aspects of the field, which led to formation of the principal hypothesis of the thesis, it is clearly written and gives an excellent and accurate account for the state-of-the-art of the research field.
The hypothesis and aims are clearly formulated and the experimental approaches have been properly designed to assess the hypothesis. I have to underline here that the question and aims are highly original and addresses an outstanding problem of high importance in cancer metabolism.
The methods are described in sufficient detail allowing to clearly understand how results were generated. The first section of the results describes the generation and biochemical/bioenergetic characterisation of the NDUFS3 deficient cell lines using the zinc finger technology. These cell lines then were used in the following sections for measure tumorigenic potential both in vitro and in vivo. The most important conclusion comes from these chapters, is that the lack of complex I activity reduces tumour formation and growth in all models studied. The role of complex I is elegantly demonstrated in the last chapter where the re-expression of NDUFS3 in NDUFS3 deficient cells re-established tumour growth, and again its repression led to almost complete tumour growth arrest. These data pave the way towards the development of novel therapeutic strategies targeting complex I, in concert with the fundamental aim of the thesis.
In addition, the thesis puts forward the hypothesis that complex I regulates HIF1alpha stabilisation and further explores whether this can account for the observed regulation of tumour growth by complex I. The data indicate that the lack of hypoxia induced stabilisation of HIF1alpha is due to alpha-ketoglutarate accumulation, as demonstrated by metabolomic studies. Although probably the lack of HIF1alpha stabilisation cannot be accounted for the whole picture which emerges from the in vivo studies, it provides a set of extremely valuable data for further studies.

Overall, the thesis by Renaud Vatrinet is an excellent work. It gives a very clear and well written account of an exceptionally important topic in cancer metabolism. The work itself is highly original and completed to a very high experimental standard.

UCL RESEARCH DEPARTMENT OF CELL AND DEVELOPMENTAL BIOLOGY
University College London, Anatomy Building, Gower Street, London, WC1E 6BT
Tel: +44 (0)20 7679 3346
http://www.cdb.ucl.ac.uk/

Accordingly, I have no major concerns, and would only list the following minor comments.

1. A few typos have been flagged for correction.
2. p56. While 'NDUFS3$^{+/+}$ cells are clones having reversed the mutations induced and therefore they express NDUFS3', thus represent the best available control, this in my opinion does not represent a clearly 'isogenic control', since these cells are coming from independent clones, thus genetic variability cannot be excluded.
3. Fig. 14: needs specifying that the experiments were performed on isolated mitochondria
4. p58. 'oxygen consumption rate measurement revealed that disruption of CI in NDUFS3$^{-/-}$ cell lines was sufficient to abrogate mitochondrial respiration' : This is a very important finding, which is however rather surprising, since the rest of the complexes, in particular complex II is still intact, thus could drive some respiration. I feel that this finding should be further discussed, at least in the discussion.
5. p63. 'While the lack of CI does not affect proliferation *in vitro*, it can nevertheless be expected that the alteration would negatively affect the intricate machinery that drive cancer formation and progression.' This statement would require introduction or referencing.
6. p63. 'The clonogenic assay has showed their reduced capacity to divide infinitely' – this should require further explanation. Clonogenic assay is usually regarded as proof of survival and maintenance of mitotic capacity.
7. Fig. 26. Here NDUFS3 competent and deficient cells have been mixed in different ratios, however I could not find the description of the exact initial proportions of the two cell lines.
8. Fig. 29A: HIF1alpha stabilisation under different conditions is shown, but there is no quantification presented.
9. p73.: 'Further, immunohistochemical analysis of collagen fibres by Masson's trichrome staining, revealed that 143B CI-deficient masses, and not CI-competent ones, displayed stromal invasion containing host vessels.' This description is not very clear. It would be beneficial to explain more in detail what stromal invasion means, and how this differs from the CI competent tumours.
10. While the work is clearly a team work, it would be correct to describe the approximate contribution of the candidate.

Gyorgy Szabadkai, MD, PhD
Professor of Physiology
Department of Cell and Developmental Biology,
Consortium for Mitochondrial Research (CfMR),
University College London,
Gower Street, WC1E 6BT,
London, UK
T.: +44 (0)2076797362
F.: +44 (0)2079167968
http://www.ucl.ac.uk/mitochondria

IRCAN
INSTITUT DE RECHERCHE SUR LE CANCER ET LE VIEILLISSEMENT, NICE
INSTITUTE FOR RESEARCH ON CANCER AND AGING, NICE

Evaluation of the thesis of Renaud Vatrinet

Nice, 30th March, 2017

To whom is concerned,

The thesis of Mr Renaud Vatrinet concerns the "Targeting Mitochondrial Respiratory Complex1: a novel anticancer strategy". Mr Varinet has endeavored to understand the involvement of the mitochondrial complex 1 in oncocytic tumors under conditions of hypoxia. Although the link between Complex 1 and HIF1 has already been established within the team, Mr. Vatrinet's main goal has been to generate *in vivo* models to support *in vitro* observations.

The thesis of Mr Vatrinet is very well written and is based on a well detailed and well referenced Introduction. The State-of-the-art is well documented and almost completed, as a more detailed paragraph on HIF-2 would have been appropriate. The working hypotheses are clear and the Materials and Methods is complete and will allow those who will continue the work to be able to make experiments identical to Mr Varinet.

The results obtained by Mr Vatrinet are of high quality. They are not debatable and reveal a high scientific quality. The Discussion is well conducted and of valuable scientific interest. Mr Vatrinet shows that although complex 1-deficient cells can adapt their metabolism to sustain proliferation, Complex 1 is however required to sustain cell tumorigenic properties. Notwithstanding the decline in xenografts growth rate, long term in vivo experiments have shown that the lack of Complex 1 did not prevent tumors training and progression, suggesting that they have successfully met the biomass production requirements. However, when NDUFS3 was removed from the xenograft, it was found that this had a negative effect on its growth. In addition, removing NDUFS3 from xenografts have successfully recovered one key oncocytic feature that is the accumulation of defective mitochondria. The most important finding of this study is that it can be used to treat benign oncocytic phenotype. As said before, I would have liked that Mr. Vatrinet looks at the potential role of HIF2 in these tumors specifically. But maybe it will be the subject of another study later.

In summary, it is a very good thesis that I have greatly enjoyed reading, with which I learned a lot and that I will keep in my archives as soon as I will ask myself about Complex 1.

I have only few minor comments related to some references that are missing and, as I said before, related to a more accurate paragraph relted to HIF2.

Dr Nathalie Mazure

IRCAN - CNRS UMR 7284, INSERM U 1081, UNS
Faculté de Médecine, 28, Avenue de Valombrose - 06107 NICE Cedex 02 - France
Tel. standard : +33 (0)4 93 37 76 99 - Fax +33 (0)4 93 37 76 76 - www.ircan.org

This work was supported by EU FP7 Marie Curie ITN MEET (grant No. 317433)

Thanks to:

Prof. Anna Maria Porcelli, Department of Pharmacy and Biotechnology, University of Bologna, Italy

Prof. Giuseppe Gasparre, Department of Surgical and Medical Sciences, University of Bologna, Italy

Serena Paterlini, Department of Surgical and Medical Sciences, University of Bologna, Italy

Prof. Barbara Kofler, Department of Pediatrics, Paracelsus Medical University, Salzburg, Austria

Dr Ivana Kurelac, Department of Surgical and Medical Sciences, University of Bologna, Italy

Dr Luisa Iommarini, Department of Pharmacy and Biotechnology, University of Bologna, Italy

Silvia Vidali, Department of Pediatrics, Paracelsus Medical University, Salzburg, Austria

Laura Amato, Department of Surgical and Medical Sciences, University of Bologna, Italy

Dr Rene Feichtinger, Department of Pediatrics, Paracelsus Medical University, Salzburg, Austria

Monica De Luise, Department of Surgical and Medical Sciences, University of Bologna, Italy

Dr Giulia Girolimetti, Department of Surgical and Medical Sciences, University of Bologna, Italy

Felix Locker, Department of Pediatrics, Paracelsus Medical University, Salzburg, Austria

Dr Christian Bergamini, Department of Pharmacy and Biotechnology, University of Bologna, Italy

Dr Moira Ragazzi, Anatomic Pathology Unit, Arcispedale Santa Maria Nuova – IRCCS, Italy

Dr Marta Columbaro, Rizzoli Orthopaedic Institute, Laboratory RAMSES, Bologna, Italy

Dr Michele Vidone, Department of Surgical and Medical Sciences, University of Bologna, Italy

Sepideh Aminzadeh-gohari, Department of Pediatrics, Paracelsus Medical University, Salzburg, Austria

Giulia Leone, Department of Pharmacy and Biotechnology, University of Bologna, Italy

Dr Franz Zimmermann, Department of Pediatrics, Paracelsus Medical University, Salzburg, Austria

Prof. Johannes Mayr, Department of Pediatrics, Paracelsus Medical University, Salzburg, Austria

Prof. Michela Rugolo, Department of Pharmacy and Biotechnology, University of Bologna, Italy

Dr Anna Maria Ghelli, Department of Pharmacy and Biotechnology, University of Bologna, Italy

Dr Claudia Zanna, Department of Pharmacy and Biotechnology, University of Bologna, Italy

Prof. Marco Seri, Department of Surgical and Medical Sciences, University of Bologna, Italy

Prof. Vincenzo Scarlato, Department of Pharmacy and Biotechnology, University of Bologna, Italy

Prof. Giovanni Capranico, Department of Pharmacy and Biotechnology, University of Bologna, Italy

For having read and corrected this thesis, I thank:

Prof. Gyorgy Szabadkai, University College of London, UK

Dr Nathalie Mazure, CNRS, Nice, France

I also thank:

The "MEETers" Eligio Iannetti, Sarah Foriel, Silvia Vidali, Mara Mennuni, Mikael Pezet, Manar Aoun, Michele Giunta, Sasha (Oleksandr) Lytovchenko, Selena Trifunov, Umut Cagin, Eliska Konarikova, Laura Sanchez Caballero, Lavinija Matakovic, and our dissemination assistants Marco Argentina and Marialuisa Russo.

For their help and advices throughout my training: Sabrina Dusi, Mario Fogazza, Valentina Troppeano, Laura Pradella, Andreas Koller, Susanne Brunner, Kerstin Graf, Bernard Okere, Lorena Marchio, Chiara Montironi and Sara Colucelli.